

Function of the *Zymomonas mobilis* terminal enzymes of the methylerythritol phosphate pathway, IspG and IspH, in *Escherichia coli*

By

Jyotsna Misra

A dissertation submitted in partial fulfillment of the requirements for the degree of

Doctor of Philosophy

(Biochemistry)

at the

UNIVERSITY OF WISCONSIN-MADISON

2023

Date of final oral examination: 12/06/2023

The dissertation is approved by the following members of the Final Oral Committee:

Patricia J. Kiley, Professor, Biomolecular Chemistry

Robert C. Landick, Professor, Biochemistry

Vatsan Raman, Associate Professor, Biochemistry

Daniel Amador Noguez, Associate Professor, Bacteriology

Abstract

Isoprenoids are one of the largest classes of natural products, exhibiting diversity in structure and function. They also include compounds that are essential for cellular life across the biological world. In bacteria, isoprenoids are derived from two precursors, isopentenyl diphosphate and dimethyl allyl diphosphate, primarily by the methyl erythritol phosphate pathway. *Zymomonas mobilis* has the potential for methyl erythritol phosphate pathway engineering by diverting some of glucose that is typically efficiently converted into ethanol to produce isoprenoid precursors. IspG and IspH catalyze the terminal steps in the methyl erythritol phosphate pathway and contain [4Fe-4S] clusters. The two oxidation-reduction reactions catalyzed by IspG and IspH are major limiting steps in the production of isoprenoid precursors in *Z. mobilis* and in vivo they show O₂ sensitivity. Here, we compare and contrast the function of IspG and IspH from *Z. mobilis* and *E. coli* under aerobic and anaerobic growth conditions. Under anaerobic conditions, we show that both *Z. mobilis* IspH and IspG are able to partially complement in *E. coli*. SUF Fe-S cluster biogenesis pathway levels were found not to be limiting for *Z. mobilis* IspH and IspG function in *E. coli*. Under aerobic conditions, *Z. mobilis* IspH confers a severe oxygen sensitive growth phenotype to *E. coli*. However, the co-expression of cognate *Z. mobilis* IspG partially rescues this growth phenotype in *E. coli*. No evidence was found for a physical association between *Z. mobilis* IspG and IspH to explain the beneficial effect of IspG. Taken together, our data suggests that co-expression of *Z. mobilis* IspG and IspH need to be co-optimized to improve flux via the methyl erythritol phosphate pathway.

Acknowledgements

I am grateful to my advisor Dr. Patricia Kiley and my sincere thanks to her for the guidance and mentorship during my time in the lab. She always believed in me and helped me to become a more confident scientist. I would like to thank the previous and current members of the Kiley Lab for all the scientific discussions over the years that helped in shaping my scientific work. I would like to give a special mention to Dr. Erin Mettert, for teaching me various laboratory techniques, creating bacterial strains and always helping me with any protocol or reagent I needed for the experiment. I would also like to say thank you to all my lab mates Wamiah, Piyush, Rajdeep, Isabel, Tomas, Tessa, Jacob, Rose for making my time in the Kiley lab memorable, it was amazing to work with all of you.

I would also like to thank all my thesis committee members Dr. Bob Landick, Dr. Daniel Amador Noguez and Dr. Vatsan Raman for their support and mentorship throughout my time as an IPiB graduate student. Their valuable feedbacks on my work helped me to improve as a scientist.

I would not have made it to here without the unconditional love and support of my family: my maternal and paternal grandparents, my mum and dad, my sister Jyoti, my brother Shiva. Also, I want to thank my best friend Gaurav and all my friends for being there for me during my time in graduate school.

I would like to thank Laura Vanderploeg for helping me with posters and pictures of the bacterial plates.

Table of contents

Abstract.....	ii
Acknowledgement.....	iii
Chapter 1: Introduction.....	1
Abstract.....	2
Isoprenoid biosynthesis.....	3
Biosynthesis of isoprenoid precursors: IDP and DMADP.....	6
Rational engineering of MEP pathway to optimize isoprenoid production in <i>Z. mobilis</i>	9
Structure of IspG (4-hydroxy-3-methylbut-2-enyl diphosphate synthase).....	11
Enzymatic reaction catalyzed by IspG.....	14
Structure of IspH (4-hydroxy-3-methylbut-2-enyl diphosphate reductase).....	17
Proposed classes of IspH.....	20
Enzymatic reaction catalyzed by IspH.....	21
Fe-S clusters are the oldest and versatile co-factors of protein.....	25
Evolution of Fe-S clusters.....	26
Organization of Fe-S cluster biogenesis in <i>E. coli</i> and <i>Z. mobilis</i>	26
The Isc pathway.....	28
The Suf pathway.....	28
IscR plays a key role in regulation of Isc and Suf pathway.....	32
Fe-S cluster homeostasis.....	32
References.....	34

Chapter 2: Functional differences between the <i>Escherichia coli</i> and <i>Zymomonas mobilis</i>	
enzymes that catalyze the terminal steps of the methylerythritol phosphate pathway.....	47
Abstract.....	48
Introduction.....	49
Results.....	52
Discussion.....	84
Materials and methods.....	90
References.....	96
Chapter 3: Final discussion and conclusions.....	101
Why do <i>Z. mobilis</i> IspG and IspH poorly complement the corresponding <i>E. coli</i> mutants?.....	102
Why is <i>Z. mobilis</i> IspH function in <i>E. coli</i> so sensitive to O ₂ ?.....	103
Why does co-expression of IspG improve the function of IspH?.....	105
Why IspG improves the growth toxicity of IspH under aerobic conditions?.....	106
References.....	108
Appendix 1: Supplemental material for chapter 2.....	110
Appendix 2: Additional assays of <i>Z. mobilis</i> IspH and IspG.....	141
Appendix 3: Metabolomics profiling to study flux through the MEP pathway in <i>E. coli</i>.....	165

List of Figures

Figure 1-1 Isoprenoids are diverse in structure and function.....	5
Figure 1-2 Biosynthesis of isoprenoid precursors.....	8
Figure 1-3 Structure of IspG.....	13
Figure 1-4 Reaction mechanism of IspG.....	16
Figure 1-5 Structure of IspH.....	19
Figure 1-6 Reaction mechanism of IspH.....	24
Figure 1-7 Organization of suf operon in <i>Z. mobilis</i> and <i>E. coli</i>	31
Figure 2-1 Viability of MG1655 (MVA ⁺) $\Delta ispG \Delta ispH$ with plasmid variants.....	55
Figure 2-2 Viability of MG1655 (MVA ⁺) $\Delta ispG$ with plasmid variants.....	58
Figure 2-3 Viability of MG1655 (MVA ⁺) $\Delta ispH$ with plasmid variants.....	61
Figure 2-4 Viability of MG1655 (MVA ⁺) $\Delta ispG \Delta ispH$ with plasmid variants.....	64
Figure 2-5 <i>Z. mobilis</i> IspG and IspH cluster degradation assay.....	68
Figure 2-6 Viability of cells under aerobic conditions in the presence of mevalonate.....	71
Figure 2-7 Viability of MG1655 (MVA ⁺) $\Delta ispH$ or MG1655 (MVA ⁺) $\Delta ispH, P_{fnr} suf_{ZM}$ with plasmid variants.....	75
Figure 2-8 Viability of MG1655 (MVA ⁺) $\Delta ispH$ or MG1655 (MVA ⁺) $\Delta ispH, P_{fnr} suf_{EC}$ with plasmid variants.....	77
Figure 2-9 Interaction studies of IspG and IspH.....	81
Figure 2-10 Model describing our findings of <i>Z. mobilis</i> and <i>E. coli</i> IspH and IspG function.....	83
Figure A1-1 Viability of cells assayed under aerobic and anaerobic conditions.....	119
Figure A1-2 Optimization of the detection of IspH in cell extracts.....	121

Figure A1-3 Blot with increasing IPTG concentration for <i>E. coli</i> strains.....	123
Figure A1-4 Mean values of IspH and IspG protein levels quantified by antibody against strep-tag II under anaerobic conditions.....	125
Figure A1-5 Mean values of IspH and IspG protein levels quantified by antibody against strep-tag II under aerobic conditions.....	127
Figure A1-6 Viability of cells assayed at 100 & 200 μ M IPTG under aerobic and anaerobic conditions.....	129
Figure A1-7 Comparison of Suf D levels under aerobic conditions.....	131
Figure A1-8 Multiple sequence alignment of <i>E. coli</i> and <i>Z. mobilis</i> IspG.....	133
Figure A1-9 Multiple sequence alignment of <i>E. coli</i> and <i>Z. mobilis</i> IspH.....	135
Figure A2-1 β - galactosidase assay of <i>PsodA</i> , <i>PfepB</i> , <i>PhyaA</i> , <i>PiscR</i> , <i>PsufA</i> under aerobic and anaerobic conditions	145, 147, 150, 153
Figure A2-2 Measurement of Fe ²⁺ release from the [4Fe-4S] cluster of <i>Z. mobilis</i> IspH.....	157
Figure A2-3 <i>Z. mobilis</i> IspH does not co-elute with <i>Z. mobilis</i> IspG C- terminus strep-tag II..	160
Figure A3-1 Fold change of various metabolites of the MEP pathway.....	168
Figure A3-2 Fold change of downstream metabolites.....	170

List of Tables

Table A1-1 List of E. coli strains used in Chapter 2.....	111
Table A1-2 List of plasmids used in Chapter 2.....	113
Table A1-3 List of primers used in Chapter 2.....	113
Table A2-1 Strains used in the study in Appendix 2.....	115
Table A2-2 Plasmids used in the study in Appendix 2.....	117

CHAPTER 1
INTRODUCTION

Abstract

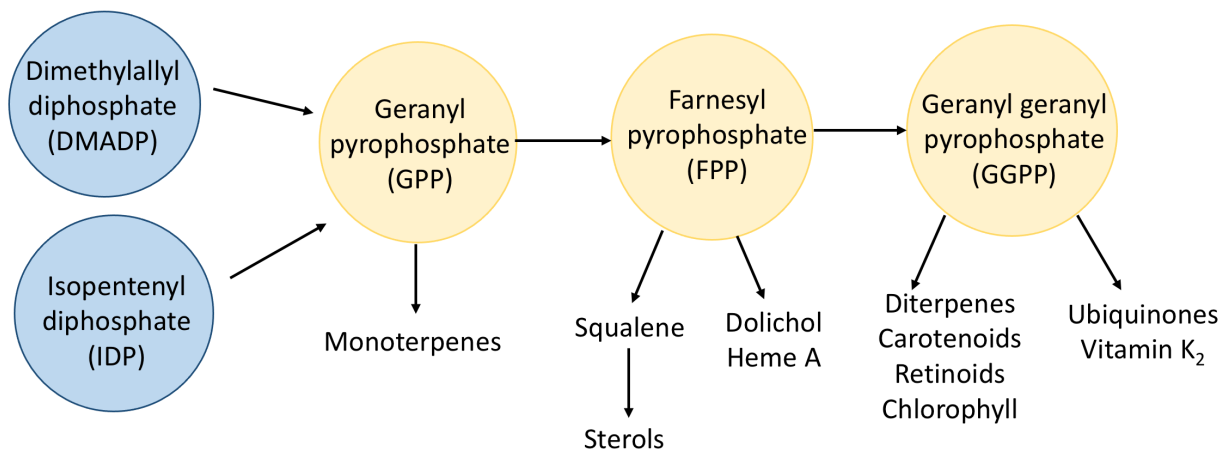
Isoprenoids can be used as a substitute for petroleum in the production of plastics and biofuels. The bacterium *Zymomonas mobilis* produces isoprenoid precursors, dimethylallyl diphosphate and isopentenyl diphosphate from glucose via the methyl erythritol phosphate pathway. IspG and IspH catalyze the final two steps of the MEP pathway and contain [4Fe-4S] clusters in their respective active sites. Biochemical studies of these enzymes from other organisms show that the Fe-S clusters are not stable to O₂. Accumulation of 2C-methyl-D-erythritol 2,4-cyclodiphosphate, the substrate of IspG, is known to occur under oxidative stress conditions in some bacteria and plants and in *Z. mobilis* when shifted to aerobic conditions, suggesting Fe-S cluster instability may be affecting activity of these enzymes in vivo. One well studied enzyme is IspH from *E. coli*. In the absence of substrate, the structure of IspH shows it to be in an open conformation, which might make its [4Fe-4S] more accessible to oxygen damage. Studies also point to the variation in the N- and C-termini of IspH as playing a role in differences of IspH sensitivity to oxidative conditions. IspG from *E. coli* is also reported to be oxygen sensitive and apart from three cysteine residues, glutamic acid acts as the fourth ligand for its [4Fe-4S] cluster. In this chapter, I provide an overview of the MEP pathway in bacteria. I review our knowledge of IspG and IspH structures and mechanism. I describe how substrate binding of IspH might impact [4Fe-4S] cluster stability and how substrate availability could impact their activity and the MEP pathway under aerobic and anaerobic conditions. I review what is known about the MEP pathway in *Z. mobilis*. Finally, I describe what is known about Fe-S cluster biogenesis in *Z. mobilis* since this pathway is responsible for generating the [4Fe-4S] clusters of IspG and IspH.

Isoprenoid biosynthesis

Isoprenoids are a large and structurally diverse group of biological compounds¹. These compounds play an important role in metabolic and regulatory processes. For example, sterols are components of eukaryotic cell membranes, carotenoids and chlorophyll take part in photosynthesis, and ubiquinone is a component of the electron transport chain²⁻⁴. In addition, isoprenoids have various commercial applications as pigments, fragrances, pharmaceuticals, agrochemicals and also have the potential to be used as biofuels or precursors to biofuels^{5,6}. Isoprenoids are composed of isoprene units (C₅) and are biosynthesized from their precursors, isopentenyl diphosphate (IDP) and its isomer dimethylallyl diphosphate (DMADP)⁷. IDP and DMADP are made from two distinct pathways: the mevalonate (MVA) pathway and the methylerythritol 4-phosphate (MEP) pathway. The C₅ isoprene units are condensed or cyclized to form geranyl pyrophosphate (GPP, C₁₀), farnesyl pyrophosphate (FPP, C₁₅), geranyl geranyl pyrophosphate (GGPP, C₂₀) and decaprenyl pyrophosphate (DPP, C₅₀)⁸, depending on the organism (Figure 1-1). In bacteria IDP and DMADP are used in the formation of the undecaprenyl (C₅₅) and decaprenyl diphosphates required for bacterial cell wall biosynthesis, in quinone biosynthesis, and protein prenylation. Thus, isoprenoid biosynthesis is required for survival in bacteria^{9,10}.

Figure 1-1: Isoprenoids are diverse in structure and function

Isoprenoids are biosynthesized from two precursor molecules: Isopentenyl diphosphate (IDP) and dimethylallyl diphosphate (DMADP). They are one of the largest classes of natural products and include various essential compounds.



Biosynthesis of isoprenoid precursors: IDP and DMADP

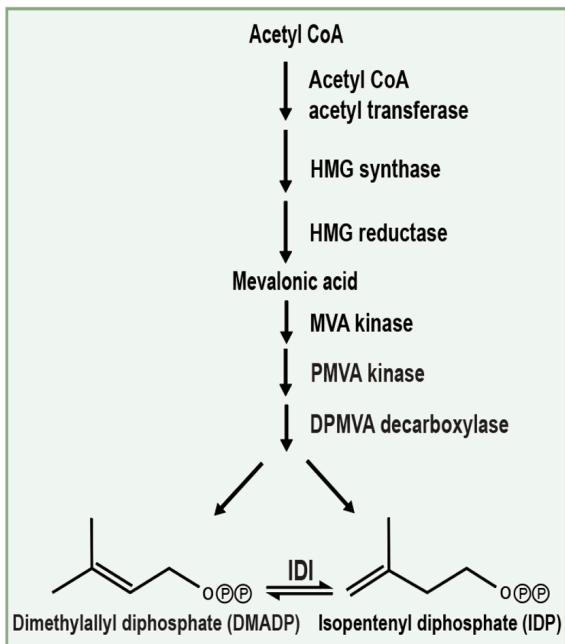
The MEP pathway is present in most prokaryotes; including *E. coli* and *Z. mobilis*, green algae, plant chloroplasts¹¹. The MEP pathway produces IDP and DMADP from glyceraldehyde 3-phosphate (G3P) and pyruvate which are glycolytic intermediates¹². This process comprises seven enzymatic reactions. G3P and pyruvate are converted to 1-deoxy-D-xylulose-5-phosphate (DXP) catalyzed by DXP synthase. This step is crucial in the pathway and is also the rate limiting step in *Z. mobilis*¹³. DXP reducto isomerase (DXR) converts DXP to methyl erythritol-4-phosphate (MEP). Enzymes IspC, IspD, IspE, IspF, catalyze 2C-methyl-D-erythritol 2,4-cyclodiphosphate (MEcDP) from MEP. IspG is involved in conversion of MEcDP to 4-hydroxy-3-methyl-but-2-enyl diphosphate (HMBDP). HMBDP is converted to IDP or DMADP catalyzed by IspH. IDP isomerase (IDI) isomerizes IDP and DMADP (Figure 1-2)^{14,15}. This enzyme is lacking in *Z. mobilis*.

The MVA pathway is present in archaea, fungi, plant cytoplasm and in some gram-positive bacteria². The pathway is connected to the central carbon metabolism through acetyl CoA. Two molecules of acetyl CoA are condensed sequentially to produce acetoacetyl CoA catalyzed by acetoacetyl CoA thiolase and HMG CoA synthase to produce 3-hydroxy-3-methylglutaryl CoA (HMG CoA) which is reduced by HMG CoA reductase to mevalonate⁸. Mevalonate is then phosphorylated sequentially by mevalonate kinase and mevalonate-5-phosphate kinase and decarboxylated by mevalonate-5-diphosphate decarboxylase to produce IDP or DMADP (Figure 1-2)^{16,17}.

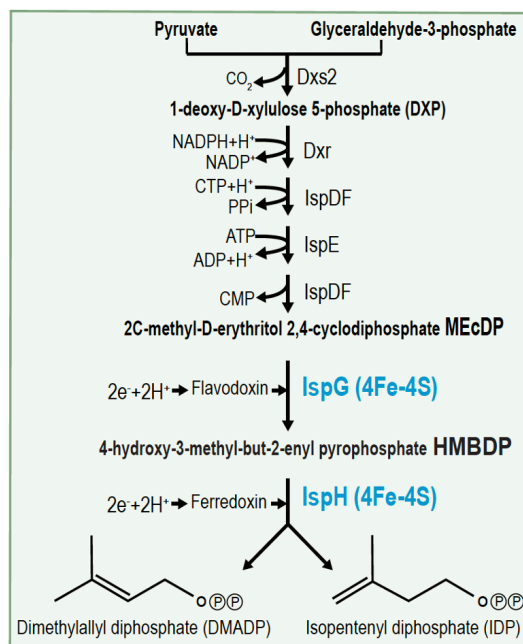
Figure 1-2: Biosynthesis of isoprenoid precursors

Biosynthesis of isoprenoid precursors, IDP and DMADP occur through either of the two pathways:

Mevalonic acid (MVA) pathway or methylerythritol phosphate (MEP) pathway



Mevalonic acid pathway



Methylerythritol phosphate pathway

Rational engineering of MEP pathway to optimize isoprenoid production in *Z. mobilis*

Zymomonas mobilis is an aerotolerant anaerobe and prolific ethanologen and is recognized as a promising platform for biofuel production^{18,19}. As such it has many remarkable characteristics for engineering of the MEP pathway to produce isoprenoids. Analysis of KEGG pathways indicates that *Z. mobilis* has all of the genes of the MEP pathway except IDI and IspDF are fused. 1-deoxy-D-xylulose 5-phosphate synthase (DXS2) catalyzes conversion of pyruvate and glyceraldehyde-3-phosphate to 1-deoxy-D-xylulose 5-phosphate (DXP). 1-deoxy-D-xylulose reductoisomerase (DXR) catalyzes conversion of 1-deoxy-D-xylulose 5-phosphate (DXP) to methylerythritol 4-phosphate (MEP). The bifunctional enzyme MEP cytidyl transferase / MEcDP synthase (IspDF) converts methylerythritol 4-phosphate (MEP) to 4-diphosphocytidyl-2-C-methyl-D-erythritol (CDP-ME). CDP-ME kinase (IspE) catalyzes CDP-ME to 4-diphosphocytidyl-2-C-methyl-D-erythritol 2-phosphate (CDP-MEP). IspDF catalyzes CDP-MEP synthesis to MEcDP. MEcDP is converted to HMBDP by IspG which is the penultimate enzyme of the pathway. IspH is the terminal enzyme and catalyzes HMBDP to IDP or DMADP. Downstream metabolites are made from IDP/ DMADP, which is catalyzed by geranyl pyrophosphate synthase (GPPS) to geranyl pyrophosphate (GPP). Farnesyl pyrophosphate is produced from geranyl pyrophosphate by farnesyl pyrophosphate synthase. Hopanoids, which are a subclass of isoprenoids, are produced from the MEP pathway and are found in the lipid membranes of *Z. mobilis*. Hopanoids are considered to be quite abundant in *Z. mobilis* indicating significant flux of carbon through the MEP pathway²⁰.

Z. mobilis uses the Entner-Doudoroff (ED) pathway, which leads to high uptake of glucose that is converted to ethanol at the same time maintaining low biomass¹⁹. This metabolism, specific

to *Z. mobilis* can perhaps be leveraged for the production of isoprenoids using lignocellulosic biomass from crops like *Miscanthus giganteus* (miscanthus) and *Panicum virgatum* (switchgrass). These crops provide an abundant sugar source that can potentially be converted into liquid fuels and other bioproducts if carbon sent to ethanol in *Z. mobilis* can be redirected towards the MEP pathway²¹⁻²³. Various inhibitory compounds example weak acids, aldehydes, furans, phenolics are produced in hydrolysates during the pre-treatment step of lignocellulose biomass to make the sugars available for microbial degradation and is a point of consideration while engineering the MEP pathway of *Z. mobilis* as these inhibitors have an impact on the growth and metabolism²⁴⁻²⁷.

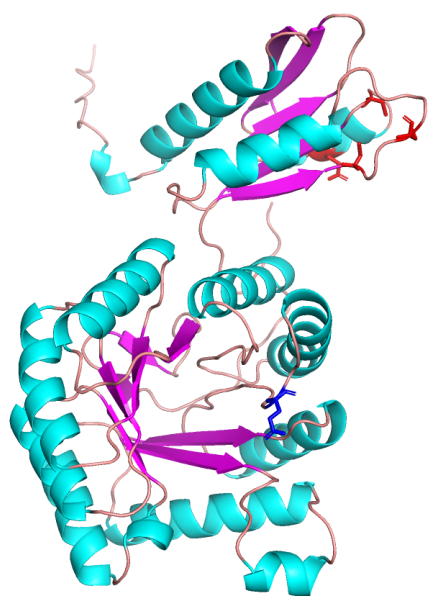
Previous work of *Z. mobilis* grown with switch grass or miscanthus hydrolysates identified oxidative stress response and Fe-S cluster biogenesis pathway genes as hydrolysate tolerance genes suggesting that these genes are essential in mitigating damage caused by reactive oxygen species levels²⁸. Redox imbalance in both the elevated sulfur assimilation pathways and alterations in the reduced pools of glutathione, which is formed from glutamate, glycine and cysteine, leads to an oxidizing intracellular environment that could adversely affect oxidatively labile [Fe-S] cluster proteins, IspG and IspH of the MEP pathway. When *Z. mobilis* is exposed to oxygen, there is significant accumulation of MEcDP and HMBDP, substrates of IspG and IspH among all other metabolites assayed from the MEP pathway²⁹. In addition, with overexpression of 1-deoxy-D-xylulose 5-phosphate synthase DXS, IspG and IspH enzyme activity are the primary constraints in the MEP pathway³⁰.

Structure of IspG (4-hydroxy-3-methylbut-2-enyl diphosphate synthase)

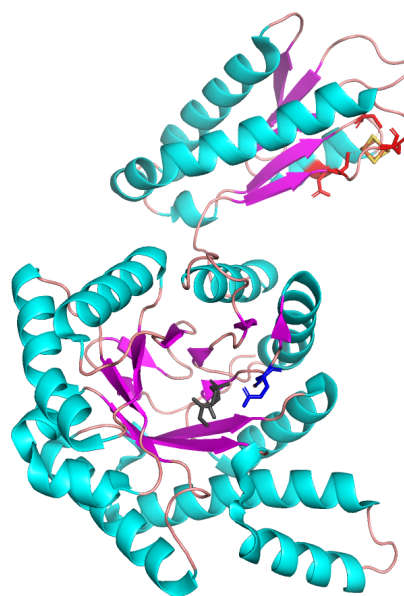
IspG from *T. thermophilus* and *A. aeolicus* crystallizes as a homodimer and has two domains: domain A and B. The A domain belongs to the TIM barrel superfamily while the [4Fe-4S] cluster is present in the B domain (Figure 1-3a). The active site is located at the interface of the N-terminal domain of one subunit with the C-terminal domain of the adjacent subunit which forms a catalytically active head-to tail dimer and catalysis proceeds in the closed active site cavities of the dimer^{31,32}. The X-ray crystal structure of IspG, bound with its substrate, MEcDP, shows that the [4Fe-4S] cluster is coordinated by glutamate and three cysteines in the absence of substrate. In the presence of substrate, this glutamate residue is replaced with the C3 oxygen of MEcDP³³. Upon binding of MEcDP, another glutamate residue is involved in the protonation of MEcDP and plays a key role in the catalysis³⁴. The three cysteines and glutamate residue that ligand the [4Fe-4S] cluster and the catalytic glutamate is conserved in *Z. mobilis* and *E. coli* IspG. (Figure 1-3b). A hinge-bend around the flexible loop connecting domain A and domain B during catalysis allows the substrate loading and the product release, which requires a transition to an open conformation. It has been reported that in plants, and some parasites and bacteria that there is an extra domain in IspG which plays primarily a structural role³⁵⁻³⁷.

Figure 1-3: Structure of IspG (A-1) Alpha fold structure prediction of *Z. mobilis* IspG (AF-Q5NR50-F1) (A-2) X-ray crystal structure of *Thermus thermophilus* IspG with HMBDP (4S39) (B) X-ray crystal structure of *Aquifex aeolicus* (3NOY)

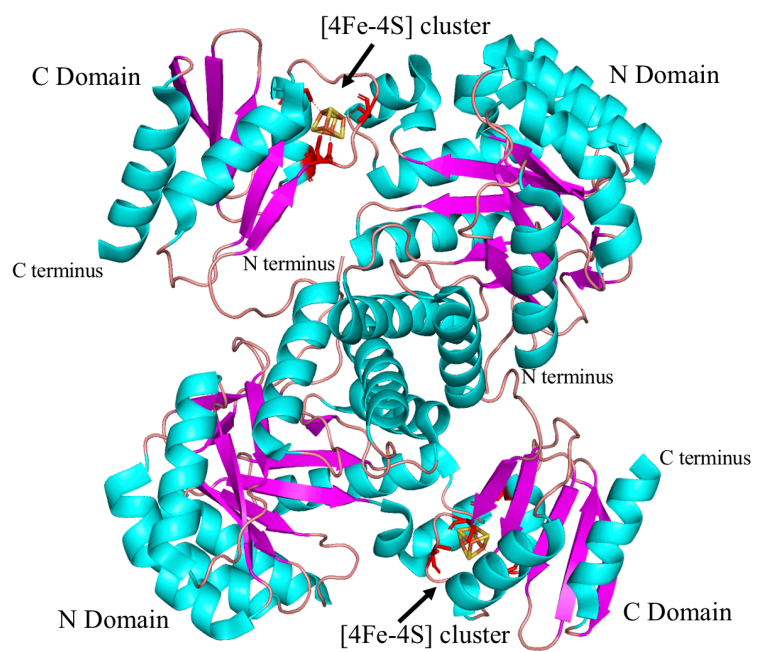
(A-1) Structure of *Z. mobilis* IspG predicted from Alpha fold. The N Domain folds as a TIM barrel and the C domain houses the [4Fe-4S] cluster. Three cysteine residues and a glutamate residue are shown in red color, which ligand to the Fe atoms of the [4Fe-4S] cluster. The glutamate residue involved in catalysis is shown in blue color. (A-2) A representation of one monomer of the X-ray structure of *Thermus thermophilus* IspG dimer with HMBDP shown in grey color and the ligands which bind the [4Fe-4S] cluster are in red color and the catalytic glutamate is in blue color. (B) Structure of IspG from *Aquifex aeolicus* shows IspG as homodimer with [4Fe-4S] cluster and the two major domains. are labelled.



(A-1)



(A-2)



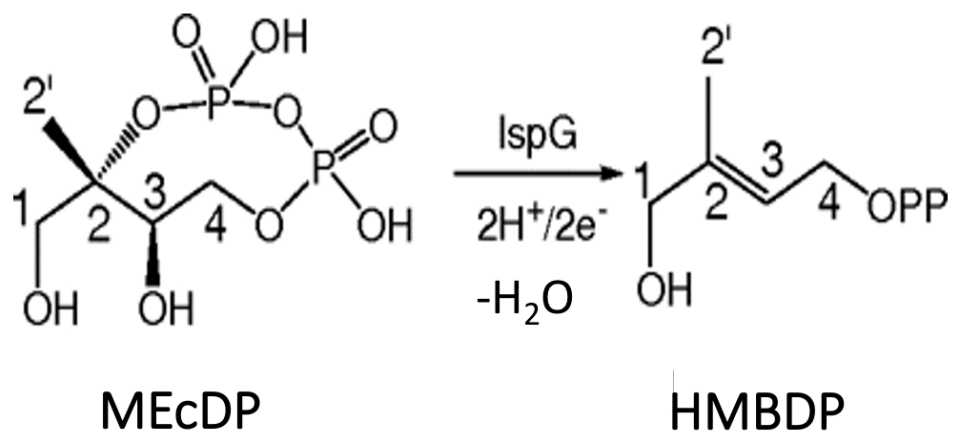
(B)

Enzymatic reaction catalyzed by IspG

IspG catalyzes the conversion of MEcDP to HMBDP in *Thermus thermophilus*, which involves the opening of the ring and formation of intermediates at the C2 carbon atom of MEcDP. Upon binding of MEcDP, displacement of glutamate (E350), which coordinates the fourth iron atom of the [4Fe-4S] cluster occurs. The second glutamate (E232) is involved in deprotonation of the C3 hydroxy group of MEcDP allowing formation of an Fe-O bond. The second carbon of MEcDP is reduced by the sequential transfer of two electrons from the [4Fe-4S] cluster of IspG. Another glutamate residue is involved in the protonation and the hydroxyl group attached to the third carbon of MEcDP is released as a water molecule during the process (Figure 1-4). The active site of IspG, which facilitates the binding of the phosphate moiety of MEcDP, include basic amino acids like arginine and lysine³⁴. Protein electron carriers like ferredoxin/ flavodoxin transfer electrons to the [4Fe-4S] cluster of IspG. In *E. coli*, flavodoxin I transfer electrons to the [4Fe-4S] cluster of IspG³⁸ and ferredoxin in plants³⁹. The protein electron carrier for *Z. mobilis* IspG is unknown. From the genome annotation, there are 2 flavodoxins (ZMO 0860, ZMO 1851) and 3 ferredoxins (ZMO 1818, ZMO 0220, ZMO 2028) that are possible protein electron carrier for IspG.

Figure 1-4: Reaction mechanism of IspG

IspG leads to reductive dehydroxylation of MEcDP to make HMBDP for isoprenoid biosynthesis through the methyl erythritol phosphate pathway. (This figure is adapted from reference⁴⁰).

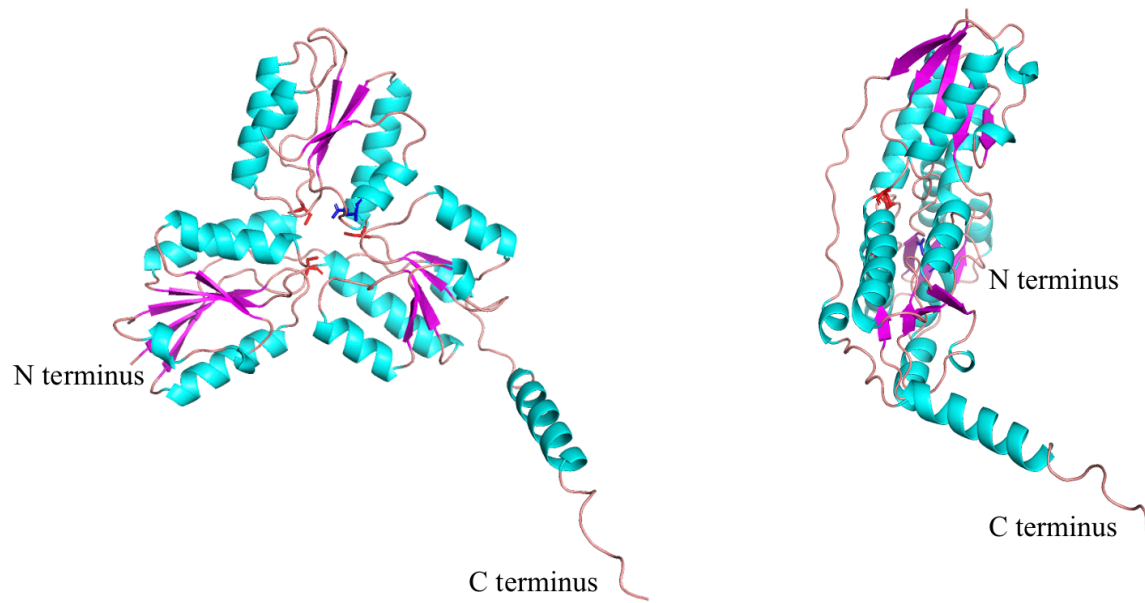


Structure of IspH (4-hydroxy-3-methylbut-2-enyl diphosphate reductase)

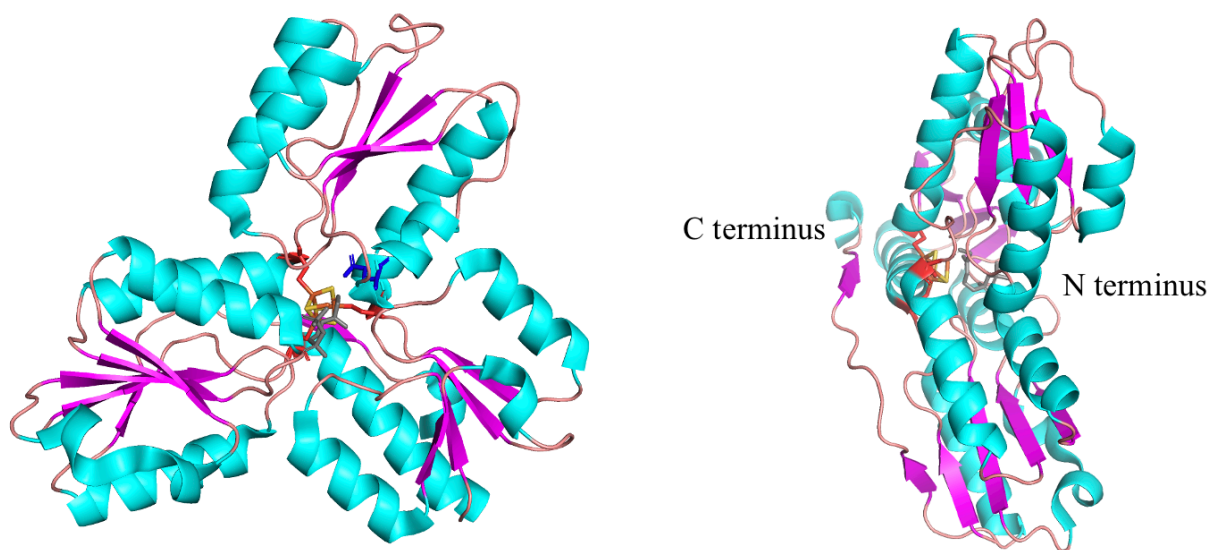
X-ray crystallographic structure of IspH from *Aquifex aeolicus*, *E. coli* and apicomplexan *Plasmodium falciparum* show that it has a basic “trefoil” arrangement of three α/β domains that surround a central Fe-S core^{41,42} (Figure 1-5). IspH from *E. coli* and *P. falciparum* exist as monomers in solution while IspH from *A. aeolicus* is predicted to assemble into homodimer. In *A. aeolicus*, the Fe-S cluster is protected through dimerization from surrounding solvent. However, in *E. coli* and *P. falciparum* the Fe-S cluster is covered by an additional C-terminal extension⁴¹⁻⁴⁴. The clover leaf like structure of *E. coli* IspH shows the three cysteine (C12, C96, C197) residues coordinate with the three Fe atoms of the [4Fe-4S] cluster. The cysteine residues involved in [4Fe-4S] cluster binding is conserved in *E. coli* and *Z. mobilis* IspH. The crystal structure of *E. coli* IspH in the presence of its substrate, shows that HMBDP acts as the fourth ligand of the [4Fe-4S] cluster as it coordinates one Fe atom of the cluster while the three cysteine residues maintain the coordination with the other three Fe atoms of the cluster. This coordination motif of IspH [4Fe-4S] cluster is similar to that found in aconitase⁴⁵. In addition, IspH bound with HMBDP is in a closed conformation. However, in the absence of the substrate, it is present in an open conformation. This conformational change in the presence of bound HMBDP is reported to stabilize the Fe-S cluster of IspH and protect it from O₂ or reactive oxygen species induced degradation^{46,47}.

Figure 1-5: Structure of IspH (A) Front and side view of alpha fold structure prediction of *Z. mobilis* IspH (AF-Q5NP61-F1) (B) Front and side view of X-ray crystal structure of *E. coli* IspH with bound HMBDP (3KE8)

(A) *Z. mobilis* IspH is predicted to fold into 3 domains consisting of the trefoil α/β structure and in the center are three cysteine residues shown in red color, which are the predicted ligands to 3 Fe atoms of the [4Fe-4S] cluster. Glutamate (E126) residue shown in blue color is proposed to be involved in the catalytic activity. In addition, the C-terminal extension is predicted to fold into an α -helix structure. (B) X-ray crystal structure of *E. coli* IspH bound with HMBDP and the catalytic glutamate residue is shown in blue color. The three cysteines which bind to [4Fe-4S] cluster is shown in red color.



(A)



(B)

Proposed classes of IspH

A recent study proposed that IspH could be grouped into four classes based on amino acid sequence differences and differences in domain structure. The authors proposed that aromatic residues near the [4Fe-4S] cluster may shield the cluster from oxidative damage, since mutagenesis studies showed substitutions of aromatic residues of *E. coli* or *A. aeolicus* IspH made the [4Fe-4S] cluster more labile to O₂. They also showed that for *E. coli* IspH, the C-terminal extension affects the sensitivity of the cluster to oxygen as a C-terminal truncation mutant had increased oxygen sensitivity in the presence as well as absence of substrate. Based on the arrangement of aromatic residues near the three cysteines that coordinate the [4Fe-4S] cluster and on the presence or absence of N-terminal and C-terminal extensions, they proposed a new classification of IspH enzymes⁴⁷.

Class A enzymes are primarily found in anaerobic and microaerophilic bacteria, which have Phe14 and Tyr98 adjacent to the first and second conserved cluster-binding cysteine residues, respectively. Class B enzymes are found in aerobic bacteria, which have Tyr198 adjacent to the third conserved Cys together with Phe302 close to the cluster and are characterized by the addition of the conserved C-terminal extension with Phe302 located in the C-terminus tail. Class C enzymes are found in cyanobacteria and green plants and have the class A core structure in addition to an N-terminal extension with the conserved Tyr72. Class D enzymes are found in apicomplexan parasites, which have the basic class B motif together with C-terminal and N-terminal extensions with a conserved Trp in C-terminal extension. The extensions are proposed to influence interactions with redox partners, oxygen sensitivity and electron-transfer rates. The authors also proposed that the occurrence of these four IspH classes are related to the type of metabolic

lifestyle- photosynthesis, aerobic respiration, pathogenesis and oxygen levels in the organism's environment⁴⁷. *Z. mobilis* IspH falls into Class B as it has the C-terminus extension when aligned to *E. coli* IspH with the conserved Tyr residue.

Enzymatic reaction catalyzed by IspH

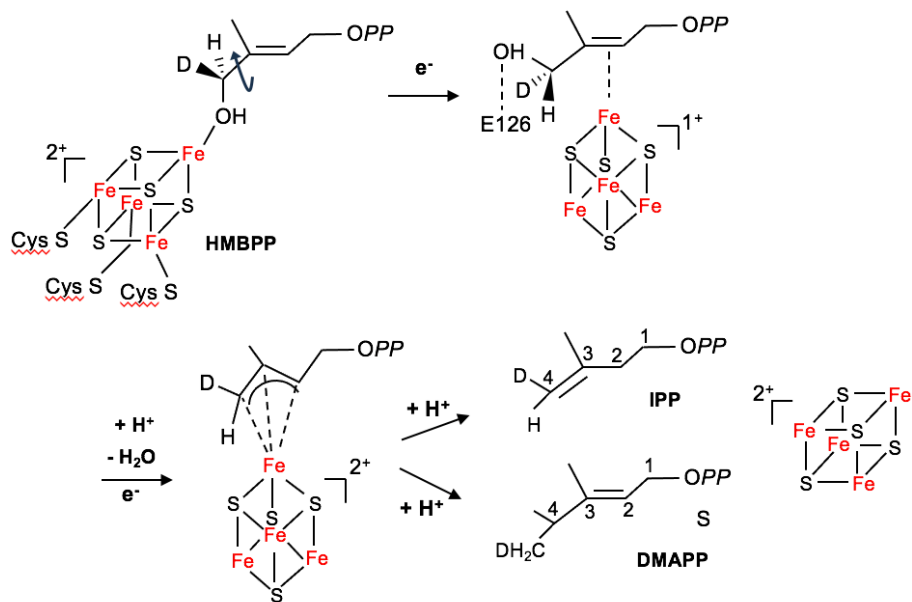
In *E. coli* entry of HMBDP to the active site of IspH causes a change in the conformation that displaces a bound water molecule to the Fe of the [4Fe-4S] cluster and closes the catalytic pocket, which protects the [4Fe-4S] cluster from the surrounding solvent (Figure 1-6). This step is essential as it prefers IspH [4Fe-4S] catalyzed reductive dehydroxylation of HMBDP over the solvent mediated hydrolysis of the diphosphate of HMBDP⁴⁸. The hydroxy moiety attached to the C1 of HMBDP binds to the apical iron of the iron-sulfur cluster of IspH. The [4Fe-4S] cluster is reduced and the hydroxyl methyl group of HMBDP subsequently rotates away from the [4Fe-4S] cluster of IspH and forms hydrogen bond with a catalytic glutamic acid E126 residue, which releases proton and dehydroxylation occurs which is released as water⁴⁹. After another electron reduction of HMBDP, an allyl anion intermediate is formed which is bound to the [4Fe-4S] cluster of IspH³⁷. Protonation occurs by E126 residue. It is been proposed that because of steric constraints imposed by the [4Fe-4S] cluster, protonation preferentially occurs at C3 over C1, releasing the two products, IPP and DMAPP at a ratio of 6:1⁵⁰. The active site of IspH facilitates the binding of the phosphate moiety of HMBDP which include polar and basic amino acids⁴⁶.

Apart from its function as a reductase in the MEP pathway, IspH also shows promiscuity in substrate tolerance and its catalytic activity in vitro. IspH has been shown to

catalyze the conversion of acetylenes to aldehydes and ketone through its acetylene hydratase activity⁴⁸. It can also catalyze the reductive conversion of HMBDP to isoprene and DMADP to isoamylene⁵¹. These findings of IspH function shows its unusual function with substrates other than HMBDP.

Figure 1-6: Reaction mechanism of IspH

IspH which is the terminal enzyme of the MEP pathway causes reductive dehydroxylation of HMBDP which is released as water molecule as well as transfers two electrons to HMBDP from the [4Fe-4S] cluster. (This figure is adapted from reference⁵²).



Fe-S clusters are the oldest and versatile co-factors of protein

Fe-S clusters are diverse in structure as well as in function⁵³. Fe-S clusters are made of iron atoms and elemental sulfur. The common types of Fe-S clusters are: cubane [4Fe-4S], cubane [3Fe-4S] and planar [2Fe-2S]. Usually, Fe-S clusters are ligated to proteins by four cysteine residues. However histidine, aspartate, arginine and glutamate residues have also been known to serve as ligands for the Fe-S cluster^{54,55,56}. Non cysteinyl ligation at one Fe atom of the [4Fe-4S] cluster is known to assist binding of substrate to the cluster in different hydratase and dehydratase class of enzymes; the classic example is aconitase⁵⁷. This is also the case for IspH.

Fe-S clusters are involved in various biological processes. They are best known for their roles in catalyzing electron transfer reactions, notably in aerobic and anaerobic respiration or other metabolic redox reactions^{58,59}. They regulate activity of transcription factors such as IscR, SoxR, and FNR, and function in DNA repair such as endonuclease III and MutY^{60,61,62}. Additionally, they can also play structural roles, such as the [4Fe-4S] cluster of the glutamine 5-phosphoribosyl-1-pyrophosphate amido transferase in *Bacillus subtilis*. The focus of this thesis is on two [4Fe-4S] enzymes: IspG (4-hydroxy-3-methylbut-2-enyl diphosphate synthase) and IspH (4-hydroxy-3-methylbut-2-enyl diphosphate reductase) that promote reduction of their substrates using ferredoxin or flavodoxin redox partners. Although ferredoxins are also Fe-S proteins, flavodoxins use flavin mononucleotide to carry out electron transfer reactions⁶³.

Evolution of Fe-S clusters

Fe-S clusters are one of the oldest cofactors as it is accepted that these clusters originated during the first billion years of life when the earth's atmosphere was anaerobic and there was plenty of ferrous iron and sulfide present⁶⁴. In early earth, Fe atoms with inorganic sulfur were thought to self-assemble to form Fe-S clusters, which were possibly the first catalysts used in evolving organisms because of their versatile redox potential⁵⁴. Once atmospheric oxygen levels increased as photosynthetic life formed on earth^{64,65}, proteins that had Fe-S clusters as co-factors became sensitive to oxidative damage. In modern proteins, Fe-S clusters labile to oxygen release ferrous iron and depending on environmental oxygen levels can generate superoxide, hydrogen peroxide and hydroxyl radicals by Fenton chemistry⁶⁶. Further, superoxide and hydrogen peroxide can damage the dehydratase class of Fe-S enzymes and hydroxyl radicals can additionally damage various components of cellular machinery such as DNA, proteins, and lipids^{67,68}. To adapt to such oxidants, cells evolved protective mechanisms to avoid the destruction of Fe-S clusters and other macromolecules from these powerful oxidants⁶⁹. This involves regulating genes which encode enzymes that eliminate superoxide and hydrogen peroxide and Fe-S cluster biogenesis machinery to replace or repair Fe-S clusters damaged by oxygen or ROS⁷⁰⁻⁷⁴.

Organization of Fe-S cluster biogenesis in *E. coli* and *Z. mobilis*

There are three main types of Fe-S cluster biogenesis machineries in bacteria - ISC (iron-sulfur cluster), SUF (sulfur utilization factor), and NIF (Nitrogen-fixing)^{58,75,76}. In *E. coli*, *de novo* Fe-S cluster assembly is carried out by the ISC pathway, which is the housekeeping iron-sulfur cluster biogenesis pathway and the SUF pathway, which is functional under oxidative stress and

iron limitation conditions^{77,78}. The NIF system is found mainly in nitrogen-fixing bacteria and takes part in the assembly of the Fe-S clusters of nitrogenase that fixes nitrogen⁷⁹.

In *Z. mobilis*, the *isc* operon is not present. Rather housekeeping Fe-S biogenesis occurs by the SUF biogenesis pathway²⁹. Accordingly, the [4Fe-4S] cluster of IspG and IspH enzymes of the MEP pathway are predicted to be provided by the SUF pathway proteins. The NIF system is also present in *Z. mobilis* and is predicted to be involved in the biogenesis of Fe-S clusters required for nitrogen fixation as *Z. mobilis* is capable of fixing dinitrogen gas as a sole nitrogen source^{80,81}.

Fe-S clusters are incorporated into proteins by a process which requires three components: cysteine desulfurase enzyme, scaffold protein and carrier protein. The source of iron is not clear for any of the three Fe-S cluster biogenesis pathways; however, sulfur is provided for Fe-S cluster assembly from L-cysteine assisted by cysteine desulfurases. For assembly of Fe-S clusters, iron and sulfur are assembled on a scaffold protein. The delivery of Fe-S clusters into apo-protein targets occurs with the help of a carrier protein(s). Electrons are supplied for Fe-S cluster reduction by electron transfer proteins, which are also involved in the synthesis of Fe-S clusters^{82,83}.

The Isc pathway

In *E. coli*, the ISC pathway is the major housekeeping pathway in Fe-S biogenesis⁸⁴. The *isc* operon comprises *iscRSUA-hscBA-fdx-iscX*. The first gene in the *isc* operon is *iscR*, which encodes an Fe-S transcription factor and also regulates expression of the iron-sulfur biogenesis pathway. Adjacent to *iscR*, is *iscS* that encodes for the cysteine desulfurase, which supplies sulfur from the amino acid cysteine for Fe-S cluster biogenesis^{85,86}. The *iscS* gene is followed by *iscU*, which encodes the scaffold protein for Fe-S cluster assembly. The *hscB* and *hscA* genes encode for HscB and HscA, which are required by the scaffold protein to deliver Fe-S cluster to the target apo protein or through IscA, which is a carrier protein⁸⁷⁻⁹². The *fdx* gene encodes for a ferredoxin that transfers single electrons required for Fe-S cluster biogenesis⁹³. The *iscX* gene encodes for IscX, which appears to function as a regulator of IscS in order to convert cysteine to alanine and has also been suggested to provide iron for Fe-S cluster biosynthesis⁹⁴.

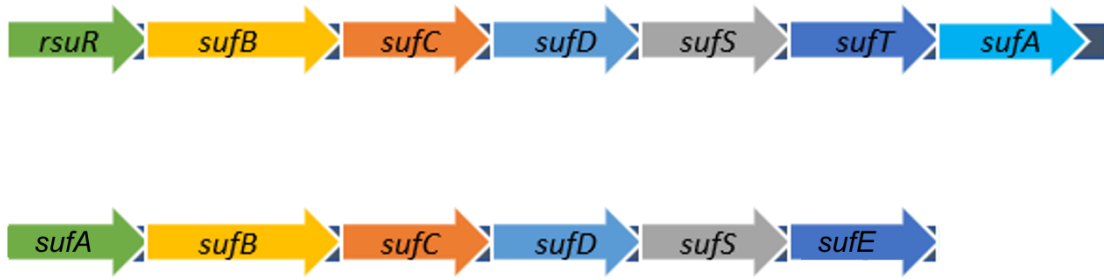
The Suf pathway

In *E. coli*, the *suf* operon comprises *sufABCDSE* and there is similarity in function between the Isc and Suf pathway proteins⁹⁵. The *sufA* gene encodes for SufA, which is a carrier protein similar to IscA in the *isc* operon⁹⁶. The *sufB* gene encodes for SufB, which is a scaffold protein along with SufC, which hydrolyzes ATP and SufD, which is a paralog of SufB⁹⁵. The cysteine desulfurase complex is formed from SufS and SufE, which provides sulfur from cysteine to the Fe-S cluster synthesized by SUF system^{97,98}.

In *Z. mobilis*, the *suf* operon comprises *sufBCDSTA* and *sufE* is present elsewhere in the genome. The first gene in the *suf* operon, ZMO0422, designated *rsuR*, is a homolog of the *E. coli* transcriptional regulator IscR that regulates Fe-S cluster biogenesis^{29,99}. RsuR is a dimeric protein which binds a [4Fe-4S] cluster and represses transcription of the *suf* operon under anaerobic conditions. However, RsuR cannot bind and repress the *suf* operon under aerobic condition as it lacks its [4Fe-4S] cluster due to oxidative damage. Thus, *suf* expression is derepressed under aerobic conditions in *Z. mobilis* as it is in *E. coli*. *sufBCDSA* is orthologous to *E. coli* proteins except *sufT* (Isabel Askenasy, Manuscript in preparation).

Figure 1-7: Organization of *suf* operon in *Z. mobilis* and *E. coli*

The *suf* operon in *Z. mobilis* (top panel) consist of *sufBCDSTA* and *sufE* is present elsewhere in the genome unlike *E. coli* *suf* operon (bottom panel) which consist of *sufABCDSE*. *IscR* regulates the expression of the *E. coli* *suf* operon while *RsuR* regulates the expression of *suf* operon in *Z. mobilis*.



IscR plays a key role in regulation of Isc and Suf pathway

In *E. coli*, IscR regulates the expression of the ISC and SUF Fe-S cluster biogenesis systems. Under anaerobic conditions as the turnover of Fe-S clusters is low, the demand for the biosynthesis of Fe-S clusters is low. Under these conditions, the [2Fe-2S] form of IscR (Holo-IscR) is present. [2Fe-2S] IscR binds and represses transcription of the *isc* operon, which in turn decreases the expression of IscR and Isc proteins. This regulates the levels of Fe-S cluster synthesis under anaerobic conditions^{85,100}.

Under oxidative stress and iron starvation conditions, holo-IscR^{100,101} shifts to apo-IscR causing upregulation of the ISC pathway as well increasing IscR levels as it is unable to repress the *isc* operon genes. Apo IscR also activates the *suf* operon genes causing an increase in the biosynthesis of the Fe-S clusters^{99,102-104}.

Fe-S cluster homeostasis

Both the ISC and SUF Fe-S cluster biogenesis machineries do show functional redundancy. However, the SUF pathway seems to takeover for the ISC pathway under stress conditions. This is supported by the fact that the two pathways are not always interchangeable^{85,105}. For example, the ISC pathway provides Fe-S cluster to [4Fe-4S] FNR (Fumarate nitrate reductase). However, in the absence of the ISC pathway, SUF can partially substitute⁷⁸. Thus, by using two Fe-S cluster biosynthesis pathways, *E. coli* is able to maintain Fe-S cluster homeostasis both under aerobic and anaerobic conditions. *E. coli* is viable if either the *isc* or the *suf* operon genes are deleted. However, deletion of both the operons causes lethality^{75,99}. This is due to *ispH* and *ispG*,

which are essential genes. Without any iron-sulfur cluster biosynthesis, the proteins become non-functional causing lethality^{50,106-109}.

In my thesis, I test and compare the function of IspG and IspH from *Z. mobilis* and *E. coli* under aerobic and anaerobic conditions using the eukaryotic mevalonic acid pathway as an alternative isoprenoid producing pathway. I also test the stability of [4Fe-4S] cluster of IspG and IspH under aerobic conditions from *Z. mobilis*. As *Z. mobilis* IspG improves the function of IspH in *E. coli*, I also tested the formation of higher order complex between IspG and IspH.

REFERENCES

1. Chang WC, Song H, Liu HW, Liu P. Current development in isoprenoid precursor biosynthesis and regulation. *Curr Opin Chem Biol.* 2013;17(4):571-579.
2. Lichtenthaler HK. The 1-Deoxy-D-Xylulose-5-Phosphate Pathway of Isoprenoid Biosynthesis in Plants. *Annu Rev Plant Physiol Plant Mol Biol.* 1999;50:47-65.
3. Vickers CE, Gershenzon J, Lerdau MT, Loreto F. A unified mechanism of action for volatile isoprenoids in plant abiotic stress. *Nat Chem Biol.* 2009;5(5):283-291.
4. Penuelas J, Munne-Bosch S. Isoprenoids: an evolutionary pool for photoprotection. *Trends Plant Sci.* 2005;10(4):166-169.
5. Tetali SD. Terpenes and isoprenoids: a wealth of compounds for global use. *Planta.* 2019;249(1):1-8.
6. Holstein SA, Hohl RJ. Isoprenoids: remarkable diversity of form and function. *Lipids.* 2004;39(4):293-309.
7. Withers ST, Keasling JD. Biosynthesis and engineering of isoprenoid small molecules. *Appl Microbiol Biotechnol.* 2007;73(5):980-990.
8. Navale GR, Dharne MS, Shinde SS. Metabolic engineering and synthetic biology for isoprenoid production in *Escherichia coli* and *Saccharomyces cerevisiae*. *Appl Microbiol Biotechnol.* 2021;105(2):457-475.
9. Nowicka B, Kruk J. Occurrence, biosynthesis and function of isoprenoid quinones. *Biochim Biophys Acta.* 2010;1797(9):1587-1605.
10. Boronat A, Rodriguez-Concepcion M. Terpenoid biosynthesis in prokaryotes. *Adv Biochem Eng Biotechnol.* 2015;148:3-18.

11. Rohmer M. The discovery of a mevalonate-independent pathway for isoprenoid biosynthesis in bacteria, algae and higher plants. *Nat Prod Rep.* 1999;16(5):565-574.
12. Eisenreich W, Bacher A, Arigoni D, Rohdich F. Biosynthesis of isoprenoids via the non-mevalonate pathway. *Cell Mol Life Sci.* 2004;61(12):1401-1426.
13. Zhao L, Chang WC, Xiao Y, Liu HW, Liu P. Methylerythritol phosphate pathway of isoprenoid biosynthesis. *Annu Rev Biochem.* 2013;82:497-530.
14. Rohmer M, Knani M, Simonin P, Sutter B, Sahm H. Isoprenoid biosynthesis in bacteria: a novel pathway for the early steps leading to isopentenyl diphosphate. *Biochem J.* 1993;295 (Pt 2)(Pt 2):517-524.
15. Wang C, Zada B, Wei G, Kim SW. Metabolic engineering and synthetic biology approaches driving isoprenoid production in *Escherichia coli*. *Bioresour Technol.* 2017;241:430-438.
16. Lv X, Xu H, Yu H. Significantly enhanced production of isoprene by ordered coexpression of genes *dxs*, *dxr*, and *idi* in *Escherichia coli*. *Appl Microbiol Biotechnol.* 2013;97(6):2357-2365.
17. Farhi M, Marhevka E, Masci T, et al. Harnessing yeast subcellular compartments for the production of plant terpenoids. *Metab Eng.* 2011;13(5):474-481.
18. Swings J, De Ley J. The biology of *Zymomonas*. *Bacteriol Rev.* 1977;41(1):1-46.
19. He MX, Wu B, Qin H, et al. *Zymomonas mobilis*: a novel platform for future biorefineries. *Biotechnol Biofuels.* 2014;7:101.
20. Hermans MA, Neuss B, Sahm H. Content and composition of hopanoids in *Zymomonas mobilis* under various growth conditions. *J Bacteriol.* 1991;173(17):5592-5595.

21. Martien JI, Amador-Noguez D. Recent applications of metabolomics to advance microbial biofuel production. *Curr Opin Biotechnol.* 2017;43:118-126.
22. Somerville C, Youngs H, Taylor C, Davis SC, Long SP. Feedstocks for lignocellulosic biofuels. *Science.* 2010;329(5993):790-792.
23. Youngs H, Somerville C. Development of feedstocks for cellulosic biofuels. *F1000 Biol Rep.* 2012;4:10.
24. Yang S, Tschaplinski TJ, Engle NL, et al. Transcriptomic and metabolomic profiling of *Zymomonas mobilis* during aerobic and anaerobic fermentations. *BMC Genomics.* 2009;10:34.
25. Yang S, Land ML, Klingeman DM, et al. Paradigm for industrial strain improvement identifies sodium acetate tolerance loci in *Zymomonas mobilis* and *Saccharomyces cerevisiae*. *Proc Natl Acad Sci U S A.* 2010;107(23):10395-10400.
26. Yang S, Pan C, Tschaplinski TJ, et al. Systems biology analysis of *Zymomonas mobilis* ZM4 ethanol stress responses. *PLoS One.* 2013;8(7):e68886.
27. Jeon YJ, Xun Z, Su P, Rogers PL. Genome-wide transcriptomic analysis of a flocculent strain of *Zymomonas mobilis*. *Appl Microbiol Biotechnol.* 2012;93(6):2513-2518.
28. Skerker JM, Leon D, Price MN, et al. Dissecting a complex chemical stress: chemogenomic profiling of plant hydrolysates. *Mol Syst Biol.* 2013;9:674.
29. Martien JI, Hebert AS, Stevenson DM, et al. Systems-Level Analysis of Oxygen Exposure in *Zymomonas mobilis*: Implications for Isoprenoid Production. *mSystems.* 2019;4(1).

30. Khana DB, Tatli M, Rivera Vazquez J, et al. Systematic Analysis of Metabolic Bottlenecks in the Methylerythritol 4-Phosphate (MEP) Pathway of *Zymomonas mobilis*. *mSystems*. 2023;8(2):e0009223.
31. Lee M, Grawert T, Quitterer F, et al. Biosynthesis of isoprenoids: crystal structure of the [4Fe-4S] cluster protein IspG. *J Mol Biol*. 2010;404(4):600-610.
32. Rekittke I, Nonaka T, Wiesner J, et al. Structure of the E-1-hydroxy-2-methyl-but-2-enyl-4-diphosphate synthase (GcpE) from *Thermus thermophilus*. *FEBS Lett*. 2011;585(3):447-451.
33. Rekittke I, Jomaa H, Ermler U. Structure of the GcpE (IspG)-MEcPP complex from *Thermus thermophilus*. *FEBS Lett*. 2012;586(19):3452-3457.
34. Quitterer F, Frank A, Wang K, et al. Atomic-Resolution Structures of Discrete Stages on the Reaction Coordinate of the [Fe₄S₄] Enzyme IspG (GcpE). *J Mol Biol*. 2015;427(12):2220-2228.
35. Liu YL, Guerra F, Wang K, et al. Structure, function and inhibition of the two- and three-domain 4Fe-4S IspG proteins. *Proc Natl Acad Sci U S A*. 2012;109(22):8558-8563.
36. Okada K, Hase T. Cyanobacterial non-mevalonate pathway: (E)-4-hydroxy-3-methylbut-2-enyl diphosphate synthase interacts with ferredoxin in *Thermosynechococcus elongatus* BP-1. *J Biol Chem*. 2005;280(21):20672-20679.
37. Wang W, Oldfield E. Bioorganometallic chemistry with IspG and IspH: structure, function, and inhibition of the [Fe(4)S(4)] proteins involved in isoprenoid biosynthesis. *Angew Chem Int Ed Engl*. 2014;53(17):4294-4310.

38. Puan KJ, Wang H, Dairi T, Kuzuyama T, Morita CT. fldA is an essential gene required in the 2-C-methyl-D-erythritol 4-phosphate pathway for isoprenoid biosynthesis. *FEBS Lett.* 2005;579(17):3802-3806.
39. Seemann M, Tse Sum Bui B, Wolff M, Miginiac-Maslow M, Rohmer M. Isoprenoid biosynthesis in plant chloroplasts via the MEP pathway: direct thylakoid/ferredoxin-dependent photoreduction of GcpE/IspG. *FEBS Lett.* 2006;580(6):1547-1552.
40. Wang W, Li J, Wang K, Huang C, Zhang Y, Oldfield E. Organometallic mechanism of action and inhibition of the 4Fe-4S isoprenoid biosynthesis protein GcpE (IspG). *Proc Natl Acad Sci U S A.* 2010;107(25):11189-11193.
41. Reikittke I, Wiesner J, Rohrich R, et al. Structure of (E)-4-hydroxy-3-methyl-but-2-enyl diphosphate reductase, the terminal enzyme of the non-mevalonate pathway. *J Am Chem Soc.* 2008;130(51):17206-17207.
42. Grawert T, Rohdich F, Span I, et al. Structure of active IspH enzyme from Escherichia coli provides mechanistic insights into substrate reduction. *Angew Chem Int Ed Engl.* 2009;48(31):5756-5759.
43. Reikittke I, Olkhova E, Wiesner J, et al. Structure of the (E)-4-hydroxy-3-methyl-but-2-enyl-diphosphate reductase from Plasmodium falciparum. *FEBS Lett.* 2013;587(24):3968-3972.
44. Krissinel E, Henrick K. Inference of macromolecular assemblies from crystalline state. *J Mol Biol.* 2007;372(3):774-797.
45. Beinert H, Kennedy MC, Stout CD. Aconitase as Iron-Regulatory Protein, Enzyme, and Iron-Regulatory Protein. *Chem Rev.* 1996;96(7):2335-2374.

46. Grawert T, Span I, Eisenreich W, et al. Probing the reaction mechanism of IspH protein by x-ray structure analysis. *Proc Natl Acad Sci U S A*. 2010;107(3):1077-1081.
47. Rao G, Oldfield E. Structure and Function of Four Classes of the 4Fe-4S Protein, IspH. *Biochemistry*. 2016;55(29):4119-4129.
48. Span I, Wang K, Wang W, et al. Discovery of acetylene hydratase activity of the iron-sulphur protein IspH. *Nat Commun*. 2012;3:1042.
49. Wang W, Wang K, Span I, et al. Are free radicals involved in IspH catalysis? An EPR and crystallographic investigation. *J Am Chem Soc*. 2012;134(27):11225-11234.
50. Wolff M, Seemann M, Tse Sum Bui B, et al. Isoprenoid biosynthesis via the methylerythritol phosphate pathway: the (E)-4-hydroxy-3-methylbut-2-enyl diphosphate reductase (LytB/IspH) from *Escherichia coli* is a [4Fe-4S] protein. *FEBS Lett*. 2003;541(1-3):115-120.
51. Ge D, Xue Y, Ma Y. Two unexpected promiscuous activities of the iron-sulfur protein IspH in production of isoprene and isoamylene. *Microb Cell Fact*. 2016;15:79.
52. Chaignon P, Petit BE, Vincent B, Allouche L, Seemann M. Methylerythritol Phosphate Pathway: Enzymatic Evidence for a Rotation in the LytB/IspH-Catalyzed Reaction. *Chemistry*. 2020;26(5):1032-1036.
53. Fontecave M. Iron-sulfur clusters: ever-expanding roles. *Nat Chem Biol*. 2006;2(4):171-174.
54. Beinert H. Iron-sulfur proteins: ancient structures, still full of surprises. *J Biol Inorg Chem*. 2000;5(1):2-15.
55. Beinert H, Holm RH, Munck E. Iron-sulfur clusters: nature's modular, multipurpose structures. *Science*. 1997;277(5326):653-659.

56. Meyer J. Iron-sulfur protein folds, iron-sulfur chemistry, and evolution. *J Biol Inorg Chem.* 2008;13(2):157-170.
57. Lill R. Function and biogenesis of iron-sulphur proteins. *Nature.* 2009;460(7257):831-838.
58. Johnson DC, Dean DR, Smith AD, Johnson MK. Structure, function, and formation of biological iron-sulfur clusters. *Annu Rev Biochem.* 2005;74:247-281.
59. Yoch DC, Carithers RP. Bacterial iron-sulfur proteins. *Microbiol Rev.* 1979;43(3):384-421.
60. Porello SL, Cannon MJ, David SS. A substrate recognition role for the [4Fe-4S]₂₊ cluster of the DNA repair glycosylase MutY. *Biochemistry.* 1998;37(18):6465-6475.
61. Fuss JO, Tsai CL, Ishida JP, Tainer JA. Emerging critical roles of Fe-S clusters in DNA replication and repair. *Biochim Biophys Acta.* 2015;1853(6):1253-1271.
62. Cunningham RP, Asahara H, Bank JF, et al. Endonuclease III is an iron-sulfur protein. *Biochemistry.* 1989;28(10):4450-4455.
63. Campbell IJ, Bennett GN, Silberg JJ. Evolutionary Relationships Between Low Potential Ferredoxin and Flavodoxin Electron Carriers. *Front Energy Res.* 2019;7.
64. Imlay JA. Iron-sulphur clusters and the problem with oxygen. *Mol Microbiol.* 2006;59(4):1073-1082.
65. Flint DH, Tuminello JF, Emptage MH. The inactivation of Fe-S cluster containing hydrolyases by superoxide. *J Biol Chem.* 1993;268(30):22369-22376.
66. Wardman P, Candeias LP. Fenton chemistry: an introduction. *Radiat Res.* 1996;145(5):523-531.
67. Imlay JA. Pathways of oxidative damage. *Annu Rev Microbiol.* 2003;57:395-418.

68. Cabiscol E, Tamarit J, Ros J. Oxidative stress in bacteria and protein damage by reactive oxygen species. *Int Microbiol.* 2000;3(1):3-8.
69. Venkateswara Rao P, Holm RH. Synthetic analogues of the active sites of iron-sulfur proteins. *Chem Rev.* 2004;104(2):527-559.
70. Imlay JA. Cellular defenses against superoxide and hydrogen peroxide. *Annu Rev Biochem.* 2008;77:755-776.
71. Imlay JA. The molecular mechanisms and physiological consequences of oxidative stress: lessons from a model bacterium. *Nat Rev Microbiol.* 2013;11(7):443-454.
72. Crack JC, Green J, Hutchings MI, Thomson AJ, Le Brun NE. Bacterial iron-sulfur regulatory proteins as biological sensor-switches. *Antioxid Redox Signal.* 2012;17(9):1215-1231.
73. Fleischhacker AS, Kiley PJ. Iron-containing transcription factors and their roles as sensors. *Curr Opin Chem Biol.* 2011;15(2):335-341.
74. Crack JC, Green J, Thomson AJ, Le Brun NE. Iron-sulfur cluster sensor-regulators. *Curr Opin Chem Biol.* 2012;16(1-2):35-44.
75. Takahashi Y, Tokumoto U. A third bacterial system for the assembly of iron-sulfur clusters with homologs in archaea and plastids. *J Biol Chem.* 2002;277(32):28380-28383.
76. Zheng L, Cash VL, Flint DH, Dean DR. Assembly of iron-sulfur clusters. Identification of an iscSUA-hscBA-fdx gene cluster from *Azotobacter vinelandii*. *J Biol Chem.* 1998;273(21):13264-13272.
77. Outten FW, Djaman O, Storz G. A suf operon requirement for Fe-S cluster assembly during iron starvation in *Escherichia coli*. *Mol Microbiol.* 2004;52(3):861-872.

78. Mettert EL, Outten FW, Wanta B, Kiley PJ. The impact of O₂ on the Fe-S cluster biogenesis requirements of *Escherichia coli* FNR. *J Mol Biol.* 2008;384(4):798-811.
79. Johnson DC, Dos Santos PC, Dean DR. NifU and NifS are required for the maturation of nitrogenase and cannot replace the function of isc-gene products in *Azotobacter vinelandii*. *Biochem Soc Trans.* 2005;33(Pt 1):90-93.
80. Kremer TA, LaSarre B, Posto AL, McKinlay JB. N₂ gas is an effective fertilizer for bioethanol production by *Zymomonas mobilis*. *Proc Natl Acad Sci U S A.* 2015;112(7):2222-2226.
81. Martien JI, Trujillo EA, Jacobson TB, et al. Metabolic Remodeling during Nitrogen Fixation in *Zymomonas mobilis*. *mSystems.* 2021;6(6):e0098721.
82. Loiseau L, Gerez C, Bekker M, et al. ErpA, an iron sulfur (Fe S) protein of the A-type essential for respiratory metabolism in *Escherichia coli*. *Proc Natl Acad Sci U S A.* 2007;104(34):13626-13631.
83. Py B, Gerez C, Huguenot A, et al. The ErpA/NfuA complex builds an oxidation-resistant Fe-S cluster delivery pathway. *J Biol Chem.* 2018;293(20):7689-7702.
84. Blanc B, Gerez C, Ollagnier de Choudens S. Assembly of Fe/S proteins in bacterial systems: Biochemistry of the bacterial ISC system. *Biochim Biophys Acta.* 2015;1853(6):1436-1447.
85. Schwartz CJ, Giel JL, Patschkowski T, et al. IscR, an Fe-S cluster-containing transcription factor, represses expression of *Escherichia coli* genes encoding Fe-S cluster assembly proteins. *Proc Natl Acad Sci U S A.* 2001;98(26):14895-14900.

86. Mihara H, Kurihara T, Yoshimura T, Esaki N. Kinetic and mutational studies of three NifS homologs from *Escherichia coli*: mechanistic difference between L-cysteine desulfurase and L-selenocysteine lyase reactions. *J Biochem.* 2000;127(4):559-567.
87. Agar JN, Krebs C, Frazzon J, Huynh BH, Dean DR, Johnson MK. IscU as a scaffold for iron-sulfur cluster biosynthesis: sequential assembly of [2Fe-2S] and [4Fe-4S] clusters in IscU. *Biochemistry.* 2000;39(27):7856-7862.
88. Raulfs EC, O'Carroll IP, Dos Santos PC, Unciuleac MC, Dean DR. In vivo iron-sulfur cluster formation. *Proc Natl Acad Sci U S A.* 2008;105(25):8591-8596.
89. Chandramouli K, Johnson MK. HscA and HscB stimulate [2Fe-2S] cluster transfer from IscU to apoferredoxin in an ATP-dependent reaction. *Biochemistry.* 2006;45(37):11087-11095.
90. Silberg JJ, Hoff KG, Tapley TL, Vickery LE. The Fe/S assembly protein IscU behaves as a substrate for the molecular chaperone Hsc66 from *Escherichia coli*. *J Biol Chem.* 2001;276(3):1696-1700.
91. Vinella D, Brochier-Armanet C, Loiseau L, Talla E, Barras F. Iron-sulfur (Fe/S) protein biogenesis: phylogenomic and genetic studies of A-type carriers. *PLoS Genet.* 2009;5(5):e1000497.
92. Vinella D, Loiseau L, Ollagnier de Choudens S, Fontecave M, Barras F. In vivo [Fe-S] cluster acquisition by IscR and NsrR, two stress regulators in *Escherichia coli*. *Mol Microbiol.* 2013;87(3):493-508.
93. Chandramouli K, Unciuleac MC, Naik S, Dean DR, Huynh BH, Johnson MK. Formation and properties of [4Fe-4S] clusters on the IscU scaffold protein. *Biochemistry.* 2007;46(23):6804-6811.

94. Kim JH, Bothe JR, Frederick RO, Holder JC, Markley JL. Role of IscX in iron-sulfur cluster biogenesis in *Escherichia coli*. *J Am Chem Soc.* 2014;136(22):7933-7942.
95. Perard J, Ollagnier de Choudens S. Iron-sulfur clusters biogenesis by the SUF machinery: close to the molecular mechanism understanding. *J Biol Inorg Chem.* 2018;23(4):581-596.
96. Gupta V, Sendra M, Naik SG, et al. Native *Escherichia coli* SufA, coexpressed with SufBCDSE, purifies as a [2Fe-2S] protein and acts as an Fe-S transporter to Fe-S target enzymes. *J Am Chem Soc.* 2009;131(17):6149-6153.
97. Outten FW, Wood MJ, Munoz FM, Storz G. The SufE protein and the SufBCD complex enhance SufS cysteine desulfurase activity as part of a sulfur transfer pathway for Fe-S cluster assembly in *Escherichia coli*. *J Biol Chem.* 2003;278(46):45713-45719.
98. Loiseau L, Ollagnier-de-Choudens S, Nachin L, Fontecave M, Barras F. Biogenesis of Fe-S cluster by the bacterial Suf system: SufS and SufE form a new type of cysteine desulfurase. *J Biol Chem.* 2003;278(40):38352-38359.
99. Mettert EL, Kiley PJ. Coordinate regulation of the Suf and Isc Fe-S cluster biogenesis pathways by IscR is essential for viability of *Escherichia coli*. *J Bacteriol.* 2014;196(24):4315-4323.
100. Giel JL, Nesbit AD, Mettert EL, Fleischhacker AS, Wanta BT, Kiley PJ. Regulation of iron-sulphur cluster homeostasis through transcriptional control of the Isc pathway by [2Fe-2S]-IscR in *Escherichia coli*. *Mol Microbiol.* 2013;87(3):478-492.
101. Desnoyers G, Morissette A, Prevost K, Masse E. Small RNA-induced differential degradation of the polycistronic mRNA *iscRSUA*. *EMBO J.* 2009;28(11):1551-1561.

102. Lee KC, Yeo WS, Roe JH. Oxidant-responsive induction of the suf operon, encoding a Fe-S assembly system, through Fur and IscR in *Escherichia coli*. *J Bacteriol.* 2008;190(24):8244-8247.
103. Yeo WS, Lee JH, Lee KC, Roe JH. IscR acts as an activator in response to oxidative stress for the suf operon encoding Fe-S assembly proteins. *Mol Microbiol.* 2006;61(1):206-218.
104. Lee JH, Yeo WS, Roe JH. Induction of the sufA operon encoding Fe-S assembly proteins by superoxide generators and hydrogen peroxide: involvement of OxyR, IHF and an unidentified oxidant-responsive factor. *Mol Microbiol.* 2004;51(6):1745-1755.
105. Jang S, Imlay JA. Hydrogen peroxide inactivates the *Escherichia coli* Isc iron-sulphur assembly system, and OxyR induces the Suf system to compensate. *Mol Microbiol.* 2010;78(6):1448-1467.
106. Grawert T, Kaiser J, Zepeck F, et al. IspH protein of *Escherichia coli*: studies on iron-sulfur cluster implementation and catalysis. *J Am Chem Soc.* 2004;126(40):12847-12855.
107. Tanaka N, Kanazawa M, Tonosaki K, Yokoyama N, Kuzuyama T, Takahashi Y. Novel features of the ISC machinery revealed by characterization of *Escherichia coli* mutants that survive without iron-sulfur clusters. *Mol Microbiol.* 2016;99(5):835-848.
108. Trotter V, Vinella D, Loiseau L, Ollagnier de Choudens S, Fontecave M, Barras F. The CsdA cysteine desulphurase promotes Fe/S biogenesis by recruiting Suf components and participates to a new sulphur transfer pathway by recruiting CsdL (ex-YgdL), a ubiquitin-modifying-like protein. *Mol Microbiol.* 2009;74(6):1527-1542.

109. Xiao Y, Zahariou G, Sanakis Y, Liu P. IspG enzyme activity in the deoxyxylulose phosphate pathway: roles of the iron-sulfur cluster. *Biochemistry*. 2009;48(44):10483-10485.

CHAPTER 2

Functional differences between the *Escherichia coli* and *Zymomonas mobilis* enzymes that catalyze the terminal steps of the methylerythritol phosphate pathway

Jyotsna Misra and Patricia J Kiley

A version of this manuscript will be submitted for publication

I performed all the experiments described here. Erin Mettert made the strains

ABSTRACT

Isoprenoids are a diverse family of compounds that are synthesized from two isomeric compounds, isopentenyl diphosphate (IDP) and dimethylallyl diphosphate (DMADP), which in most bacteria are produced from the essential methylerythritol phosphate pathway. The last two enzymes of this pathway, IspG and IspH, are [4Fe-4S] cluster proteins and in *Zymomonas mobilis*, the intermediates, MEcDP and HMBDP, accumulate in cells in response to O₂ suggesting lability of the IspG and IspH Fe-S clusters. Here we show using complementation assays in *Escherichia coli* that even under anaerobic conditions, *Z. mobilis* IspG and IspH are not as functional as their *E. coli* counterparts, requiring higher levels of expression to rescue viability. A deficit of the SUF Fe-S cluster biogenesis pathway did not explain the inefficient *Z. mobilis* IspH and IspG complementation since no improvement was observed in *E. coli* strains expressing the *Z. mobilis* SUF Fe-S cluster biogenesis pathway or having increased expression of the *E. coli* SUF pathway. Complementation of single and double mutants with various combinations of *Z. mobilis* and *E. coli* IspG and IspH indicated that optimal growth required the pairing of IspG and IspH from the same species, although no evidence was found for complex formation between the two proteins. Further, *Z. mobilis* IspH conferred a severe O₂ sensitive growth defect to *E. coli* that could be partially rescued by co-expression of *Z. mobilis* IspG. In vitro analysis confirmed the O₂ sensitivity of the [4Fe-4S] cluster of both *Z. mobilis* IspG and IspH. Taken together, our data indicate the important role of the cognate protein IspG in improving the function of *Z. mobilis* IspH under both aerobic and anaerobic conditions.

INTRODUCTION

Isoprenoids comprise a chemically diverse family of natural products that have various functions throughout the biological world¹⁻³. Isoprenoids also have commercial value because of their use as colorants, flavoring agents, vitamins, fragrances, and their potential to be used as alternative fuel sources^{4,5}. Isoprenoid precursors, isopentenyl diphosphate (IDP) and dimethylallyl diphosphate (DMADP), are synthesized from one of two conserved pathways. The methylerythritol phosphate (MEP) pathway is found in eubacteria, green algae and plant plastids⁶ while the mevalonate (MVA) pathway is found in *Streptomyces*, Archaea, plant cytosol and other eukaryotes. Recent studies have focused on the MEP pathway as a possible platform for engineering of isoprenoid compounds⁷.

Studies of *Zymomonas mobilis*, a Gram-negative, alpha-proteobacterium are providing new insights into the control of flux through the MEP pathway that may prove useful in expanding use of this ethanol producing organism for production of isoprenoid-based biofuels. *Z. mobilis* naturally makes large amounts of hopanoids, a class of isoprenoids⁸, and converts 96% of glucose to ethanol by the Entner-Doudoroff glycolytic pathway under anaerobic conditions⁹. Thus, *Z. mobilis* is an excellent microbe for engineering the MEP pathway because of its streamlined catabolism and because of the potential to redeploy more carbon from glucose to optimize IDP and DMADP production¹⁰.

The last two steps of the MEP pathway require the enzymes IspG and IspH and these have been identified as key metabolic bottlenecks in *Z. mobilis* overexpression studies¹¹. Mechanistic studies of these enzymes from various sources indicate that IspG catalyzes the

reductive ring opening of 2-C-methyl-D-erythritol 2,4-cyclodiphosphate (MEcDP) to 4-hydroxy-3-methyl-but-2-enyl diphosphate (HMBDP). The structure of IspG from *T. thermophilus* and *A. aeolicus* reveals the protein is a dimer, with each monomer coordinating an [4Fe-4S] cluster via a Glu and three Cys residues^{12,13}. In contrast, IspH from *E. coli* is a monomer coordinating the [4Fe-4S] cluster via three Cys residues and the substrate HMBDP^{14,15}. The reduced cluster promotes the reductive dehydroxylation of HMBDP, generating the isomers IDP and DMADP. However, in its reduced [4Fe-4S]¹⁺ state, IspH from *Bacillus* sp. N16-5 also catalyzes the promiscuous conversion of HMBDP to isoprene and DMADP to isoamylene¹⁶. In contrast, in its oxidized [4Fe-4S]²⁺ state, *E. coli* IspH has also been shown to have a promiscuous activity that catalyzes the conversion of acetylenes to ketones and aldehydes via an acetylene hydratase activity¹⁷. These data suggest that Fe-S cluster redox state is one feature that influences optimal metabolic flux through this pathway.

The Fe-S clusters of these enzymes are generally considered to be O₂ sensitive since anaerobic conditions are required for isolation of active enzyme^{18,19}. Indeed, when *Z. mobilis* was shifted from anaerobic to aerobic growth conditions, the substrates of IspG and IspH, MEcDP and HMBDP, respectively, accumulate transiently suggesting that the Fe-S clusters of *Z. mobilis* IspG and IspH are also labile to O₂. The *suf* operon, encoding the sole Fe-S biogenesis pathway of *Z. mobilis*, was also upregulated in response to O₂ suggesting an increase in demand for Fe-S cluster biogenesis perhaps to replace or repair O₂ damaged enzymes²⁰. In recent work in *E. coli*, the role of heterologous Fe-S biogenesis pathways was investigated and shown to be important in the function of several types of Fe-S cluster enzymes from analogous sources²¹. Taken together, these observations suggest that cluster occupancy may also be limiting metabolic flux of the MEP pathway in some circumstances.

Here, we investigate the function of *Z. mobilis* IspG and IspH in *E. coli*, taking advantage of established genetic tools to study MEP pathway function, which is essential for viability. Previous studies suggest that the [4Fe-4S] cluster of *Z. mobilis* IspG and IspH could be sensitive to oxygen and insufficient levels impede metabolic flux²⁰, highlighting the importance of IspG and IspH enzymes in engineering the MEP pathway in *Z. mobilis* to make more isoprenoids. By comparing the function of *Z. mobilis* IspG and IspH to *E. coli* orthologs under aerobic and anaerobic conditions, we define several features of *Z. mobilis* IspG and IspH that may limit its activity in cells. These results also indicate that this genetic approach provides an experimentally tractable system for interrogating *Z. mobilis* IspG and IspH function, which will guide future engineering of the MEP pathway in *Z. mobilis*.

RESULTS

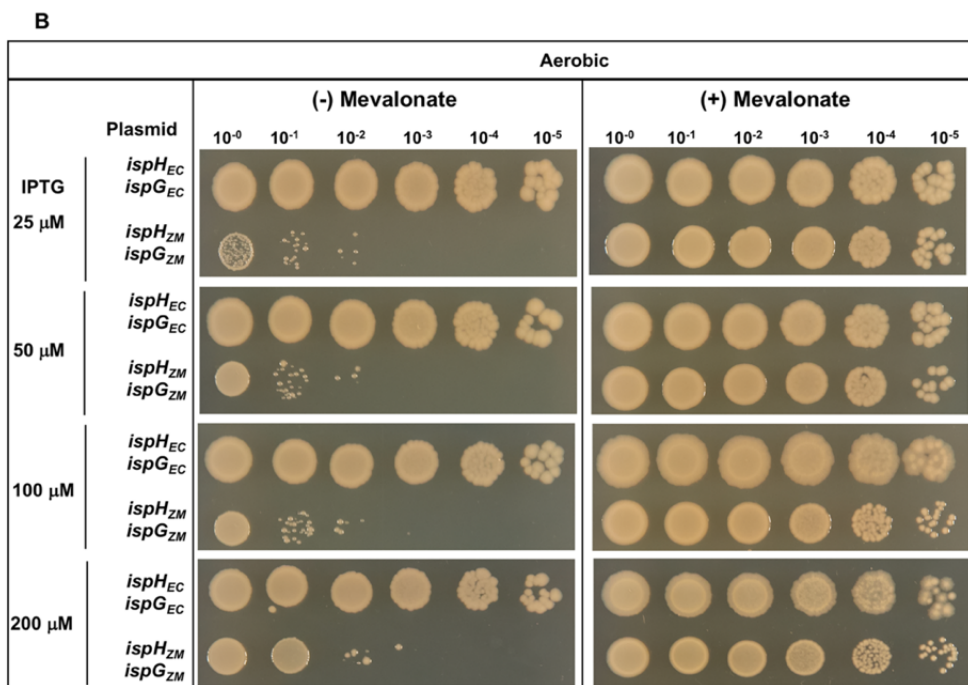
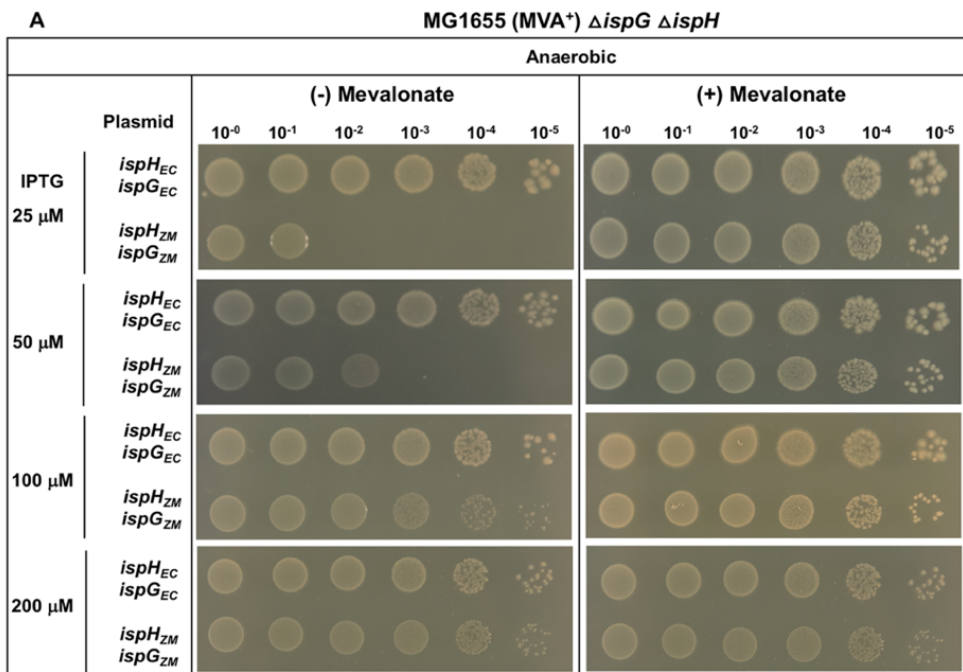
***Z. mobilis* IspG and IspH partially complement an *E. coli* mutant lacking the analogous proteins under anaerobic conditions**

The function of IspG and IspH from *Z. mobilis* was compared to analogous proteins from *E. coli* using an *E. coli* strain deleted for chromosomal *ispG* and *ispH*, but containing a gene cassette that maintains viability by conditional production of isoprenoids from the eukaryotic mevalonic acid pathway (MVA⁺) when supplied with mevalonate. Expression of plasmid encoded *ispG* and *ispH* for comparison of *Z. mobilis* to *E. coli* proteins was controlled by an IPTG inducible promoter. Complementation of MG1655 Δ *ispG* Δ *ispH* (MVA⁺) with indicated plasmids was assayed by plating serial dilutions of liquid cultures grown under permissive conditions (with mevalonate) onto solid media with or without mevalonate under anaerobic conditions at the indicated IPTG concentrations (Figure 1A). *E. coli* *ispG* and *ispH* fully rescued growth of this strain over a range of IPTG concentrations (0, 25 μ M, 50 μ M, 100 μ M, 200 μ M) since the number and size of the colonies was similar at the highest dilution tested (10^{-5}) whether or not mevalonate was present. Indeed, even in the absence of IPTG, sufficient IspH and IspG are produced to complement the mutant (Fig. S1). In contrast, *Z. mobilis* *ispG* and *ispH* were unable to fully complement the mutant phenotype at 0, 25 and 50 μ M IPTG as growth was not observed beyond the 10^{-2} dilution in the absence of mevalonate, in contrast to the robust growth observed with mevalonate. Growth at the 10^{-1} dilution is the sensitivity limit of this assay and likely represents dilution of the preexisting pool of mevalonate and mevalonate pathway components, since we routinely observe growth up to the 10^{-1} dilution with the plasmid vector alone (Figure S1). At 100 and 200 μ M IPTG induction, colonies were observed with *Z. mobilis* *ispG* and *ispH* at the 10^{-5} dilution similar to *E. coli*. However, the size of the colonies was smaller in the absence of

mevalonate than with mevalonate and smaller than those produced by *E. coli ispG* and *ispH*. These results indicate that *Z. mobilis* IspG and IspH function to produce isoprenoid precursors in *E. coli*, although less efficiently than their *E. coli* counterparts.

Figure 2-1 Viability of MG1655 (MVA⁺) Δ *ispG* Δ *ispH* with plasmid variants

MG1655 (MVA⁺) Δ *ispG* Δ *ispH* with plasmid variants containing *ispG* and *ispH* from either *Z. mobilis* (*ispH_{ZM} ispG_{ZM}*) or *E. coli* (*ispH_{EC} ispG_{EC}*) were grown in LB with mevalonate, arabinose and spectinomycin. After 16 hours of overnight growth, bacteria were washed with LB to remove mevalonate and were normalized to OD₆₀₀ 1. The bacteria were then diluted in LB and 5 μ l was used from each dilution tube to spot on solid TYE media with and without mevalonate (1mM) containing the indicated concentrations of IPTG (25 μ M, 50 μ M, 100 μ M or 200 μ M) to induce *ispG* and *ispH* co-expression with or without mevalonate (1mM). The agar plates were then incubated at 37°C overnight either under aerobic or anaerobic conditions.

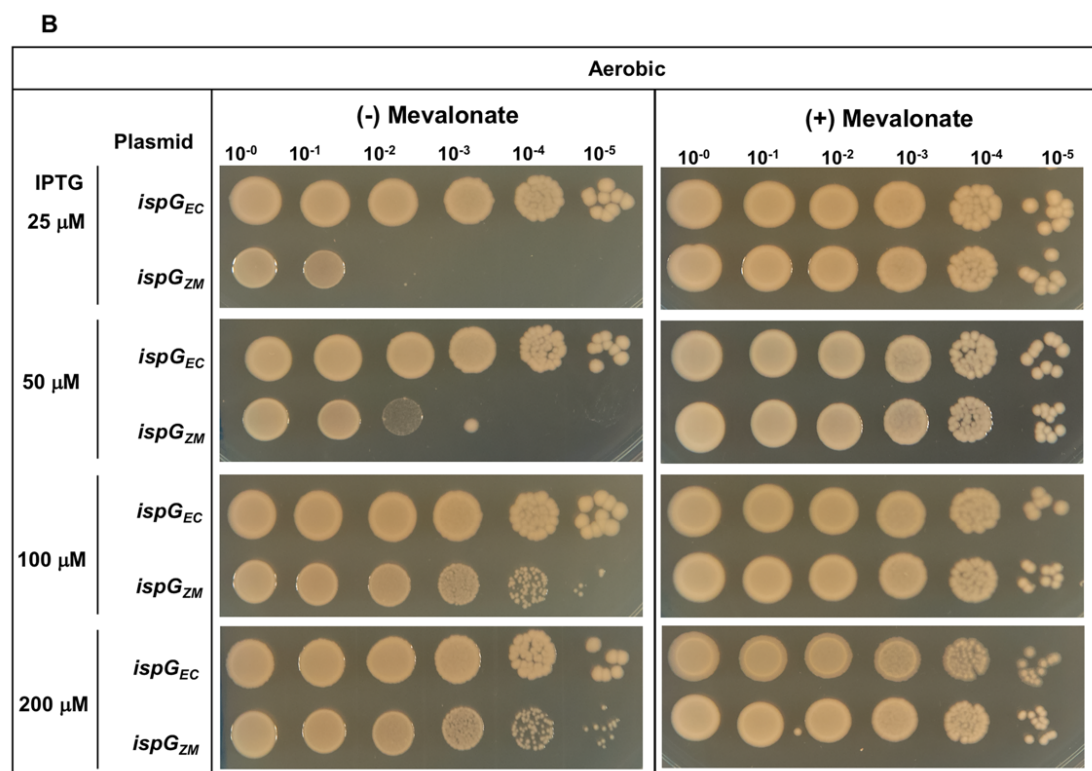
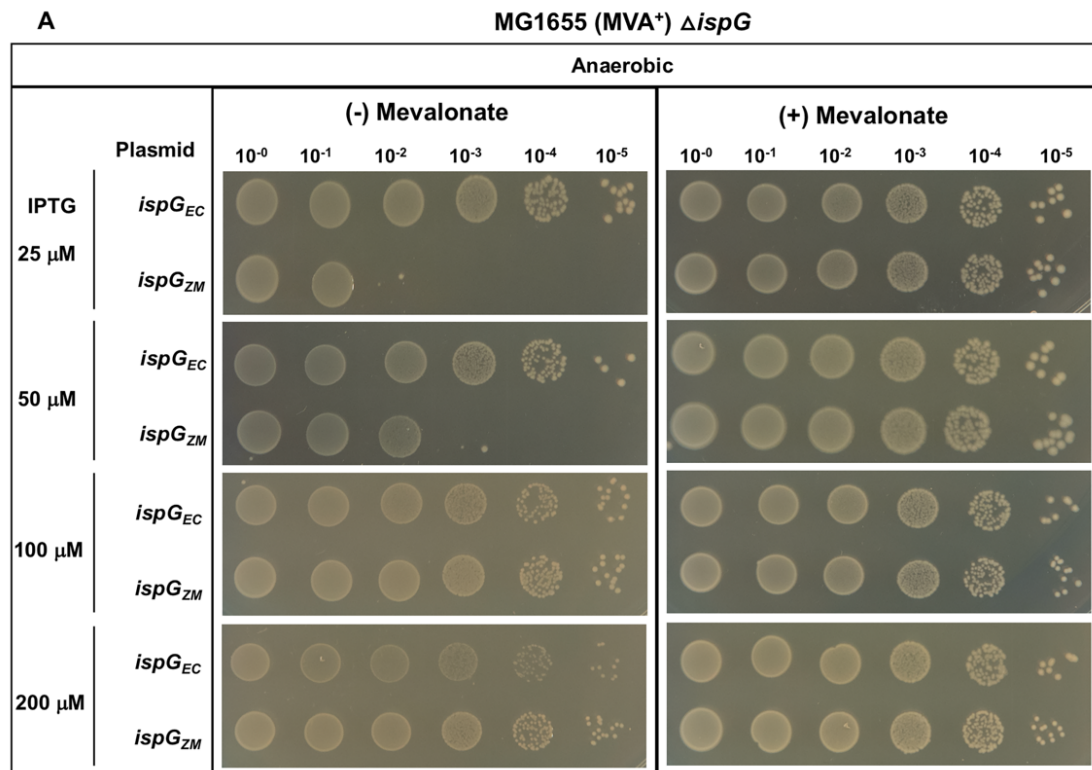


***Z. mobilis* IspG is not as functional as *E. coli* IspG under anaerobic conditions**

To dissect whether both *Z. mobilis ispG* and *ispH* were equally inefficient in producing isoprenoids in *E. coli*, we tested the function of each gene separately. Using MG1655 Δ *ispG* (MVA⁺), we compared viability of strains containing plasmid encoded *E. coli* and *Z. mobilis ispG* using the same growth assay. As expected, *E. coli ispG* was able to restore growth at all IPTG concentrations as colonies were observed at each 10⁻⁵ dilution. In contrast, complementation by *Z. mobilis ispG* was inefficient at lower IPTG concentration (25, 50 μ M IPTG) but was similar to *E. coli ispG* at 100 and 200 μ M IPTG and the colonies observed at the 10⁻⁵ dilution were similar in size to that of the permissive condition (Figure 2A). Overall, the pattern of results mostly mirrored the complementation of Δ *ispG* Δ *ispH* strain by *Z. mobilis ispG* and *ispH*. Western blot analysis of Strep-tag II IspG demonstrated that protein levels of *E. coli* and *Z. mobilis* IspG were similar following liquid growth at the various IPTG concentrations (Figure S3 and S4). Thus, it is likely that differences in activity and not protein levels explain the partial complementation by *Z. mobilis* IspG.

Figure 2-2 Viability of MG1655 (MVA⁺) Δ *ispG* with plasmid variants

MG1655 (MVA⁺) Δ *ispG* with plasmid variants containing *ispG* from *Z. mobilis* (*ispG_{ZM}*) or *E. coli* (*ispG_{EC}*) were grown in LB with mevalonate, arabinose and spectinomycin. After 16 hours of overnight growth, bacteria were washed with LB to remove mevalonate and were normalized to OD₆₀₀ 1. The bacteria were then diluted in LB and 5 μ l was used from each dilution tube to spot on solid TYE media with and without mevalonate (1mM) containing the indicated concentrations of IPTG (25 μ M, 50 μ M, 100 μ M or 200 μ M) to induce *ispG* and *ispH* co-expression with or without mevalonate (1mM). The agar plates were then incubated at 37°C overnight either under aerobic or anaerobic conditions.

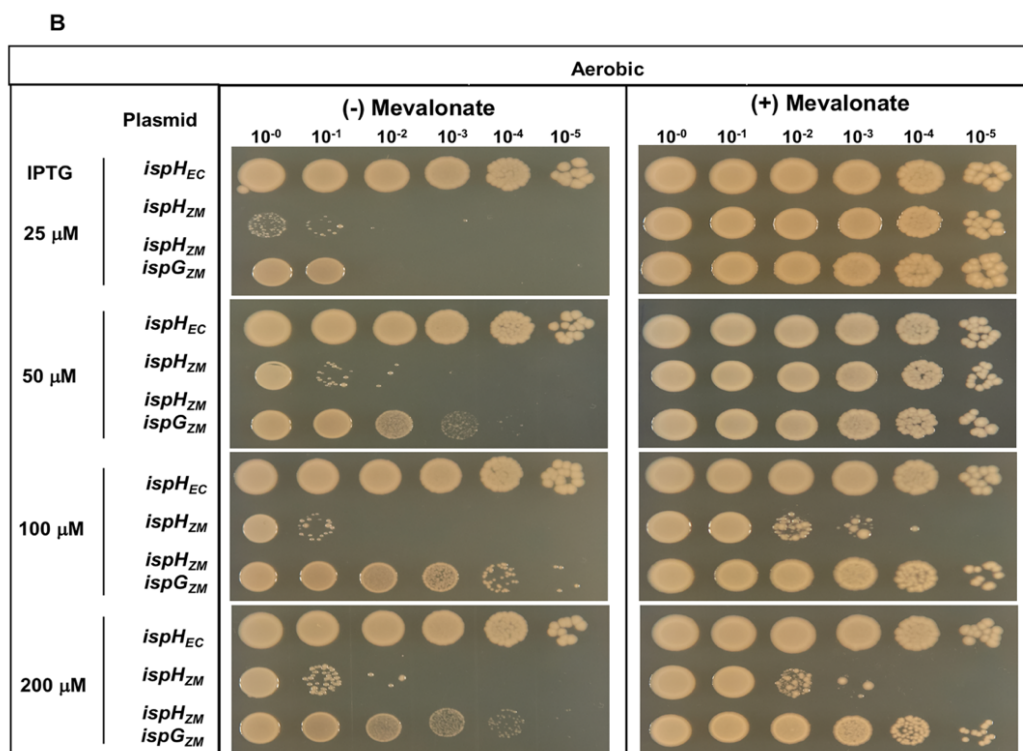
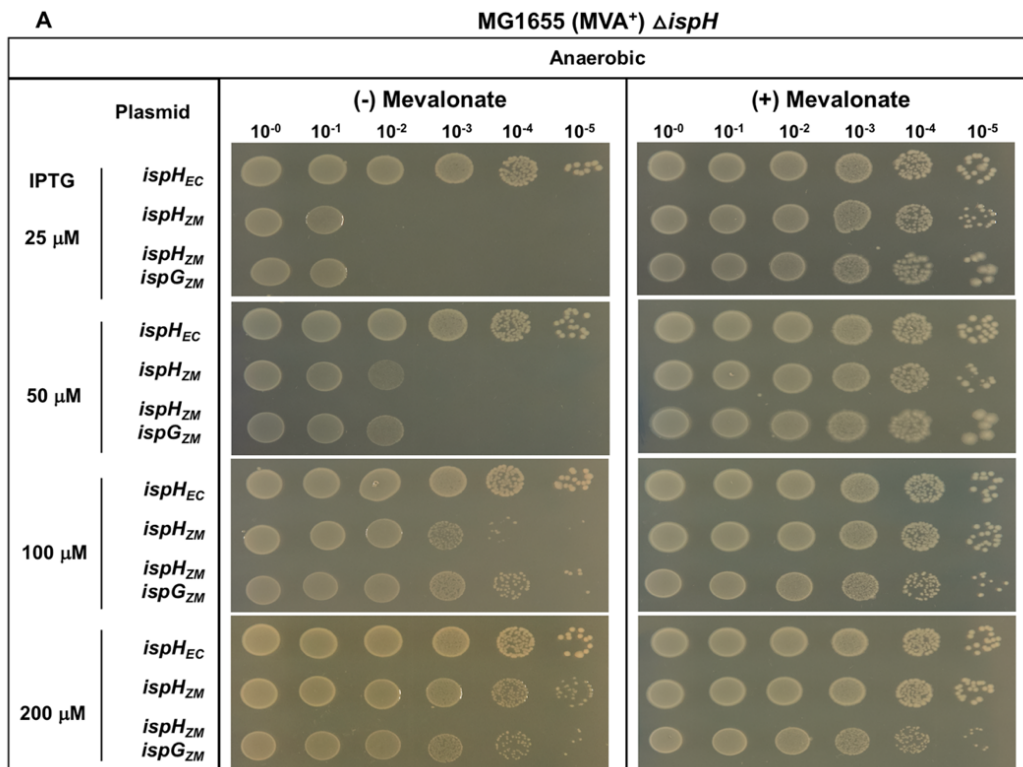


***Z. mobilis* IspH is less functional than *Z. mobilis* IspG in complementing their respective *E. coli* mutants under anaerobic conditions**

The function of *Z. mobilis ispH* was compared to that of its *E. coli* ortholog using growth of MG1655 Δ *ispH* (MVA⁺) as an assay. As expected, *E. coli ispH* was able to complement the function of the mutant at all IPTG concentrations. In contrast *Z. mobilis ispH* only partially complemented MG1655 Δ *ispH* (MVA⁺) at 50 and 100 μ M IPTG and no complementation was observed at 25 μ M IPTG. However, at 200 μ M IPTG, a similar number of colonies was present as *E. coli ispH* although the colony size was smaller compared to *E. coli ispH* or when grown on media containing mevalonate (Figure 3A). Thus, *Z. mobilis ispH* was less efficient than *Z. mobilis ispG* in complementing the corresponding *E. coli* mutants and less efficient than *Z. mobilis ispG* and *ispH* in complementing Δ *ispG* Δ *ispH* suggesting a requirement for its cognate partner, IspG. Western blot analysis of Strep-tag II IspH demonstrated that protein levels of *E. coli* and *Z. mobilis* IspH were similar following liquid growth at the various IPTG concentration assayed (Figure S2-S4). Thus, it is likely that differences in activity and not protein levels explain the difference in complementation between *Z. mobilis* and *E. coli* IspH.

Figure 2-3 Viability of MG1655 (MVA⁺) Δ *ispH* with plasmid variants

MG1655 (MVA⁺) Δ *ispH* with plasmid variants containing *ispH* from *Z. mobilis* (*ispH_{ZM}*) or *E. coli* (*ispH_{EC}*) or *ispG* & *ispH* from *Z. mobilis* (*ispH_{ZM}ispG_{ZM}*) were grown in LB with mevalonate, arabinose and spectinomycin. After 16 hours of overnight growth, bacteria were washed with LB to remove mevalonate and were normalized to OD₆₀₀ 1. The bacteria were then diluted in LB and 5 μ l was used from each dilution tube to spot on solid TYE media with and without mevalonate (1mM) containing the indicated concentrations of IPTG (25 μ M, 50 μ M, 100 μ M or 200 μ M) to induce *ispG* and *ispH* co-expression with or without mevalonate (1mM). The agar plates were then incubated at 37°C overnight either under aerobic or anaerobic conditions.

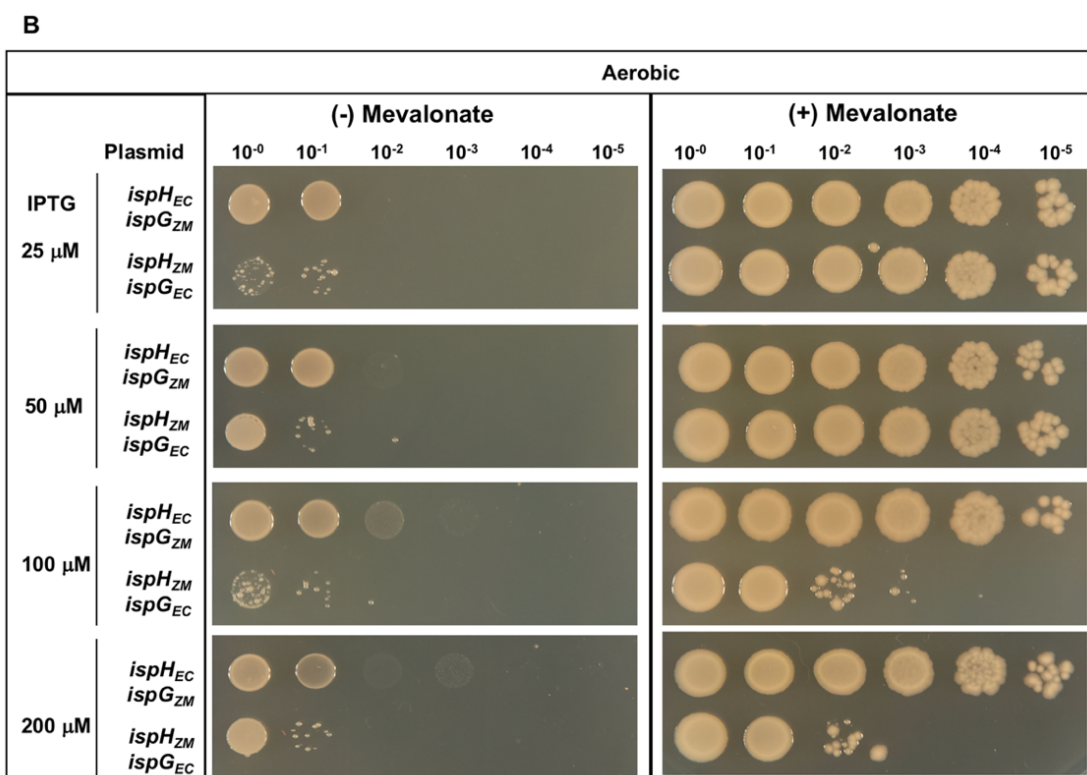
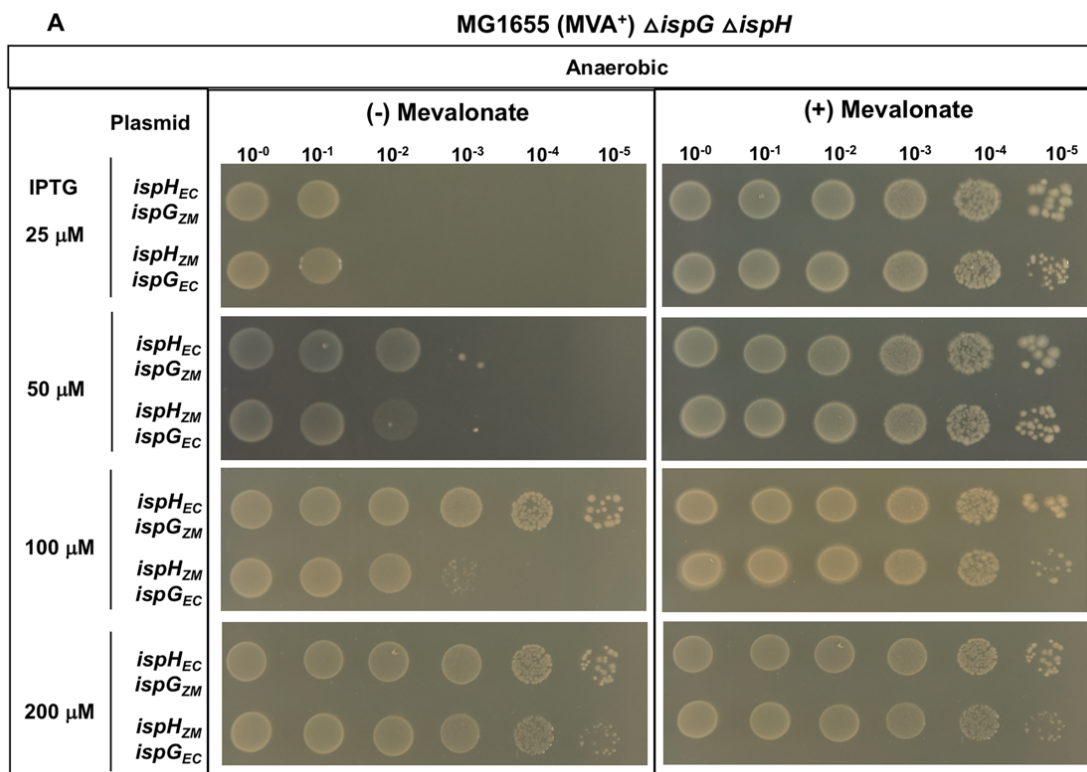


***Z. mobilis* IspH function is optimal when paired with its cognate IspG**

To test the preference of IspG and IspH for their cognate partner, the analogous genes from each species were swapped. When *E. coli ispG* was co-expressed with *Z. mobilis ispH* in *E. coli* $\Delta ispG \Delta ispH$ (MVA⁺), we observed that this pair functioned more poorly in complementation (Figure 4A) under anaerobic conditions than either *Z. mobilis ispG* and *ispH* or *E. coli ispG* and *ispH* (Figure 1A) indicating that *E. coli* IspG was not an adequate substitute for *Z. mobilis* IspG. In addition, when *E. coli ispH* was co-expressed with *Z. mobilis ispG*, we observed that the complementation efficiency was reduced (Figure 4A) compared to *E. coli ispG* and *ispH* and slightly increased as compared to *Z. mobilis ispG* and *ispH* (Figure 1A), suggesting that *E. coli* IspH could function with *Z. mobilis* IspG but less efficiently than *E. coli* IspG. These data indicate that IspH function exhibits a preference for its cognate IspG suggesting that *ispG* and *ispH* may have co-evolved to function optimally with its cognate partner through an unknown mechanism. Since *E. coli* IspG could not a sufficient substitute for *Z. mobilis* IspG in the swap assays, we tested if co-expressing *Z. mobilis ispG* with *ispH* improved the function of *Z. mobilis* IspH under anaerobic conditions in a strain lacking *E. coli ispH* but retaining chromosomal *E. coli ispG*. We observed a 10-fold increase in the number of colonies at 100 μ M IPTG with plasmid encoded *Z. mobilis ispG ispH* than with *ispH* alone (Figure 3A) indicating that co-expression of *Z. mobilis* IspH with IspG improved complementation of *E. coli* $\Delta ispH$ (MVA⁺). To address whether co-expression with IspG altered IspH protein levels, western blot analysis of Strep-tag II IspH was performed from cultures grown with a range of IPTG concentrations, which showed that levels of *Z. mobilis* IspH did not change significantly in the presence or absence of IspG (Figure S4). Altogether, our data indicate that *Z. mobilis* IspH functions best in this assay with IspG from the same organism.

Figure 2-4 Viability of MG1655 (MVA⁺) $\Delta ispG \Delta ispH$ with plasmid variants

MG1655 (MVA⁺) $\Delta ispG \Delta ispH$ with plasmid variants containing *ispG* from *E. coli* and *ispH* from *Z. mobilis* (*ispH_{ZM} ispG_{EC}*) or *ispG* from *Z. mobilis* & *ispH* from *E. coli* (*ispH_{EC} ispG_{ZM}*) were grown in LB with mevalonate, arabinose and spectinomycin. After 16 hours of overnight growth, bacteria were washed with LB to remove mevalonate and were normalized to OD₆₀₀ 1. The bacteria were then diluted in LB and 5 μ l was used from each dilution tube to spot on solid TYE media with and without mevalonate (1mM) containing the indicated concentrations of IPTG (25 μ M, 50 μ M, 100 μ M or 200 μ M) to induce *ispG* and *ispH* co-expression with or without mevalonate (1mM). The agar plates were then incubated at 37°C overnight either under aerobic or anaerobic conditions.



Z. mobilis* IspG and IspH confer an O₂ sensitive phenotype to *E. coli*Δ*ispG*Δ*ispH

IspG and IspH each have [4Fe-4S] cluster cofactors that are generally considered O₂ sensitive¹⁸ and in *Z. mobilis* the substrates of these enzymes accumulate when anaerobic cultures are shifted to aerobic conditions²⁰. To determine if there were differences in enzyme function in the presence of O₂ when the clusters are expected to be less stable, we used the same complementation assay described above but incubated plates under aerobic conditions. *E. coli ispG* and *ispH* complemented the function of *E. coli*Δ*ispG*Δ*ispH* (MVA⁺) at all IPTG concentrations (25 - 200 μM) similar to anaerobic conditions. In contrast, *Z. mobilis ispG* and *ispH* showed at least a 100-fold reduction in viability under aerobic conditions (Figure 1B) compared to anaerobic conditions at 100 and 200 μM IPTG (Figure 1A). This result suggested that *Z. mobilis* IspG and IspH [4Fe-4S] clusters may be more sensitive to O₂ than its *E. coli* orthologs, conferring an O₂ sensitive phenotype to growth.

Z. mobilis* IspG does not confer O₂ sensitivity to *E. coli

To examine whether both *Z. mobilis ispG* and *ispH* were responsible for the O₂ sensitive phenotype in *E. coli*, we tested the function of each gene individually under aerobic conditions. As expected, *E. coli ispG* was able to restore growth of MG1655Δ*ispG* (MVA⁺) at all IPTG concentrations. For *Z. mobilis ispG* the pattern of growth observed under aerobic conditions (Figure 2B) was nearly identical to that observed under anaerobic conditions (Fig 2A); there appears to be only a small reduction in colony forming units at equivalent IPTG concentrations under aerobic conditions. These results suggest that *Z. mobilis* IspG is not the major driver of the O₂ sensitive phenotype observed with both *Z. mobilis* IspG and IspH.

Z. mobilis* IspH confers an O₂ sensitive phenotype to *E. coli

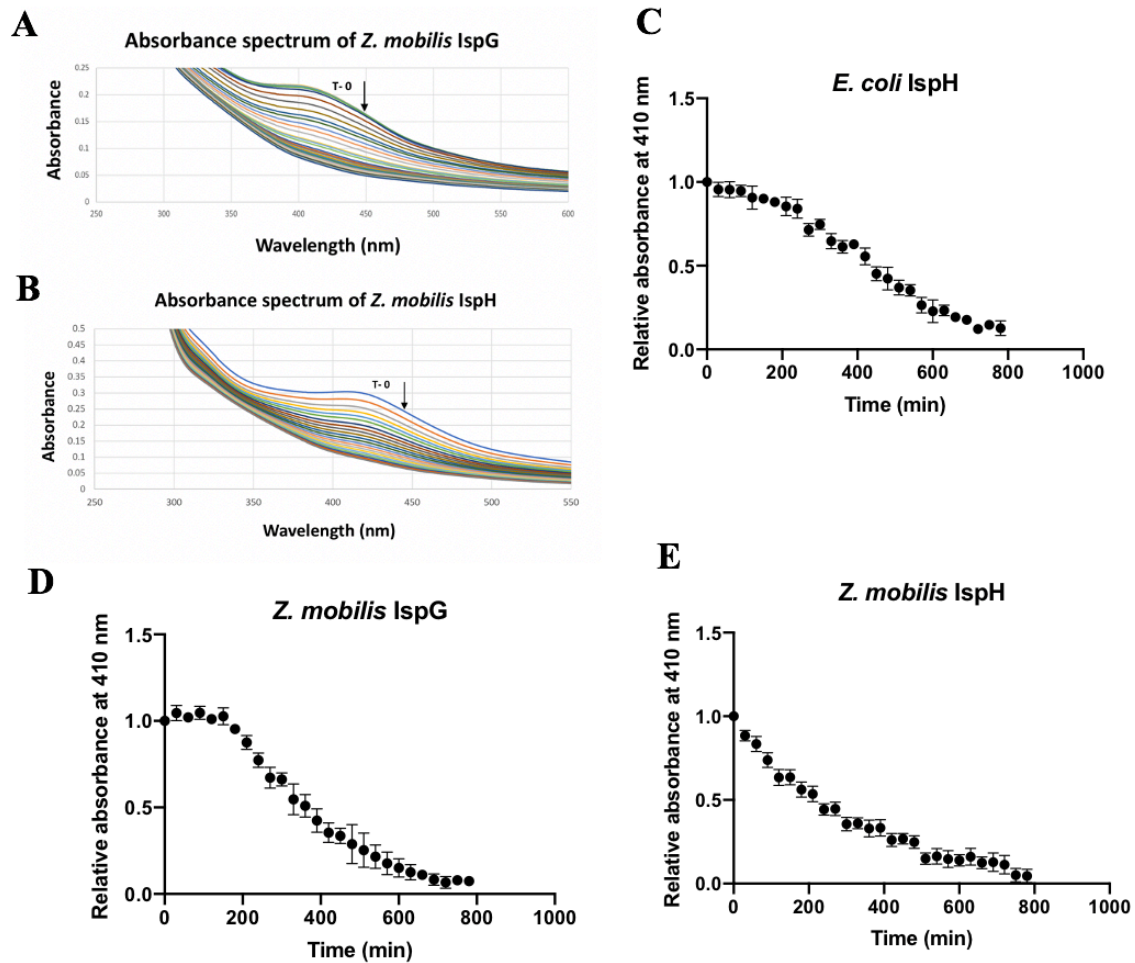
Using MG1655 Δ *ispH* (MVA⁺), we compared the function of *E. coli* and *Z. mobilis ispH* under aerobic conditions. As expected, *E. coli ispH* was able to fully complement the function of MG1655 Δ *ispH* (MVA⁺) under aerobic conditions. In contrast, *Z. mobilis ispH* was severely defective in complementation at all IPTG concentrations (Figure 3B) compared to anaerobic conditions (Figure 3A). This phenotype was not due to differences in protein levels as determined by western blots of cells grown under anaerobic (Figure S3, S4) and aerobic conditions (Figure S3 and S5).

The [4Fe-4S] cluster of IspG and IspH are sensitive to O₂ *in vitro*

Since aerobic conditions impaired the function of *Z. mobilis* IspH in the complementation assays, we tested the stability of the [4Fe-4S] cluster of *Z. mobilis* IspG, *Z. mobilis* IspH and *E. coli* IspH to O₂ *in vitro* (Figure 5). The proteins were isolated anaerobically via a Strep-Tag II at their C-termini yielding protein with the characteristic absorbance spectra of a [4Fe-4S] cluster (Figure 5A,B). Anaerobic protein (60 μ M) was then exposed to air and the change in the characteristic absorbance peak at 410 nm was monitored over a 12-hour time period. We used *E. coli* IspH as a control since the lability of the [4Fe-4S] cluster to O₂ was previously reported¹⁸. All three proteins lost the [4Fe-4S] cluster absorbance over time indicating their sensitivity to O₂ (Figure 5C-E). Although the [4Fe-4S] cluster of *Z. mobilis* IspH appeared to be the most sensitive to O₂, differences in the initial cluster occupancy between the three samples precluded a more rigorous analysis.

Figure 2-5 *Z. mobilis* IspG and IspH cluster degradation assay

IspH (A) and IspG (B) from *Z. mobilis* with C-terminus strep-tag II was purified under anaerobic conditions and absorbance at 410 nm characteristic of [4Fe-4S] was monitored under aerobic conditions using 60 μ M, occupancy of 4Fe between 5-10%. [4Fe-4S] cluster of (C) *E. coli* IspH, *Z. mobilis* IspH (D) and IspG (E) degraded under aerobic conditions over time. Relative absorbance at 410 nm is the normalized absorbance value at initial time point.



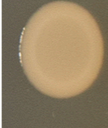
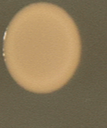
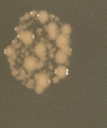
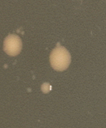


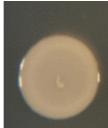
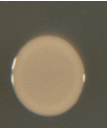
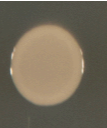
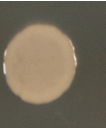


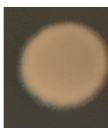
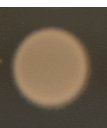




***Z. mobilis* IspH catalytic activity is required to impart an O₂ sensitive to with mevalonate**

Unexpectedly, an O₂ sensitive phenotype was also observed for expression of *Z. mobilis ispH* in *E. coli* Δ *ispH* (MVA⁺) in the presence of mevalonate as colonies were only observed at 10⁻³ dilution at 100 and 200 μ M IPTG (Figure 3B), suggesting a phenotype that could not be explained simply by the lack of isoprenoids. We considered the possibility that *Z. mobilis* IspH could be producing an off pathway inhibitory product under aerobic conditions since promiscuous activities have been noted previously^{16,17}. Thus, we tested whether the O₂ sensitive phenotype in the presence of mevalonate depended on the catalytic function of *Z. mobilis* IspH. Substitution of *Z. mobilis* IspH Glu127 to Ala should inactivate enzyme activity based on the analogous *E. coli* active site mutant, E126A¹⁴. In addition, we constructed a second substitution, *Z. mobilis* IspH C13A that should also inactivate enzyme activity because it removes one of the Cys expected to ligate the [4Fe-4S] cluster. Both *Z. mobilis* IspH variants restored aerobic growth to mevalonate grown cells as colonies were observed at 10⁻⁵ dilution (Figure 6). Furthermore, expression of *Z. mobilis ispH* in a strain containing a wild-type copy of *E. coli ispH* does not have an oxygen-sensitive growth phenotype, indicating that the function of the *E. coli* protein suppresses this activity (Fig S6). These results suggest that *Z. mobilis* IspH has an aberrant activity in the presence of O₂.

Figure 2-6 Viability of cells under aerobic conditions in the presence of mevalonate

MG1655 (MVA⁺) Δ *ispH* with plasmid variants containing *ispH* from *Z. mobilis* (*ispH_{ZM}*) with point mutations E127A or C13A were grown in LB with mevalonate, arabinose and spectinomycin. After 16 hours of overnight growth, bacteria were washed with LB to remove mevalonate and were normalized to OD₆₀₀ 1. The bacteria were then diluted in LB and 5 μ l was used from each dilution tube to spot on solid TYE media with and without mevalonate (1mM) containing the indicated concentrations of IPTG (25 μ M, 50 μ M, 100 μ M or 200 μ M) to induce *ispG* and *ispH* co-expression with or without mevalonate (1mM). The agar plates were then incubated at 37°C overnight either under aerobic conditions.

MG1655 (MVA⁺) Δ *ispH*

Plasmid	Aerobic					
	(+) Mevalonate					
	10 ⁻⁰	10 ⁻¹	10 ⁻²	10 ⁻³	10 ⁻⁴	10 ⁻⁵
<i>ispH_{ZM}</i>						
(E127A) <i>ispH_{ZM}</i>						
(C13A) <i>ispH_{ZM}</i>						

The cognate enzyme pair is required to suppress the aberrant O₂ dependent activity of *Z. mobilis* IspH

We reasoned that the expression of *Z. mobilis* IspG might be necessary to eliminate this aberrant activity because inhibition of growth with mevalonate was not observed when complementing MG1655 Δ *ispG* Δ *ispH*(MVA⁺) with *Z. mobilis ispG* and *ispH*. Indeed, co-expression of *Z. mobilis ispG* with *Z. mobilis ispH* significantly improved the growth of MG1655 Δ *ispH*(MVA⁺) in both the presence and absence of mevalonate at 100 and 200 μ M IPTG (Figure 3B). This improvement in growth suggests that *Z. mobilis* IspG somehow prevents this aberrant activity by *Z. mobilis* IspH.

The preference for *Z. mobilis* IspG was demonstrated in MG1655 Δ *ispG* Δ *ispH*(MVA⁺) (Figure 4A and B) in a swapping experiment with *E. coli* IspG. When *E. coli ispG* was co-expressed with *Z. mobilis ispH*, the same O₂ sensitive phenotype in the presence of mevalonate was observed. In addition, in the absence of mevalonate, a nearly 100-fold reduction in viability was observed with 100 and 200 μ M IPTG under aerobic conditions compared to growth under anaerobic conditions. Interestingly, *E. coli* IspH does not show the O₂ dependent aberrant activity when it is co-expressed with heterologous IspG from *Z. mobilis* since there is no loss in viability in the presence of mevalonate under aerobic conditions. However, we did observe that in the absence of mevalonate co-expression of *Z. mobilis ispG* with *E. coli ispH* impedes complementation of *E. coli* Δ *ispG* Δ *ispH* under aerobic conditions even though we did not observe a similar effect when complementing *E. coli* Δ *ispG* with *Z. mobilis ispG* under aerobic or anaerobic conditions. Since the major difference between these two strains are the levels of *E. coli* IspH, it suggests that *E. coli* IspH might compete with *Z. mobilis* IspG for a common cofactor under aerobic conditions impeding the

activity of *Z. mobilis* IspG. Since one common cofactor are the [4Fe-4S] clusters, we investigated if the Fe-S cluster biogenesis machinery was limiting under aerobic conditions.

Expression of the *Z. mobilis* *suf* operon in *E. coli* does not improve the function of *Z. mobilis* IspG or IspH

We focused our attention on the SUF Fe-S cluster biogenesis pathway since *Z. mobilis* has only the SUF pathway for producing its complement of Fe-S proteins, whereas *E. coli* has both the ISC and SUF pathways. In *E. coli*, the housekeeping pathway ISC, was previously shown to maturate *E. coli* IspG and IspH. To test whether the inefficient complementation of *Z. mobilis* IspG and IspH resulted from insufficient Fe-S cluster maturation due to differences in biogenesis pathways, *E. coli* strains were constructed that had the native *E. coli* *suf* operon replaced with that from *Z. mobilis* and placed under control of a constitutive promoter. Under either aerobic or anaerobic conditions, we observed no improvement in the complementation MG1655 Δ *ispH* (MVA⁺) with either *Z. mobilis* *ispH* or *Z. mobilis* *ispH* and *ispG* at 100 - 200 μ M IPTG (Figure 7) with *Z. mobilis* SUF machinery. As a control we tested the native *E. coli* *suf* operon expressed from the same constitutive promoter and it showed no difference in complementation efficiency from the parent strain (Figure 8). Western blot analysis confirmed the higher level of SufD in this strain compared to the native promoter (Figure S7).

Figure 2-7 Viability of MG1655 (MVA⁺) Δ *ispH* or MG1655 (MVA⁺) Δ *ispH*, P_{fnr} *suf*_{ZM} with plasmid variants

MG1655 (MVA⁺) Δ *ispH* or MG1655 (MVA⁺) Δ *ispH*, P_{fnr} *suf*_{ZM} with plasmid variants containing *ispH* from *Z. mobilis* (*ispH*_{ZM}) or *E. coli* (*ispH*_{EC}) or *ispG* & *ispH* from *Z. mobilis* (*ispH*_{ZM} *ispG*_{ZM}) were grown in LB with mevalonate, arabinose and spectinomycin. After 16 hours of overnight growth, bacteria were washed with LB to remove mevalonate and were normalized to OD₆₀₀ 1. The bacteria were then diluted in LB and 5 μ l was used from each dilution tube to spot on solid TYE media with and without mevalonate (1mM) containing the indicated concentrations of IPTG (25 μ M, 50 μ M, 100 μ M or 200 μ M) to induce *ispG* and *ispH* co-expression with or without mevalonate (1mM). The agar plates were then incubated at 37°C overnight either under aerobic or anaerobic conditions.

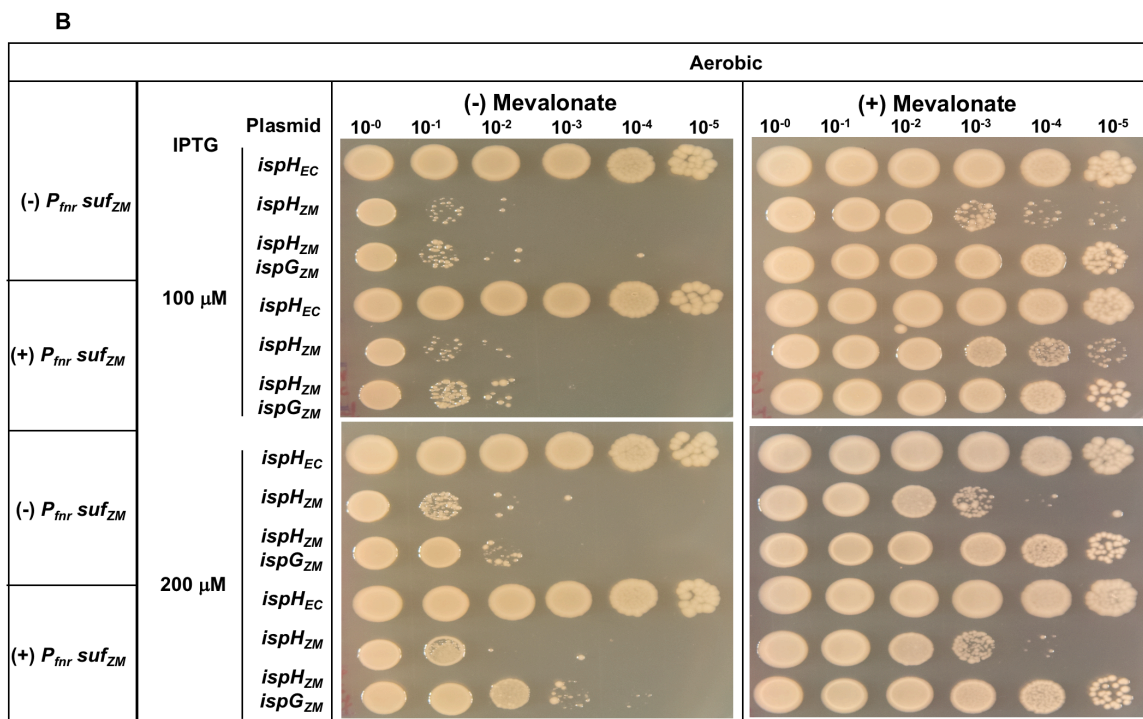
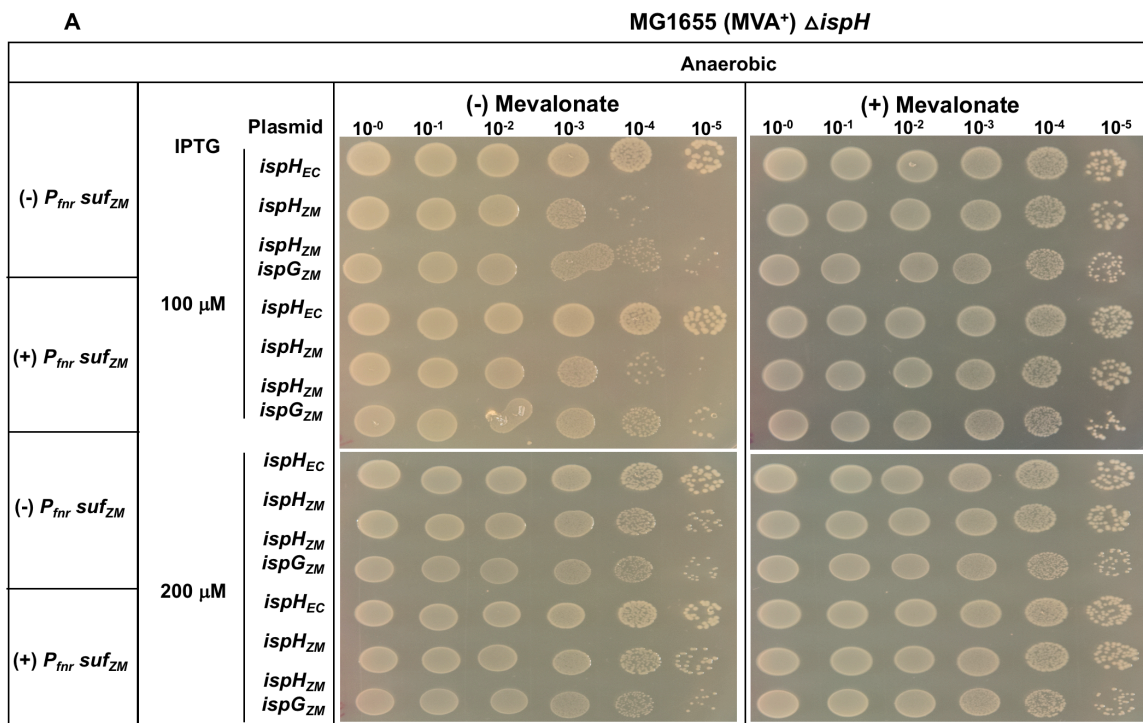
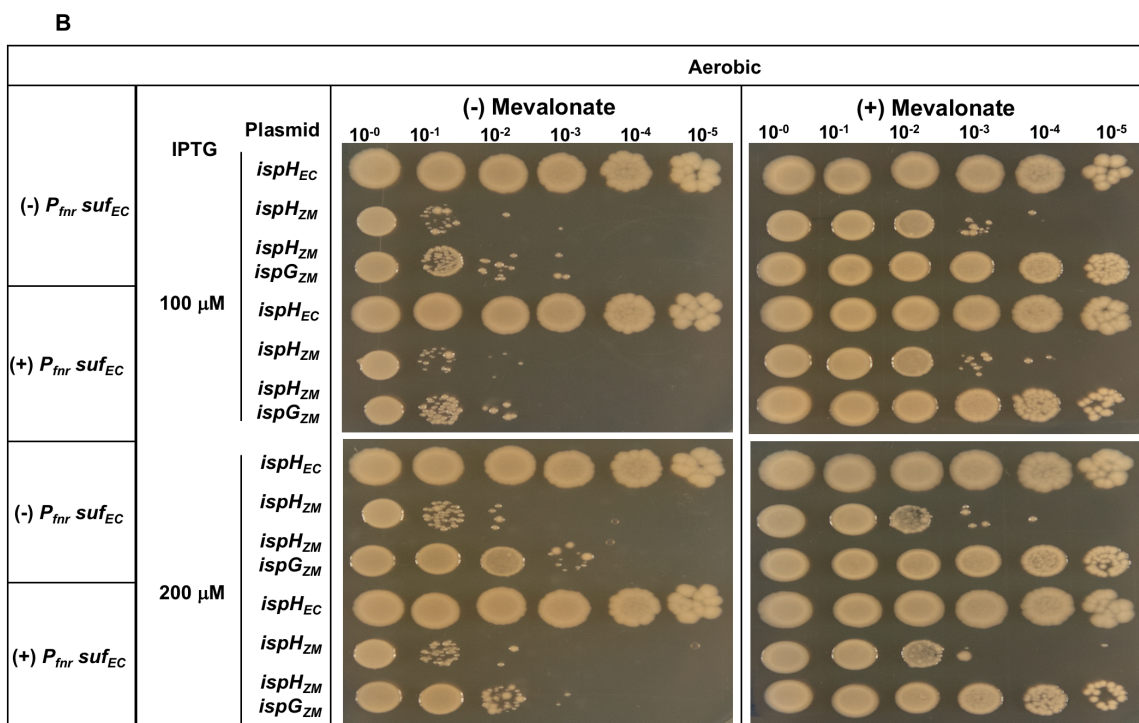
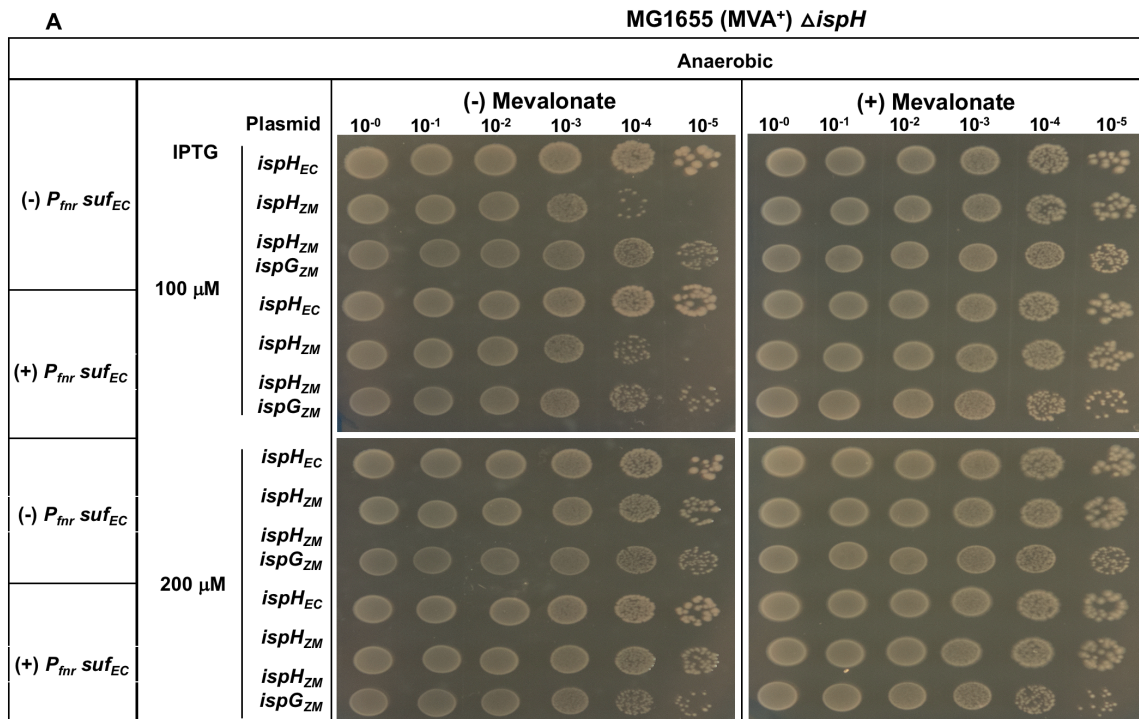


Figure 2-8 Viability of MG1655 (MVA⁺) Δ *ispH* or MG1655 (MVA⁺) Δ *ispH*, *P_{fnr} suf_{EC}* with plasmid variants

MG1655 (MVA⁺) Δ *ispH* or MG1655 (MVA⁺) Δ *ispH*, *P_{fnr} suf_{EC}* with plasmid variants containing *ispH* from *Z. mobilis* (*ispH_{ZM}*) or *E. coli* (*ispH_{EC}*) or *ispG* & *ispH* from *Z. mobilis* (*ispH_{ZM} ispG_{ZM}*) were grown in LB with mevalonate, arabinose and spectinomycin. After 16 hours of overnight growth, bacteria were washed with LB to remove mevalonate and were normalized to OD₆₀₀ 1. The bacteria were then diluted in LB and 5 μ l was used from each dilution tube to spot on solid TYE media with and without mevalonate (1mM) containing the indicated concentrations of IPTG (25 μ M, 50 μ M, 100 μ M or 200 μ M) to induce *ispG* and *ispH* co-expression with or without mevalonate (1mM). The agar plates were then incubated at 37°C overnight either under aerobic or anaerobic conditions.



Does IspG physically interact with IspH?

As the presence of IspG improved the function of IspH, we also considered the possibility of whether IspG and IspH form a complex. Using two in vitro assays to test for physical association (molecular sieve chromatography and blue native gels), we did not observe complex formation between *Z. mobilis* IspG and IspH under the conditions tested. For molecular sieve chromatography, anaerobically isolated Strep-tag-II IspH (25 μ M) and IspG (25 μ M) were mixed together and loaded onto a Superdex 200 Increase 10/300 GL molecular sieve column under anaerobic conditions (Figure 9A). The elution profile of this equimolar mixture reflected the sum of the individual profiles of IspG or IspH, indicating no physical interaction could be detected under these solution conditions. Native blue polyacrylamide gel electrophoresis analysis of an equimolar mixture of *Z. mobilis* IspG (25 μ M) and IspH (25 μ M) also showed that the proteins separated according to their native size, which for IspG was a dimer (79.8 kDa) and IspH was a monomer (37 kDa) (Figure 9B).

Since the reaction catalyzed by these proteins also require partner proteins, such as ferredoxins or flavodoxins, we reasoned that a cell-based assay might detect an interaction if other proteins were also required. We used the bacterial adenylate cyclase *two-hybrid* (BACTH) assay²² for this analysis where fusion proteins to different domains of adenylate cyclase will reconstitute activity and produce cAMP if the tested proteins oligomerize. Activity is assayed in *E. coli* Δ *cya* through the cAMP dependent expression of the *lac* operon. IspG from *E. coli* and *Z. mobilis* were individually fused with T18 at their N-termini and IspH from *Z. mobilis* and *E. coli* were individually fused with T25 at their N-termini, engineered on pUT18C and pKT25, respectively. Restoration of adenylate cyclase activity under aerobic and anaerobic conditions was assayed by

plating transformed strains on TYE X-gal, IPTG (500 μ M), Ampicillin (200 μ g/ μ l) and Kan (50 μ g/ μ l). Blue colonies were detected with the positive control, pKT25-zip and pUT18C-zip, containing strain (Figure 9C). However, for the combinations of *Z. mobilis* IspG and IspH or *E. coli* IspH and IspG, we observed only white colonies on the X-gal plates under either aerobic or anaerobic conditions, indicating a lack of adenylate cyclase activity and accordingly, no detectable interaction between IspG and IspH from either organism.

Figure 2-9 Interaction studies of IspG and IspH

(A) Elution volume of *Z. mobilis* IspH is 14 ml, *Z. mobilis* IspG is 12.8 ml. Equimolar mixture of IspG and IspH elution volume is identical to IspH / G under anaerobic conditions. (B) BTH 101 with plasmid variants (*T25ispH_{ZM}* & *T18ispG_{ZM}*), (*T25ispH_{EC}* & *T18ispG_{ZM}*), (*T25ispG_{EC}* & *T18ispG_{EC}*), (*T25* & *T18*), (*T25-zip* & *T18-zip*) under aerobic and anaerobic conditions. Anaerobic plates were exposed to oxygen to allow the oxygen dependent dimerization of the dye to form blue color. (C) Blue-Native PAGE gel with electrophoresed *Z. mobilis* IspH, IspG, IspG & IspH and standard marker under aerobic conditions. *Z. mobilis* IspH (25 μ M), *Z. mobilis* IspG (25 μ M) was used.

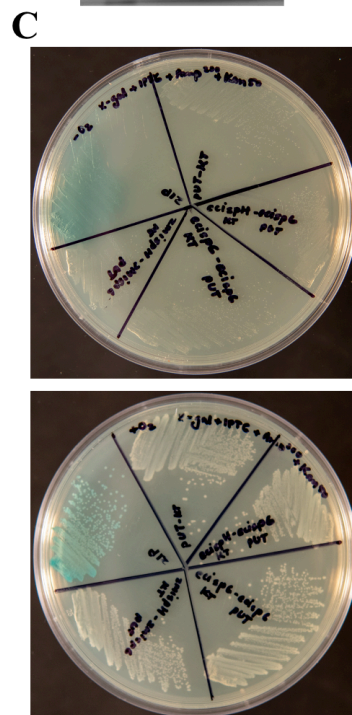
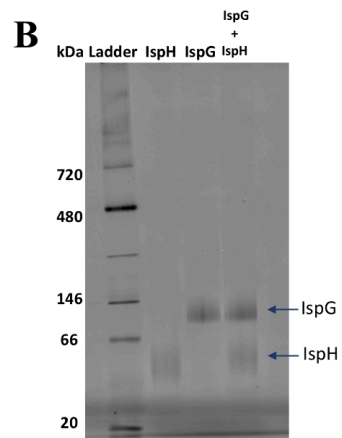
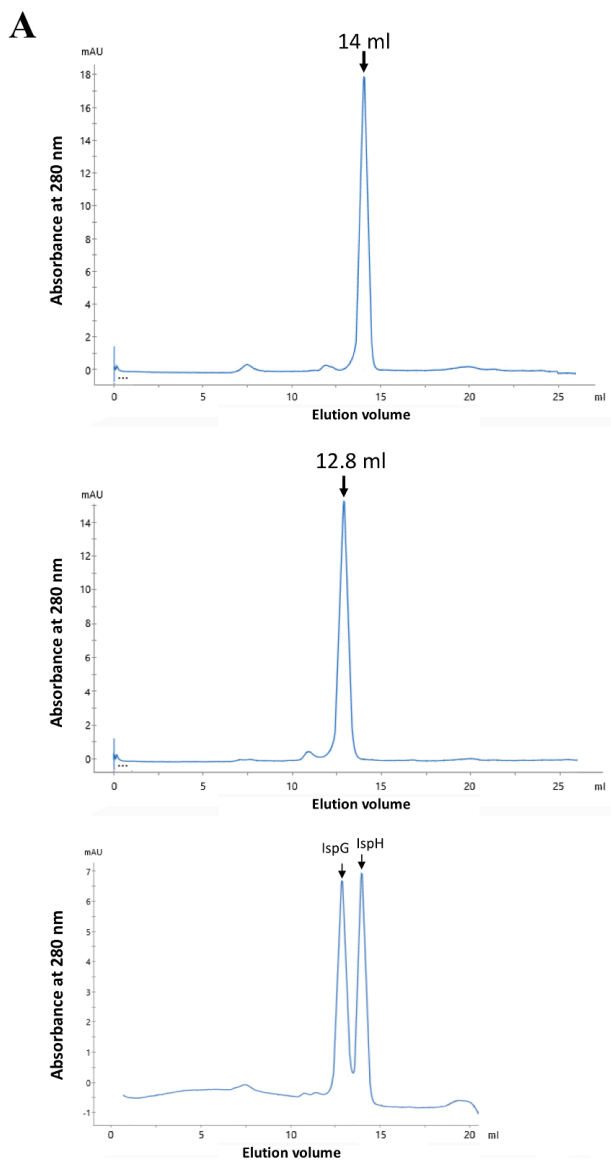
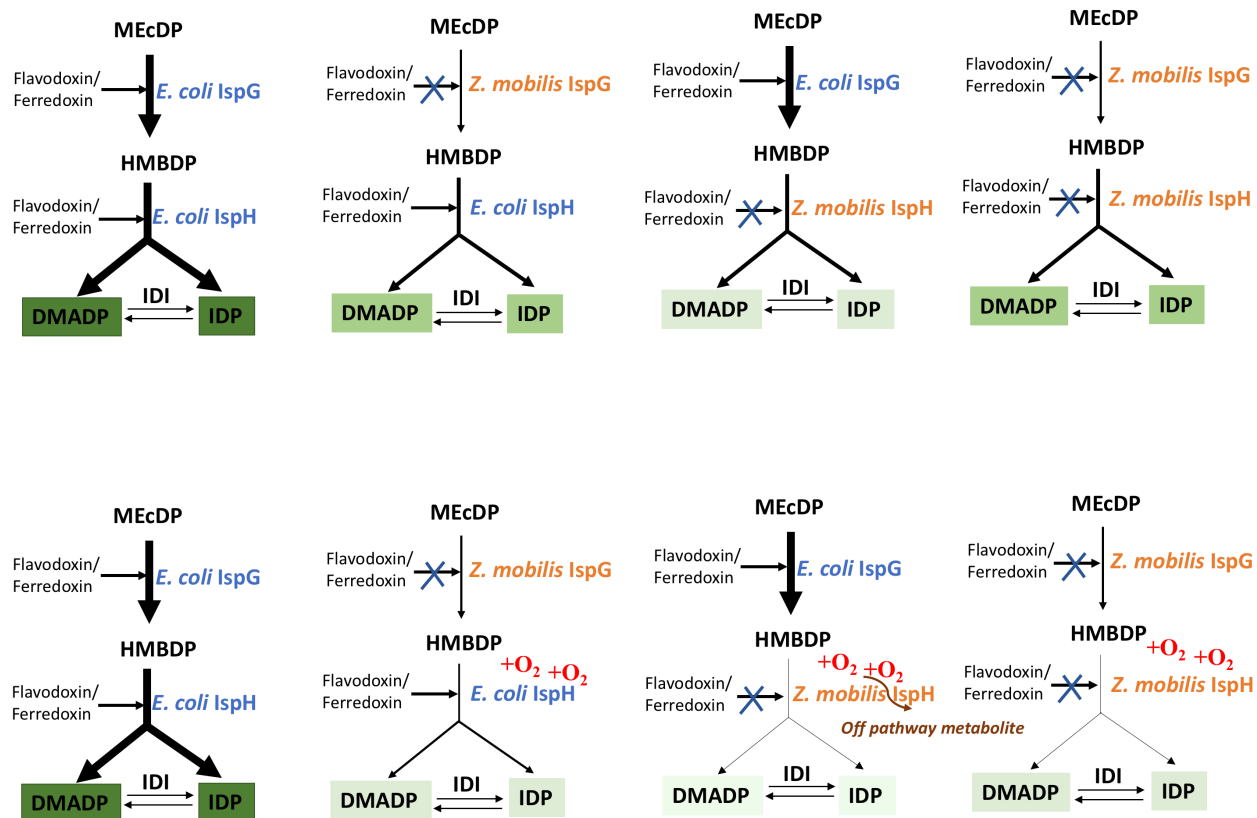


Figure 2-10 Model describing our findings of *Z. mobilis* and *E. coli* IspH and IspG function

IspG and IspH function of the MEP pathway from *Z. mobilis* and *E. coli* under anaerobic and aerobic conditions. The lines represent flux through the terminal steps of the MEP pathway, thick lines represent high flux while thin lines represent slow flux.



DISCUSSION

Optimization of the MEP pathway is of significant interest because of the value of isoprenoid-based bioproducts. The terminal steps catalyzed by the [4Fe-4S] cluster containing IspG and IspH enzymes have often been noted as bottlenecks in the pathway²⁰. Here, we focused on these two enzymes from *Z. mobilis* to begin to understand the attributes that potentially limit their function. Our analysis of *Z. mobilis* IspH and IspG proteins expressed in *E. coli* indicated that neither protein could fully complement the respective *E. coli* mutants even under anaerobic conditions, indicating significant functional differences between the *E. coli* and *Z. mobilis* proteins. Co-expression of *Z. mobilis* IspG and IspH improved the function of IspH under anaerobic conditions suggesting a functional linkage between the activity of the two enzymes despite the absence of any physical association. Finally, *Z. mobilis* IspH caused an oxygen sensitive growth phenotype that could be partially mitigated by co-expression of cognate IspG and both proteins were shown to have O₂ sensitive [4Fe-4S] cluster cofactors. Overall, these data suggest that both enzymes need to be optimized in parallel to improve MEP pathway flux.

Why *Z. mobilis* IspG poorly complements *E. coli* Δ *ispG* is not obvious from the protein sequence. Overall, *Z. mobilis* IspG is 48.4% identical over the entire length of *E. coli* IspG (Figure S8). The alpha-fold prediction of a *Z. mobilis* IspG monomer shows an overall structural similarity to the *E. coli* prediction and to either subunit of the dimeric IspG X-ray crystal structure from *Thermus thermophilus* B8. According to the crystal structure, the protein folds into two domains, a TIM barrel, and an Fe-S cluster domain. The [4Fe-4S] cluster of IspG is ligated by 3 Cys residues and one Glu and these residues are conserved for both *Z. mobilis* (Cys272, Cys275, Cys307 and Glu 314) and *E. coli* (Cys270, Cys273, Cys305, and Glu 312) IspG. The residues in *T.*

thermophilus that bind the substrate, MEcDP, and hold it in place via a hydrogen bond network between the [4Fe-4S] cluster and the TIM barrel (Arg56, Arg110, Arg141, Lys204 and Arg260) are also conserved. The substrate binds directly to the [4Fe-4S]²⁺ cluster, displacing ligation by Glu350 and brings the conserved Glu232 into proximity of the MEcDP C3 hydroxyl group forming a closed state for catalysis, in which the active site is no longer solvent exposed. It is worth noting that *Z. mobilis* IspG has 4 additional cysteines in the TIM barrel domain that are not present in *E. coli*, raising the possibility that it has another metal center. Nevertheless, the conservation of the overall structure and the key residues for binding substrate and the Fe-S cluster in all three proteins imply a conserved active site and reaction mechanism for the IspG catalyzed reductive ring opening to form HMBDP.

It is also not clear from the protein sequence of *Z. mobilis* IspH why this protein complements *E. coli* Δ *ispH* poorly. *Z. mobilis* IspH is 52.5% identical over the entire length of *E. coli* IspH (Figure S9). The alpha-fold prediction of a *Z. mobilis* IspH monomer shows an overall structural similarity to the X-ray crystal structure of *E. coli* IspH¹⁴. The protein folds as a “trefoil” arrangement consisting of three α/β domains with the Fe-S cluster bound at the center of the structure. IspH belongs to a subclass of Fe-S cluster proteins, illustrated by aconitase, where Cys residues provide three ligands to the [4Fe-4S] but the fourth Fe ligand of the [4Fe-4S] cluster is provided by the substrate and substrate availability can impact Fe-S cluster occupancy¹⁷. The X-ray structure of *E. coli* IspH shows that the C4-OH group of HMBDP displaces bound water to form the fourth Fe ligand to the [4Fe-4S] cluster²³. Cys12, Cys 96 and Cys197 form the other cluster ligands and the position of these is conserved in *Z. mobilis* IspH (FIG S9). E126, which plays a key role during catalysis to bind the CH₂OH group of HMBDP to promote the conversion

to IDP or DMADP^{15,24}, is also conserved. Thus, the conservation between *E. coli* and *Z. mobilis* of the overall IspH structure and key residues for binding substrate and the Fe-S cluster imply a conserved active site and reaction mechanism for the IspH catalyzed reductive dehydroxylation of HMBDP to IDP and DMADP.

Although we cannot rule out differences in K_M or k_{cat} contributing to the poor function of *Z. mobilis* IspG and IspH in *E. coli* since these are not known, another gap in our knowledge is the identity of the physiological redox partners that serve as the electron donors for these reactions (Figure 10). Electron transfer from redox proteins to the [4Fe-4S] cluster of both IspG and IspH is required for each catalytic cycle^{25,26}. In plants, reduced ferredoxin (FdxA) supplies electrons to the IspG [4Fe-4S] cluster, while in *E. coli*, electrons are supplied through flavodoxin I (FldA)^{27,28}. The electron transfer proteins involved in reducing the [4Fe-4S] cluster of IspG and IspH in *Z. mobilis* are unknown. From the genome annotation of *Z. mobilis*, there are 5 predicted ferredoxins (ZMO 1818, ZMO 0220, ZMO 2028, ZMO 0860, and ZMO 0456) and 1 flavodoxin (ZMO 1851) that are possible candidates for these electron transfer reactions. Previous studies suggest that organisms with multiple protein electron donors are more likely to have evolved "specialists" by optimizing binding specificity and electron transfer rates for specific enzyme partners and extended protein regions that exclude other proteins²⁹.

In support of a role for specific redox partners for IspG, a recent study showed that the majority of orthologous IspG proteins surveyed from phylogenetically representative bacteria failed to complement *E. coli* $\Delta ispG$ strains²¹. For a small subset, the lack of complementation could be explained by a preference for their native electron transfer proteins

through co-expression with its native IspG in *E. coli*. The least conserved region between *Z. mobilis* and *E. coli* IspG is at the C-terminus. Since there is no structural or biochemical information to indicate where flavodoxin or ferredoxin dock on any IspG, such variation at the C-termini could be significant in specifying a particular redox partner and thus affect function. Thus, future efforts for optimization of the MEP pathway in *Z. mobilis* should focus on identifying which accessory electron transfer proteins are required for *Z. mobilis* IspG and IspH function and determine if their co-expression with IspG and IspH improves MEP pathway function in *E. coli* or *Z. mobilis*.

A similar survey of heterologously expressed IspH orthologs in *E. coli* has not been undertaken to our knowledge. However, a phylogenetic analysis indicates considerable diversity of IspH at their N and C termini. Biochemical and bioinformatic analysis has proposed that there are four main classes of IspH. *E. coli* and *Z. mobilis* IspH belong to Class B¹⁸ because of the aromatic residues found near the [4Fe-4S] cluster of IspH as well as a longer C-terminal extension. In fact, the C-terminal extension of *Z. mobilis* IspH is longer than that of *E. coli* IspH, which could affect enzyme activity or interaction with a redox partner. We reason that maybe because *Z. mobilis* is a facultative anaerobic bacterium which prefers anaerobic growth conditions, IspH may not have evolved to protect its [4Fe-4S] cluster from oxidative degradation for transitions to aerobic growth.

We also found functional connections between IspG and IspH from *Z. mobilis* since coexpression of *Z. mobilis ispH* with *ispG* improved complementation *E. coli* Δ *ispH*. However, this result could not be explained by a physical association since all three assays (molecular sieve

analysis, native gel electrophoresis and BACTH two hybrid screen) failed to detect an interaction between the two proteins under the conditions tested. Although these results do not exclude a missing protein component in our assays, we also considered the possibility that the interactions are too transient to detect and/or may be influenced by the presence of the pathway intermediates. Since IspG catalyzes the conversion of MEcDP to HMBDP and HMBDP is a ligand to the [4Fe-4S] cluster of IspH, a reasonable expectation is that cluster stability and occupancy of IspH is linked to the availability of its substrate HMBDP, connecting it to the function of IspG. It is possible that detection of protein: protein interactions might require the appropriate electron transfer partners as well as substrates and highly occupied cluster containing IspG and IspH.

Under aerobic conditions, *Z. mobilis* IspH prevented growth of *E. coli* Δ *ispH* even in the presence of mevalonate, suggesting that the enzyme was making an inhibitory product (Fig. 10). We considered this might be due to accumulation of HMBDP in these strains since a previous study suggested that accumulation of HMBDP could be toxic to cells. However, we found that IspH activity was required for this inhibition since a catalytically inactive *Z. mobilis* variant no longer prevented growth in the presence of mevalonate. We speculate that the open conformation, which is known for *E. coli* IspH to be more prone to [4Fe-4S] cluster oxidation and degradation, must dominate under aerobic conditions. Whether this results from a lack of interaction with its cognate IspG and a decrease in HMBDP binding to stabilize the [4Fe-4S] cluster is unknown. It is worth noting that the presence of *Z. mobilis* IspG and not *E. coli* IspG suppresses this inhibitory activity, favoring the notion of a specific interaction with *Z. mobilis* IspG. If the lack of a matching ferredoxin or flavodoxin is also limiting, then the oxidized cluster would be less likely to get reduced to the functional [4Fe-4S]¹⁺ form. IspH is known to show acetylene hydratase activity

and catalyze the conversion of acetylenes to aldehyde and ketone¹⁷. We speculate that such a promiscuous activity produces a compound that is inhibiting growth. Future work will be needed to address this hypothesis.

A previous study also reported that balanced activities of IspG and IspH are important for MEP pathway function. If IspH levels were not sufficient, then HMBDP accumulated, which they suggest is toxic to cells³⁰. In this study, we observed optimal MEP pathway function when *ispG* and *ispH* were co-expressed in a strain lacking only IspH, compared to expression of *ispH* alone. However, this increase in viability cannot easily be explained by HMBDP levels since more HMBDP would be expected in the co-expression strain since it also carries a functional *E. coli ispG* on the chromosome. However, under aerobic conditions, the remarkable preference for the cognate IspH and IspG pairs in strains co-expressing different combinations of *Z. mobilis* and *E. coli* IspG and IspH deleted for *ispG* and *ispH* on the chromosome, can only be reasonably explained by specific protein:protein interactions between these proteins and not just the capacity to make HMBDP (Figure 10).

The Fe-S cluster maturation machinery does not appear to be limiting for *Z. mobilis* IspG and IspH function in *E. coli*. Previous studies showed that *E. coli* isoprenoid synthesis relies on the ISC housekeeping Fe-S maturation pathway³¹. Moreover, other studies examined the impact of levels of Fe-S cluster machinery for IspH or IspG activity expressed in *E. coli*^{15,21}. *Z. mobilis* has only the SUF Fe-S biogenesis²⁰ raising the question whether a preference for an orthologous pathway limited function in *E. coli*. However, the fact that over expression of either the *E. coli* or *Z. mobilis* Fe-S cluster maturation pathway did not improve *Z. mobilis* IspG or IspH

functions suggested there was no preference for Fe-S cluster biogenesis pathways, and this was not the source of limited function.

In summary, the results presented here reveal a species specificity of IspG and IspH function that is particularly striking under aerobic growth conditions. The knowledge gained here is central to understand the function of *Z. mobilis* IspG and IspH under aerobic and anaerobic conditions and identifying the physiological electron donors and determining the molecular basis of the species specificity will provide insight to engineering the steps catalyzed by these unique [4Fe-4S] containing enzymes and improve the flux through the MEP pathway to produce isoprenoid precursors.

MATERIALS AND METHODS

Plasmid construction

The coding region of *ispG* and *ispH* from *E. coli* and *Z. mobilis* were cloned into expression vectors for use in complementation assays. First, each coding region was amplified from either *E. coli* MG1655 or *Z. mobilis* ZM4 genomic DNA by PCR with Q5 DNA polymerase and specific primer sets (Table 3). Primer set 1 (a, b and c) and 3 (a, b and c) amplified *E. coli* *ispH* and *ispG*, respectively. Primer set 2 (a, b and c) and 4 (a, b and c) amplified *Z. mobilis* *ispH* and *ispG*, respectively. The PCR products were digested with AflIII and Sall and ligated into the same sites of pRL814 to yield pPK13575 for *E. coli* *ispG*, pPK13576 for *Z. mobilis* *ispG*, pPK13573 for *E. coli* *ispH*, and pPK13574 for *Z. mobilis* *ispH* (Table 2). For these expression plasmids, the ribosomal binding sites of *Z. mobilis* *ispH* and *ispG* were also independently optimized using the Salis algorithm³² and the analogous optimized sequence was also used for *E. coli* *ispG* and *ispH*.

The ribosomal binding site and adjacent optimized sequence were included in the primers used to amplify *ispH* and *ispG* and are highlighted in bold in the primer sequence (Table 3). To construct plasmids that co-express *ispH* and *ispG*, *Z. mobilis* and *E. coli* *ispG* were amplified from pPK13576 and pPK13575 respectively, using primer pairs, 8a and 8b or 9a and 9b, respectively. pPK13574 or pPK13573 were amplified with primers 7a and 7b, respectively and the *ispG* PCR products were inserted 121 nucleotides downstream of *ispH* by Gibson assembly (NEB) to generate plasmids pPK13635 and pPK13636. For co-expression of *ispH* from *E. coli* and *ispG* from *Z. mobilis*, *Z. mobilis* IspG (pPK13576), was amplified using primer sets (11a, 11b) and was inserted 121 nucleotides downstream of *E. coli* *ispH* in pPK13573 amplified using primer set (10a, 10b). In addition, *E. coli* IspG (pPK13575) was amplified using primer sets (13a, 13b) and inserted 121 nucleotides downstream of *Z. mobilis* *ispH* in pPK13574 amplified by primer set (12a, 12b). To generate in frame C-terminal Strep-tagged variants of IspH and IspG, DNA sequence encoding Strep-tag II was included in the primer sequence for PCR amplification of *Z. mobilis* *ispH* [primer set (14a, 14b)], *E. coli* *ispH* [primer set (15a, 15b)], *Z. mobilis* *ispG* [primer set (16a, 16b)], *E. coli* *ispG* [primer set (17a, 17b)] and KLD enzyme mix (NEB) was used for circularization to generate plasmid pPK13616, pPK13612, pPK13618, pPK13614, respectively. Strep-tag II was also added to *Z. mobilis* *ispH* on plasmid pPK13635 to produce pPK14456. For isolation of IspH, *Z. mobilis* *ispH* with Strep-tag II was constructed from PCR products of *ispH* amplified from pPK13574 using primers 18a and 18b, and pET11a, amplified by primers 19a and 19b, joined by using Gibson assembly.

Strain construction

To delete the essential genes, *ispH* and *ispG*, from *E. coli* MG1655 or its recombineering derivative PK9012³³, we used an established approach to maintain viability by first P1 transducing into these strains a synthetic operon from strain BP129 encoding the eukaryotic mevalonic acid pathway under control of the *E. coli* arabinose inducible promoter, P_{BAD} *yPMD*, *hPMK*, *yMVK*, *ecIDI*, *lacZ*, *lacY*, *lacA* (MVA^+)³¹ inserted at the *putP* locus to create PK13556 and PK13557, respectively. Primer pairs 5a and 5b and 6a and 6b were used to amplify FRT-*cat*-FRT region from PK5949 with primers containing 5' tails that are homologous to the sequence flanking the coding region of *ispH* and *ispG* respectively. PCR products were transformed into the recombineering strain PK13557 containing the eukaryotic mevalonate pathway (MVA^+) Δ *ispH*::*cat* or Δ *ispG*::*cat*; cell viability was maintained by growth on LB media containing 10 mM arabinose to induce MVA^+ and 1 mM mevalonate to bypass the MEP pathway. Mevalonate was made from 0.9M Mevalonolactone (EMD Millipore) by alkaline hydrolysis with 1M potassium hydroxide (Fischer chemical).

The Δ *ispH*::*cat* or Δ *ispG*::*cat* alleles were then P1 transduced to PK13556 (MG1655 MVA^+) resulting in PK13566 and PK13567 respectively. The *lacZYA* genes were deleted from the MVA^+ cassette resulting in PK14317 [MG1655 ($MVA^+\Delta$ *lacZYA*::*tet*)]. $MVA^+\Delta$ *lacZYA*::*tet* was P1 transduced to PK9776 (MG1655 Δ *lacY*) to yield PK14463. *ispH*::*cat* and *ispG*::*cat* alleles from PK13566 and PK13567 were then P1 transduced to PK14463 resulting in PK14464 ($MG1655\Delta$ *lacY\Delta**ispH*::*catMVA^+\Delta*lacZYA*::*tet*) and PK14465 ($MG1655\Delta$ *lacY\Delta**ispG*::*catMVA^+\Delta*lacZYA*::*tet*), respectively. Plasmids carrying the *E. coli* or *Z. mobilis* *ispH* or *Z. mobilis***

ispHispG were transformed into PK14464. Plasmids carrying *E. coli* and *Z. mobilis ispG* genes were transformed into PK14465.

PK14487 was made by removing the *cat* gene from *ispG::cat* using pCP20 plasmid³⁴ and subsequently P1 transducing the Δ *ispH::cm^r* allele from PK13566 into PK14485 (MG1655 Δ *lacY* Δ *ispGMVA⁺* Δ *lacZYA::tet*) to yield PK14487 (MG1655 Δ *lacY* Δ *ispG*, Δ *ispH::cm^r*MVA⁺ Δ *lacZYA::tet*). Plasmids containing *ispH* and *ispG* genes from *E. coli* and *Z. mobilis* were transformed in PK14487.

The *kan-Pfnr-suf_{EC}* was P1 transduced from PK 16191 to PK 14464 (MG1655 Δ *lacY* Δ *ispH::cat* MVA⁺ Δ *lacZYA::tet*) resulting in PK 14842. The *kan-Pfnr-suf_{ZM}* was P1 transduced from PK 16235 to PK 14464 (MG1655 Δ *lacY* Δ *ispH::cat*MVA⁺ Δ *lacZYA::tet*) resulting in PK 14862. Plasmids carrying the *E. coli* or *Z. mobilis ispH* or *Z. mobilis ispHispG* were transformed into PK14862.

Complementation of *E. coli* Δ *ispH*, Δ *ispG* and Δ *ispH* Δ *ispG* mutant strains

E. coli strains with relevant plasmids were tested for their ability to complement the indicated mutations by growth in the absence of mevalonate under aerobic and anaerobic conditions. Strains were grown overnight in LB media containing arabinose (10 mM), mevalonate (1 mM) and spectinomycin (100 μ g/ml). The cell suspension was normalized to OD_{600nm} 1.0 and 1 ml was centrifuged for 2 minutes, the supernatant was discarded, and the pellet was washed once with LB to remove mevalonate. The cells were pelleted again, resuspended in 1ml of LB, and 5 μ l of serial dilutions was spotted on TYE agar plates containing either mevalonate (1mM),

arabinose (10mM), IPTG (25 μ M, 50 μ M, 100 μ M, 200 μ M) and spectinomycin (100 μ g/ml) or TYE agar plates containing only IPTG (25 μ M, 50 μ M, 100 μ M, 200 μ M) and spectinomycin (100 μ g/ml). Plates were incubated in air for aerobic growth or in a sealed jar with AnaeroPack System (Mitsubishi gas chemical) for anaerobic growth at 37°C for 16 hours.

Western blot assay

Levels of plasmid encoded C- terminal Strep-tag II IspG or IspH produced following IPTG induction were measured in relevant *E. coli* strains by Western Blotting. Strains were grown overnight in LB media containing mevalonate (1mM), arabinose (10mM), spectinomycin (100 μ g/ml) for 16 hours at 37°C. Bacterial strains were sub-cultured (1:100) into the same media until the OD_{600nm} reached 0.2 and then IspH Strep-tag II or IspG expression was induced by addition of isopropyl -D-thiogalactoside (IPTG) (25 μ M, 50 μ M, 100 μ M, or 200 μ M) final concentration. After two hours, the cells were normalized to OD_{600nm} of 0.2 and 1 ml of cell suspension was pelleted. Cell pellets were resuspended in 1X SDS-loading buffer, heated to 95°C and electrophoresed by SDS-PAGE. The gel was transferred to a 0.45-micron nitrocellulose membrane (Amersham Protran) and the assay was performed with Strep-tag II antibody HRP Conjugate (EMD Millipore) according to the manufacturer's recommendations. The blot was imaged using an Azure imager and was analyzed using the Azure spot pro software.

Expression and purification of *Z. mobilis* IspH

PK13681 that contains the repaired *suf* operon which is controlled by arabinose induced P_{BAD} promoter³⁵ was transformed with *Z. mobilis* IspH Strep-tag II at C-terminus in pET vector (pPK 13650) resulting in PK 13654. The cells were grown aerobically at 37°C in 1L of terrific broth (Research Products International) containing final concentration of ferric ammonium citrate 10mg/L, 2 mM cysteine, 10 mM arabinose, and ampicillin (100 µg/L). At an OD₆₀₀ of 0.3, synthesis of IspH was induced by adding IPTG to a final concentration of 0.4 mM for 2 hours. The induced culture was sparged overnight (20 hours) with argon at 4°C. The culture was centrifuged at 8000 rpm in a Beckman JLA 10.500 rotor for 15 min at 4°C, resuspended in 50 mM Tris-HCl, 150 mM NaCl, 1mM DTT, 100µM PMSF, pH 8 under anaerobic conditions and lysed in a French Press at 20,000 psi (1 psi~6.9kPa). The lysate was centrifuged at 45,000 rpm in a Beckman 70.1 Ti rotor for 1h at 4°C. The supernatant was fractionated using a FPLC instrument (AKTA pure chromatography system, Cytiva) equipped with a StrepTrapTM HP column (5ml, GE Healthcare), equilibrated with 50 mM Tris-HCl, 150 mM NaCl, 1 mM DTT, pH 8. IspH proteins were eluted with 50 mM Tris-HCl, 150 mM NaCl, 2.5 mM desthiobiotin, 1 mM DTT, pH 8. DTT and desthiobiotin in the pooled protein fraction was separated using PD-10 desalting column containing 8.3 ml of SephadexTM G-25 resin (cytiva) with 50 mM Tris-HCl, 150 mM NaCl pH 7.5., The concentration of the protein was measured using Bradford assay³⁶. The isolation of protein was carried out anaerobically inside a Coy anerobic chamber with an atmosphere of 80% N₂, 10%CO₂ and 10%H₂.

REFERENCES

1. Rohmer M, Knani M, Simonin P, Sutter B, Sahn H. Isoprenoid biosynthesis in bacteria: a novel pathway for the early steps leading to isopentenyl diphosphate. *Biochem J.* 1993;295 (Pt 2)(Pt 2):517-524.
2. Lichtenthaler HK. The 1-Deoxy-D-Xylulose-5-Phosphate Pathway of Isoprenoid Biosynthesis in Plants. *Annu Rev Plant Physiol Plant Mol Biol.* 1999;50:47-65.
3. Holstein SA, Hohl RJ. Isoprenoids: remarkable diversity of form and function. *Lipids.* 2004;39(4):293-309.
4. Chang WC, Song H, Liu HW, Liu P. Current development in isoprenoid precursor biosynthesis and regulation. *Curr Opin Chem Biol.* 2013;17(4):571-579.
5. Martien JI, Amador-Noguez D. Recent applications of metabolomics to advance microbial biofuel production. *Curr Opin Biotechnol.* 2017;43:118-126.
6. Rohmer M. The discovery of a mevalonate-independent pathway for isoprenoid biosynthesis in bacteria, algae and higher plants. *Nat Prod Rep.* 1999;16(5):565-574.
7. Frank A, Groll M. The Methylerythritol Phosphate Pathway to Isoprenoids. *Chem Rev.* 2017;117(8):5675-5703.
8. Brenac L, Baidoo EEK, Keasling JD, Budin I. Distinct functional roles for hopanoid composition in the chemical tolerance of *Zymomonas mobilis*. *Mol Microbiol.* 2019;112(5):1564-1575.
9. He MX, Wu B, Qin H, et al. *Zymomonas mobilis*: a novel platform for future biorefineries. *Biotechnol Biofuels.* 2014;7:101.

10. Liu Y, Ghosh IN, Martien J, Zhang Y, Amador-Noguez D, Landick R. Regulated redirection of central carbon flux enhances anaerobic production of bioproducts in *Zymomonas mobilis*. *Metab Eng*. 2020;61:261-274.
11. Khana DB, Tatli M, Rivera Vazquez J, et al. Systematic Analysis of Metabolic Bottlenecks in the Methylerythritol 4-Phosphate (MEP) Pathway of *Zymomonas mobilis*. *mSystems*. 2023;8(2):e0009223.
12. Lee M, Grawert T, Quitterer F, et al. Biosynthesis of Isoprenoids: Crystal Structure of the 4Fe-4S Cluster Protein IspG. *Journal of Molecular Biology*. 2010;404(4):600-610.
13. Rekitke I, Nonaka T, Wiesner J, et al. Structure of the E-1-hydroxy-2-methyl-but-2-enyl-4-diphosphate synthase (GcpE) from *Thermus thermophilus*. *FEBS Lett*. 2011;585(3):447-451.
14. Grawert T, Rohdich F, Span I, et al. Structure of active IspH enzyme from *Escherichia coli* provides mechanistic insights into substrate reduction. *Angew Chem Int Ed Engl*. 2009;48(31):5756-5759.
15. Grawert T, Span I, Eisenreich W, et al. Probing the reaction mechanism of IspH protein by x-ray structure analysis. *Proc Natl Acad Sci U S A*. 2010;107(3):1077-1081.
16. Ge D, Xue Y, Ma Y. Two unexpected promiscuous activities of the iron-sulfur protein IspH in production of isoprene and isoamylene. *Microb Cell Fact*. 2016;15:79.
17. Span I, Wang K, Wang W, et al. Discovery of acetylene hydratase activity of the iron-sulphur protein IspH. *Nat Commun*. 2012;3:1042.
18. Rao G, Oldfield E. Structure and Function of Four Classes of the 4Fe-4S Protein, IspH. *Biochemistry*. 2016;55(29):4119-4129.

19. Zepeck F, Grawert T, Kaiser J, et al. Biosynthesis of isoprenoids. purification and properties of IspG protein from *Escherichia coli*. *J Org Chem*. 2005;70(23):9168-9174.
20. Martien JI, Hebert AS, Stevenson DM, et al. Systems-Level Analysis of Oxygen Exposure in *Zymomonas mobilis*: Implications for Isoprenoid Production. *mSystems*. 2019;4(1).
21. D'Angelo F, Fernandez-Fueyo E, Garcia PS, et al. Cellular assays identify barriers impeding iron-sulfur enzyme activity in a non-native prokaryotic host. *Elife*. 2022;11.
22. Battesti A, Bouveret E. The bacterial two-hybrid system based on adenylate cyclase reconstitution in *Escherichia coli*. *Methods*. 2012;58(4):325-334.
23. Chaignon P, Petit BE, Vincent B, Allouche L, Seemann M. Methylerythritol Phosphate Pathway: Enzymatic Evidence for a Rotation in the LytB/IspH-Catalyzed Reaction. *Chemistry*. 2020;26(5):1032-1036.
24. Span I, Grawert T, Bacher A, Eisenreich W, Groll M. Crystal structures of mutant IspH proteins reveal a rotation of the substrate's hydroxymethyl group during catalysis. *J Mol Biol*. 2012;416(1):1-9.
25. Wolff M, Seemann M, Tse Sum Bui B, et al. Isoprenoid biosynthesis via the methylerythritol phosphate pathway: the (E)-4-hydroxy-3-methylbut-2-enyl diphosphate reductase (LytB/IspH) from *Escherichia coli* is a [4Fe-4S] protein. *FEBS Lett*. 2003;541(1-3):115-120.
26. Wang W, Oldfield E. Bioorganometallic chemistry with IspG and IspH: structure, function, and inhibition of the [Fe(4)S(4)] proteins involved in isoprenoid biosynthesis. *Angew Chem Int Ed Engl*. 2014;53(17):4294-4310.

27. Puan KJ, Wang H, Dairi T, Kuzuyama T, Morita CT. *fldA* is an essential gene required in the 2-C-methyl-D-erythritol 4-phosphate pathway for isoprenoid biosynthesis. *FEBS Lett.* 2005;579(17):3802-3806.
28. Seemann M, Tse Sum Bui B, Wolff M, Miginiac-Maslow M, Rohmer M. Isoprenoid biosynthesis in plant chloroplasts via the MEP pathway: direct thylakoid/ferredoxin-dependent photoreduction of GcpE/IspG. *FEBS Lett.* 2006;580(6):1547-1552.
29. Campbell IJ, Bennett GN, Silberg JJ. Evolutionary Relationships Between Low Potential Ferredoxin and Flavodoxin Electron Carriers. *Front Energy Res.* 2019;7.
30. Li Q, Fan F, Gao X, et al. Balanced activation of IspG and IspH to eliminate MEP intermediate accumulation and improve isoprenoids production in *Escherichia coli*. *Metab Eng.* 2017;44:13-21.
31. Campos N, Rodriguez-Concepcion M, Sauret-Gueto S, Gallego F, Lois LM, Boronat A. *Escherichia coli* engineered to synthesize isopentenyl diphosphate and dimethylallyl diphosphate from mevalonate: a novel system for the genetic analysis of the 2-C-methyl-D-erythritol 4-phosphate pathway for isoprenoid biosynthesis. *Biochem J.* 2001;353(Pt 1):59-67.
32. Salis HM, Mirsky EA, Voigt CA. Automated design of synthetic ribosome binding sites to control protein expression. *Nat Biotechnol.* 2009;27(10):946-950.
33. Beauchene NA, Mettert EL, Moore LJ, Keles S, Willey ER, Kiley PJ. O₂ availability impacts iron homeostasis in *Escherichia coli*. *Proc Natl Acad Sci U S A.* 2017;114(46):12261-12266.
34. Datsenko KA, Wanner BL. One-step inactivation of chromosomal genes in *Escherichia coli* K-12 using PCR products. *Proc Natl Acad Sci U S A.* 2000;97(12):6640-6645.

35. Sourice M, Askenasy I, Garcia PS, et al. A Diverged Transcriptional Network for Usage of Two Fe-S Cluster Biogenesis Machineries in the Delta-Proteobacterium *Myxococcus xanthus*. *mBio*. 2023;14(1):e0300122.
36. Kielkopf CL, Bauer W, Urbatsch IL. Bradford Assay for Determining Protein Concentration. *Cold Spring Harb Protoc*. 2020;2020(4):102269.

CHAPTER 3

Future Directions and Conclusions

Remarkably diverse reactions are carried out by [4Fe-4S] cluster containing proteins, such as electron transfer by ferredoxins, dehydration by aconitase and reductive dehydroxylation by IspG and IspH¹⁻⁵. Our results show that neither *Z. mobilis* IspG nor IspH is able to robustly complement the relevant *E. coli* mutation with *Z. mobilis* IspH being less effective than *Z. mobilis* IspG. Furthermore, *Z. mobilis* IspH shows an extremely oxygen sensitive growth phenotype. However, co-expression of *Z. mobilis* IspG and IspH improves the function of IspH under both aerobic and anaerobic conditions. Similarly, *E. coli* IspG and IspH work best with their cognate enzymes. Thus, the co-expression of cognate IspG and IspH is crucial in considering how to optimize the function of the MEP pathway. However, my data raise a number of questions as to what the fundamental differences are between the *E. coli* and *Z. mobilis* proteins that lead to these phenotypes. Here, I address my findings in the context of these outstanding questions.

Why do *Z. mobilis* IspG and IspH poorly complement the corresponding *E. coli* mutants?

Although we found that the key residues involved in the function of these proteins is conserved between *E. coli* and *Z. mobilis*, we don't know that the activity of these enzymes are the same. In order to determine this, we would have to measure the K_m and k_{cat} of IspH and IspG from both *E. coli* and *Z. mobilis* to compare these parameters.

Another possibility is that the *E. coli* repertoire of ferredoxins and flavodoxin do not work well with *Z. mobilis* IspG and IspH to efficiently transfer electrons to the Fe-S clusters for protein activity. To address this question, the *Z. mobilis* electron donors would need to be identified and co-expressed with *Z. mobilis* IspG or IspH. From the KEGG genome annotation of *Z. mobilis*, there are 5 predicted ferredoxins (ZMO 1818, ZMO 0220, ZMO 2028, ZMO 0860, and ZMO

0456) and 1 flavodoxin (ZMO 1851) that are possible candidates for these electron transfer reactions. Questions that should be addressed are whether both *Z. mobilis* IspG or IspH use the same electron donor or if the electron donor varies between each enzyme or across species. One approach is to use the MVA⁺ strain of *E. coli*, deleted for the genes encoding the *E. coli* physiological donors and test the above candidate genes for complementation when supplied with *Z. mobilis* *ispG* and *ispH*. An alternative approach is to develop a *Z. mobilis* strain where isoprenoid precursors can be supplied by the MVA pathway and use knockout or knockdowns to identify the relevant physiological electron donors. Another important question for the field is determine the binding site for the electron donors on IspH and IspG and whether it is located near the variable N termini or C-termini or IspH. X-ray crystal studies can be used to identify the binding site.

Why is *Z. mobilis* IspH function in *E. coli* so sensitive to O₂?

I was not able to answer this question because this would require additional experimental work to study the in vitro activity of this enzyme and compare to *E. coli* IspH and *Z. mobilis* IspG. However, I present some experiments or models to consider for future studies on this system. *Z. mobilis* IspH confers a severe O₂ sensitive growth phenotype under aerobic conditions compared to *E. coli* IspH. It is known that the [4Fe-4S] cluster of *E. coli* IspH is exposed to the solvent as the crystal structure in the absence of the substrate shows that H₂O is bound to the iron in the cluster that lacks a ligand. Previous studies indicate that this makes this iron is susceptible to oxidation, resulting in loss of one Fe atom to form a [3Fe-4S] cluster or eventually its complete degradation. Because this "labile" Fe atom of the [4Fe-4S] cluster of IspH coordinates with HMBDP^{7,8}, the presence of the substrate might have a protective role for *E. coli* IspH by reducing cluster access to O₂ and other small oxidants. We did not find a large difference in vitro in the rate

of O₂-dependent cluster loss between *E. coli* IspH and *Z. mobilis* IspH. However, additional experiments are needed with higher cluster occupied protein to measure cluster loss with and without substrate. In addition, the use of the iron chelator ferrene should be used to determine if the kinetics are biphasic and if loss the "labile" iron precedes total cluster degradation. This question can also be addressed in combination with EPR spectroscopy.

It is known that *E. coli* IspH, a facultative anaerobic bacterium is a Class B member of the four reported classes of IspH⁶ enzymes. IspH from *Z. mobilis* is also a member of Class B because of the aromatic residues found near the [4Fe-4S] cluster ligands, as well as the presence of a C-terminal extension. As a matter of fact, the C-terminal extension for *Z. mobilis* IspH is longer than that of *E. coli* IspH. Whether this difference leads to differential stability of the [4Fe-4S] clusters is unknown. A genetic selection for variants of *Z. mobilis* IspH with increased activity in *E. coli* grown aerobically should identify interesting protein variants, whose biochemical analysis could help establish the relationship between protein activity, cluster stability and substrate binding and the impact of O₂. Possibly the preference of *Z. mobilis* for anaerobic growth condition has put it on a slower trajectory for evolving a mechanism to protect its [4Fe-4S] cluster from oxidative degradation upon transitions to aerobic growth than *E. coli*.

In contrast, the [4Fe-4S] cluster of IspG is fully coordinated by protein side chains in the absence of substrate, which perhaps explains our observation that *Z. mobilis* IspG was less sensitive to O₂ than *Z. mobilis* IspH both in vitro and in vivo. However, we also found that in the presence of *Z. mobilis* IspG in vivo, the oxygen sensitivity of IspH is greatly reduced. It is known that the presence of HMBDP allows *E. coli* IspH to form a closed conformation and this

conformational state is more stable to oxidative damage than when it is in an open state. Thus, one interpretation of my results is that in the presence of IspG, more HMBDP is available to drive IspH into a closed conformation, protecting the cluster and active site from damaging oxidation.

Why does co-expression of IspG improve the function of IspH?

I showed the importance of IspG on the function of [4Fe-4S] cluster containing IspH under anaerobic conditions. We hypothesize that there is a functional linkage of IspH and its cognate partner protein IspG, although we do not know the mechanism. At this time, we have no evidence for complex formation between IspH and IspG, even though this would have been the most straight forward answer, leading to more substrate for IspH and increased cluster stability. However, more experiments should be pursued to consider whether the homologous electron donors (ferredoxins and/or flavodoxin) are required to detect a ternary complex. In addition, the tags on the proteins for the two-hybrid screen should be swapped to the opposite ends in case the tag interferes with an interaction. For example, we did not observe a positive two hybrid interaction between two IspG fusions even though they are dimers in solution. Two hybrid screens for IspG and IspH can also be performed in *Z. mobilis* as the native electron donor proteins are present which is a limitation in our current two hybrid screen strain. As the clusters of IspG and IspH are labile to oxidative damage and need to be in reduced state for catalytic function, it is possible that a complex will be more stable in its native organism; accordingly, experiments should be pursued in parallel in *Z. mobilis*. In our in vitro experiments, the cluster occupancy of IspG and IspH 4Fe was between 5-10% and we did not quantify the amount of [3Fe-4S] versus [4Fe-4S] in the mixture. The [3Fe-4S] cluster type would not have favored binding of HMBDP to the cluster of IspH which may have affected its conformation and possibly binding to IspG. Experiments to improve cluster occupancy

of IspG and IspH would be helpful for future in vitro interaction studies of IspG and IspH. Nevertheless, this species-specific preference for IspH and IspG suggest that IspG and IspH function have evolved together and may be driven by the need to protect the [4Fe-4S] cluster of IspH from oxidation.

Why IspG improves the growth toxicity of IspH under aerobic conditions?

In the presence of mevalonate, expression of *Z. mobilis* IspH confers an oxygen sensitive growth phenotype, despite the fact that isoprenoid precursors are being produced by the MVA pathway. This phenotype was rescued by the catalytically inactive mutant (E127A), which we designed based on previous studies¹⁰ of *E. coli* (E126A) IspH mutant. It is of particular interest that the aberrant activity of *Z. mobilis* IspH only occurs under aerobic conditions as well as in the absence of its cognate partner protein IspG. IspH is known to show acetylene hydratase activity and catalyze the conversion of acetylenes to aldehyde and ketone¹¹. This indicates that catalytic activity of IspH is promiscuous. Based on these reports of IspH activity, we reason that the oxygen sensitive growth phenotype for *Z. mobilis* IspH in the presence of mevalonate results from a promiscuous activity, producing an inhibitory compound under aerobic conditions. Further experiments to identify the promiscuous products made by *Z. mobilis* IspH can be addressed by performing metabolomics under aerobic conditions. Indeed, co-expression of IspG and IspH rescues this phenotype under aerobic conditions in the presence of mevalonate, which supports the notion protecting the active site from O₂ via IspG, prevents this promiscuous activity of IspH. It also raises the question of whether the *Z. mobilis* physiological electron donor would also mitigate the phenotype of *Z. mobilis* IspH if shifting the cluster to its reduced state decreases the promiscuous function. This can be addressed in our *E. coli* MVA+ strain.

Taken together, my work highlights the importance of the species-specific function of IspG and IspH, although the mechanism remains unknown. Future experiments should address this mechanism, using as a guide some of the ideas provided in this chapter. A major unanswered question is whether IspG and IspH form a higher order complex to explain the species specificity. This functional importance of *Z. mobilis* IspG with IspH may reflect that IspG and IspH could have evolved together as oxygen became more prominent in the environment making the [4Fe-4S] cluster of IspH and IspG subjective to oxidative damage. This knowledge is central to understand the function of *Z. mobilis* IspG and IspH under aerobic conditions and if replacing and/or engineering these unique [4Fe-4S] containing enzymes of the MEP pathway in *Z. mobilis* with more stable [4Fe-4S] cluster variants to improve stress tolerance may improve the flux through the pathway to produce isoprenoid precursors.

REFERENCES

1. Beinert H, Kennedy MC, Stout CD. Aconitase as Ironminus signSulfur Protein, Enzyme, and Iron-Regulatory Protein. *Chem Rev.* 1996;96(7):2335-2374.
2. Beinert H, Holm RH, Munck E. Iron-sulfur clusters: nature's modular, multipurpose structures. *Science.* 1997;277(5326):653-659.
3. Ciurli S, Musiani F. High potential iron-sulfur proteins and their role as soluble electron carriers in bacterial photosynthesis: tale of a discovery. *Photosynth Res.* 2005;85(1):115-131.
4. Flint DH, Tuminello JF, Miller TJ. Studies on the synthesis of the Fe-S cluster of dihydroxy-acid dehydratase in escherichia coli crude extract. Isolation of O-acetylserine sulfhydrylases A and B and beta-cystathionase based on their ability to mobilize sulfur from cysteine and to participate in Fe-S cluster synthesis. *J Biol Chem.* 1996;271(27):16053-16067.
5. Bruschi M, Guerlesquin F. Structure, function and evolution of bacterial ferredoxins. *FEMS Microbiol Rev.* 1988;4(2):155-175.
6. Rao G, Oldfield E. Structure and Function of Four Classes of the 4Fe-4S Protein, IspH. *Biochemistry.* 2016;55(29):4119-4129.
7. Grawert T, Span I, Eisenreich W, et al. Probing the reaction mechanism of IspH protein by x-ray structure analysis. *Proc Natl Acad Sci U S A.* 2010;107(3):1077-1081.
8. Rekitke I, Jomaa H, Ermler U. Structure of the GcpE (IspG)-MEcPP complex from *Thermus thermophilus*. *FEBS Lett.* 2012;586(19):3452-3457.

9. Atkinson JT, Campbell I, Bennett GN, Silberg JJ. Cellular Assays for Ferredoxins: A Strategy for Understanding Electron Flow through Protein Carriers That Link Metabolic Pathways. *Biochemistry*. 2016;55(51):7047-7064.
10. Wang W, Wang K, Liu YL, et al. Bioorganometallic mechanism of action, and inhibition, of IspH. *Proc Natl Acad Sci U S A*. 2010;107(10):4522-4527.
11. Span I, Wang K, Wang W, et al. Discovery of acetylene hydratase activity of the iron-sulphur protein IspH. *Nat Commun*. 2012;3:1042.

Appendix 1
Supplemental material for Chapter 2

Bacterial strains, plasmids and primers used in this study are listed in Tables 1-3

Table A-1 List of *E. coli* strains used in the study in Chapter 2

Strain No.	Description	Source
PK13556	MG1655 <i>putP::P_{BAD} yPMD, hPMK, yMVK, ecIDI, lacZ, lacY, lacA</i>	This study
PK9012	MG1655 Δ <i>mutS::Tn10 λc1857 Δcro-bioA</i>	Lab collection ²³
PK13557	MG1655 Δ <i>mutS::Tn10 λc1857 Δcro-bioA P_{BAD} yPMD, hPMK, yMVK, ecIDI, lacZ, lacY, lacA</i>	This study
PK13566	MG1655 <i>P_{BAD} yPMD, hPMK, yMVK, ecIDI, lacZ, lacY, lacA ΔispH::cat</i>	This study
PK13567	PK9012 <i>P_{BAD} yPMD, hPMK, yMVK, ecIDI, lacZ, lacY, lacA ΔispG::cat</i>	This study
PK14317	MG1655 <i>P_{BAD} yPMD, hPMK, yMVK, ecIDI, ΔlacZ,Y,A::tet</i>	This study
PK 9776	MG1655 Δ <i>lacY</i>	Lab collection
PK 14463	MG1655 <i>P_{BAD} yPMD, hPMK, yMVK, ecIDI, ΔlacZ,Y,A::tet ΔlacY</i>	This study
PK14464	MG1655 <i>P_{BAD} yPMD, hPMK, yMVK, ecIDI, ΔlacZ,Y,A::tet ΔlacY ΔispH::cat</i>	This study
PK14465	MG1655 <i>P_{BAD} yPMD, hPMK, yMVK, ecIDI, ΔlacZ,Y,A::tet ΔlacY ΔispG::cat</i>	This study
PK 14478	PK 14464 with pPK13573	This study
PK 14467	PK14464 with pPK13574	This study
PK 14468	PK14464 with pPK13635	This study
PK 14473	PK14465 with pPK13575	This study
PK 14474	PK 14465 with pPK13576	This study
PK 14487	MG1655 <i>P_{BAD} yPMD, hPMK, yMVK, ecIDI, ΔlacZ,Y,A::tet ΔispG, ΔispH::cat, ΔlacY</i>	
PK 14488	PK 14487 with pPK 13635	This study
PK 14489	PK 14487 with pPK 13636	This study
PK 14490	PK 14487 with pPK 13985	This study
PK 14494	PK 14487 with pPK 13986	This study
PK 14498	PK 14464 with pPK 13612	This study
PK 14499	PK 14487 with pPK 14414	This study

PK 14481	PK 14464 with pPK13616	This study
PK 14483	PK 14464 with pPK14414	This study
PK 14484	PK 14465 with pPK13614	This study
PK 14486	PK 14465 with pPK13618	This study
PK 13681	BL21 (DE3) $\Delta him::tet \Delta iscR::kan$ pBADsuf	Lab collection
PK 13654	PK 13681 with pPK13650	This study
PK 16191	MG1655, <i>kan-Pf_{nr}-suf_{EC}</i>	This study
PK 14842	MG1655 <i>P_{BAD} yPMD, hPMK, yMVK, ecIDI, $\Delta lacZ, Y, A::tet \Delta lacY \Delta ispH::cat$, kan-Pf_{nr}-suf_{EC}</i>	This study
PK 14843	PK 14842 pPK13574	This study
PK 14844	PK 14842 pPK13635	This study
PK 14849	PK 14842 with pPK13573	This study
PK 14862	MG1655 <i>P_{BAD} yPMD, hPMK, yMVK, ecIDI, $\Delta lacZ, Y, A::tet \Delta lacY \Delta ispH::cat$, kan-Pf_{nr}-suf_{ZM}</i>	This study
PK 14869	PK 14862 pPK13574	This study
PK 14870	PK 14862 pPK13574	This study
PK 14871	PK 14862 pPK13574	This study

Table A-2 List of plasmids used in the study in Chapter 2

Plasmid No.	Description	Source
pPK 15435	pRL814 broad host range plasmid	Lab collection ²
pPK13573	pRL814 with <i>E. coli ispH</i>	This study
pPK13574	pRL814 with <i>Z. mobilis ispH</i>	This study
pPK13575	pRL814 with <i>E. coli ispG</i>	This study
pPK13576	pRL814 with <i>Z. mobilis ispG</i>	This study
pPK13635	pRL814 with <i>Z. mobilis ispH</i> and <i>ispG</i>	This study
pPK13636	pRL814 with <i>E. coli ispH</i> and <i>ispG</i>	This study
pPK13985	pRL814 with <i>E. coli ispH</i> and <i>Z. mobilis ispG</i>	This study
pPK13986	pRL814 with <i>Z. mobilis ispH</i> and <i>E. coli ispG</i>	This study
pPK 13612	pRL814 with <i>E. coli ispH</i> Strep Tag II	This study
pPK 13614	pRL814 with <i>E. coli ispG</i> Strep Tag II	This study
pPK 13616	pRL814 with <i>Z. mobilis ispH</i> Strep Tag II	This study
pPK 13618	pRL814 with <i>Z. mobilis ispG</i> Strep Tag II	This study
pPK 14414	pRL814 with <i>Z. mobilis ispH</i> Strep Tag II and <i>ispG</i>	This study
pPKD321	FRT- <i>cat</i> -FRT	BL Wanner

Table A-3 List of primers used in the study in Chapter 2

Primer number	Primer sequence (5'-3')
1a	CTCCTTCTTAAGAAAGATTCAGGTTTCATACAAAGGAGGACGGATAT GCAGATCCTGTTGGCCAACC
1b	GCGTGTCGACTTAATCGACTTCACGAATATC
1c	CTCCTTCTTAAGAAAGATTCAGGT
2a	CTCCTTCTTAAGAAAGATTCAGGTTTCATACAAAGGAGGACGGATGT GATAAAAATCATTCTGGCTC
2b	GCGTGTCGACTCAAGCCTCCTGTTCTGTATC
2c	CTCCTTCTTAAGAAAGATTC
3a	CTCCTTCTTAAGCTGAAATTAGTTTAGGAGAAAGAATATGCATAACCA GGCTCCAATTC
3b	GCGTGTCGACTTATTTTCAACCTGCTGA
3c	CTCCTTCTTAAGCTGAAATT
4a	CTCCTTCTTAAGCTGAAATTAGTTTAGGAGAAAGAATATGTCCATTCG TCCTTGGCGCC
4b	GCGTGTCGACTTATTCGGCGGCGACCGTGGC
4c	CTCCTTCTTAAGCTGAAATT
5a	TGCTGGAAATCGATCCGGCACTGGAGGCGTAACATGATTCCGGGGATC CGTCGACC

5b	GTATTTTCGCATAACTTAGGCTGCTAATGACTTAATGTGTAGGCTGGAG CTGCTTC
6a	GCAGTAACAGACGGGTAACGCGGGAGATTTTTCATGATTCCGGGGATC CGTAGACC
6b	CACGGGAAGCGAGGCGCTTCCCATCACGTTATTATTGTGTAGGCTGGAG CTGCTTC
7a	GCTTGATATCGAATTCCTG
7b	TTACTCGAGTTTGTAGAGC
8a	AGCTCTACAACTCGAGTAACTGAAATTAGTTTAGGAGAAAGAATATG TCCATTCG
8b	GCAGGAATTCGATATCAAGCTTATTCGGCGGGCACCCT
9a	AGCTCTACAACTCGAGTAACTGAAATTAGTTTAGGAGAAAG
9b	GCAGGAATTCGATATCAAGCTTATTTTCAACCTGCTGAAC
10a	GCCGAATAAGCTTGATATCGAATTCCTGCAGC
10b	AACTAATTTAGAGTTAAATCGACTTCACGAATATCGACAC
11a	AGTCGATTAAGCTCTGAAATTAGTTTAGGAGAAAGAATATGTCCATTCGT
11b	GATATCAAGCTTATTCGGCGGGCACC
12a	GTTGAAAATAAGCTTGATATCGAATTCCTGCAGC
12b	CTAATTTAGACTCAAGCCTCCTGTTCTGTATCG
13a	GCTTGAGTCTGAAATTAGTTTAGGAGAAAGAATATGCATAACCAGG
13b	TCGATATCAAGCTTATTTTCAACCTGCTG
14a	CATCCTCAATTTGAAAATAACGACACAATCTGTCCTTTC
14b	CGACCAGCCGCCAAAGCAGCCAGCCTCCTGTTCTGTATC
15a	CATCCTCAATTTGAAAATAACGACACAATCTGTCCTTTC
15b	CGACCAGCCGCCAAAGCAGCCATCGACTTCACGAATATCGAC
16a	CATCCTCAATTTGAAAATAACGACACAATCTGTCCTTTCG
16b	CGACCAGCCGCCAAAGCAGCCTTCGGCGGGCACC
17a	CATCCTCAATTTGAAAATAACGACACAATCTGTCCTTTCG
17b	CGACCAGCCGCCAAAGCAGCCTTCGGCGGGCACC
18a	AGATATACATGTGATAAAAATCATTCTGGC
18b	CTTTCGGGCTTATTTTCAAATTGAGGATGC
19a	AGCCCGAAAGGAAGCTGAG
19b	ATGTATATCTCCTTCTTAAAGTTAAACAAAATTATTTCTAG

Table A1-4. Strains used in the study in Appendix 2

Strain No.	Description	Source
PK 7564	MG1655 <i>kan-PsodA-lacZ</i>	This study
PK 12028	MG1655 <i>kan-PfepB-lacZ</i>	This study
PK 12029	MG1655 <i>kan-PfepB-lacZ, Δfnr</i>	This study
PK 7573	MG1655 <i>kan-PhyaA-lacZ</i>	Nesbit et. al, ¹¹
PK 6886	MG1655 <i>kan-PhyaA-lacZ, ΔiscR</i>	Nesbit et. al, ¹¹
PK 11099	Long <i>PsufA</i> (bp -393 to +90)- <i>lacZ</i> fusion, <i>Δfur</i>	Mettert et. al, ⁵
PK 11100	Long <i>PsufA</i> (bp -393 to +90)- <i>lacZ</i> fusion, <i>Δfur, ΔiscR</i>	Mettert et. al, ⁵
PK 10864	Short <i>PsufA</i> (bp -200 to +40)- <i>lacZ</i> fusion, <i>Δfur,</i>	Mettert et. al, ⁵
PK 10865	Short <i>PsufA</i> (bp -200 to +40)- <i>lacZ</i> fusion, <i>Δfur, ΔiscR</i>	Mettert et. al, ⁵
PK 14034	PK 7573 with pRL814 plasmid	This study
PK 14035	PK 7573 with <i>E. coli</i> IspH in pRL814 plasmid	This study
PK 14036	PK 7573 with <i>Z. mobilis</i> IspH in pRL814 plasmid	This study
PK 14037	PK 6886 with pRL814 plasmid	This study
PK 14038	PK 6886 with <i>E. coli</i> IspH in pRL814 plasmid	This study
PK 14039	PK 6886 with <i>Z. mobilis</i> IspH in pRL814 plasmid	This study
PK 14040	PK 12028 with pRL814 plasmid	This study
PK 14041	PK 12028 with <i>E. coli</i> IspH in pRL814 plasmid	This study
PK 14042	PK 12028 with <i>Z. mobilis</i> IspH in pRL814 plasmid	This study
PK 14043	PK 12029 with pRL814 plasmid	This study
PK 14044	PK 12029 with <i>E. coli</i> IspH in pRL814 plasmid	This study
PK 14045	PK 12029 with <i>Z. mobilis</i> IspH in pRL814 plasmid	This study

PK 14046	PK 11099 with pRL814 plasmid	This study
PK 14047	PK 11099 with <i>E. coli</i> IspH in pRL814 plasmid	This study
PK 14048	PK 11099 with <i>Z. mobilis</i> IspH in pRL814 plasmid	This study
PK 14000	PK 7564 with pRL814 plasmid	This study
PK 14001	PK 7564 with <i>Z. mobilis</i> IspH in pRL814 plasmid	This study
PK 14025	PK 7564 with <i>E. coli</i> IspH in pRL814 plasmid	This study
PK 14049	PK 7564 with <i>Z. mobilis</i> IspH & IspG in pRL814 plasmid	This study
PK 14050	PK 11100 with pRL814 plasmid	This study
PK 140451	PK 11100 with <i>E. coli</i> IspH in pRL814 plasmid	This study
PK 140452	PK 11100 with <i>Z. mobilis</i> IspH in pRL814 plasmid	This study
PK 140453	PK 10865 with pRL814 plasmid	This study
PK 140454	PK 10865 with <i>E. coli</i> IspH in pRL814 plasmid	This study
PK 140455	PK 10865 with <i>Z. mobilis</i> IspH in pRL814 plasmid	This study
PK 140456	PK 10864 with pRL814 plasmid	This study
PK 140457	PK 10864 with <i>E. coli</i> IspH in pRL814 plasmid	This study
PK 140458	PK 10864 with <i>Z. mobilis</i> IspH in pRL814 plasmid	This study
PK 13681	BL21 (DE3) $\Delta him::tet \Delta iscR::kan$ pBADsuf	Lab collection
PK 13654	BL21 (DE3) $\Delta him::tet \Delta iscR::kan$ pBADsuf with pPK13650	This study
PK 13652	BL21 (DE3) $\Delta him::tet \Delta iscR::kan$ pBADsuf with pPK13648	This study

PK 13655	BL21 (DE3) $\Delta him::tet$ $\Delta iscR::kan$ pBAD _{suf} with pPK13651	This study
----------	---	------------

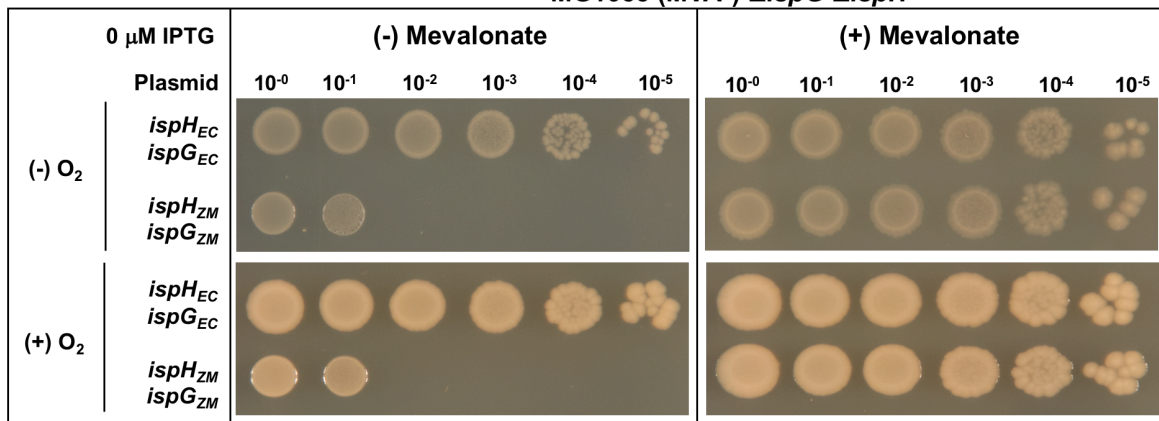
Table A1-5. Plasmids used in the study in Appendix 2

Plasmid No.	Description	Source
pPK 13712	pRL814 broad host range plasmid, Δgfp	This study
pPK13573	pRL814 with <i>E. coli ispH</i>	This study
pPK13574	pRL814 with <i>Z. mobilis ispH</i>	This study
pPK13536	pRL814 with <i>Z. mobilis ispH</i> & <i>ispG</i>	This study
pPK 13648	<i>E. coli ispH</i> strep-tag II in pET11a	This study
pPK 13650	<i>Z. mobilis ispH</i> strep-tag II in pET11a	This study
pPK 13651	<i>Z. mobilis ispG</i> strep-tag II in pET11a	This study

Figure A1-1. Viability of cells assayed under aerobic and anaerobic conditions

MG1655 (MVA⁺) $\Delta ispG \Delta ispH$ with plasmid variants containing *ispG* and *ispH* from *Z. mobilis* (*ispH_{ZM} ispG_{ZM}*) or *E. coli* (*ispH_{EC} ispG_{EC}*) were grown in LB with mevalonate, arabinose and spectinomycin.

A

MG1655 (MVA⁺) Δ *ispG* Δ *ispH*

B

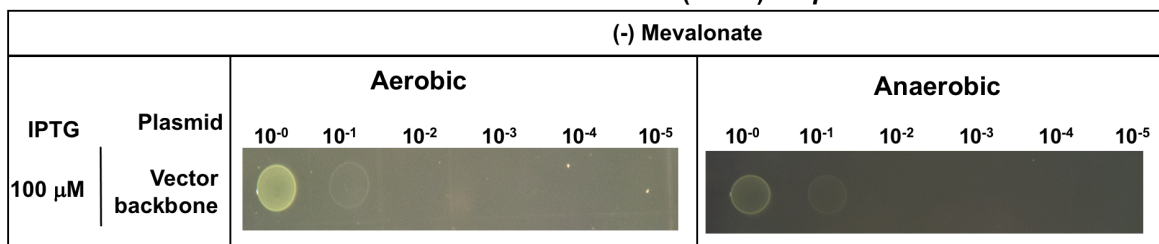
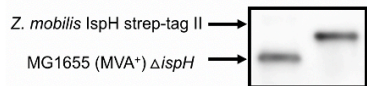
MG1655 (MVA⁺) Δ *ispH*

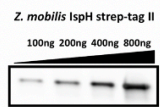
Figure A1-2. Optimization of the detection of IspH in cell extracts

(A) Detection of protein band cross-reacting with the strep-tag II antibody in MG1655 (MVA⁺) $\Delta ispH$ which lacks plasmid overexpressing IspH or IspG. (B) Increasing concentrations of isolated *Z. mobilis* IspH with strep-tag II at C terminus separated on SDS-PAGE, transferred to nitrocellulose membrane and probed with antibody against strep-tag II. The blot was imaged using an Azure imager. (C) The blot was quantified using the Azure spot pro software and strep-tag II isolated *Z. mobilis* IspH was detected in a linear range between 100-800 ng protein concentration. (D) Increasing concentration of MG1655 (MVA⁺) $\Delta ispH$ with *Z. mobilis* IspH strep-tag II at C-terminus was over expressed and probed with antibody against strep-tag II along with increasing concentration of isolated *Z. mobilis* IspH with strep-tag II at C terminus. (E) The blot was quantified and *Z. mobilis* IspH strep-tag II was detected in MG1655 (MVA⁺) $\Delta ispH$ in a linear range between 300-900 ng concentration.

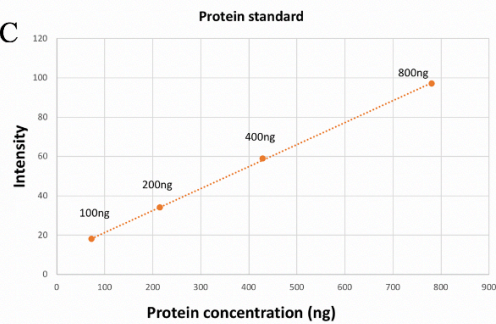
A



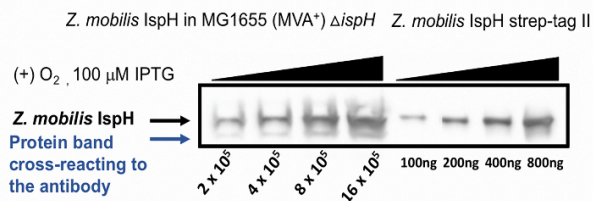
B



C



D



E

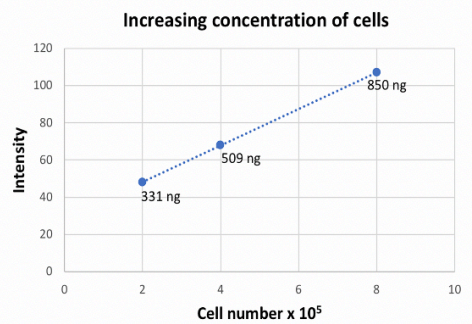


Figure A1-3. Blot with increasing IPTG concentration for *E. coli* strains

(A) MG1655 (MVA⁺) Δ *ispH* with *Z. mobilis* IspH strep-tag II at C-terminus **(B)** MG1655 (MVA⁺) Δ *ispH* with *E. coli* IspH strep-tag II at C-terminus **(C)** MG1655 (MVA⁺) Δ *ispG* with *Z. mobilis* IspG strep-tag II at C-terminus **(D)** MG1655 (MVA⁺) Δ *ispG* with *E. coli* IspG strep-tag II at C-terminus was over expressed with increasing IPTG concentration (25 μ M, 50 μ M, 100 μ M, 200 μ M) under aerobic and anaerobic conditions, separated on SDS-PAGE, transferred to nitrocellulose membrane and probed with antibody against strep-tag II. The blot was imaged using an Azure imager.

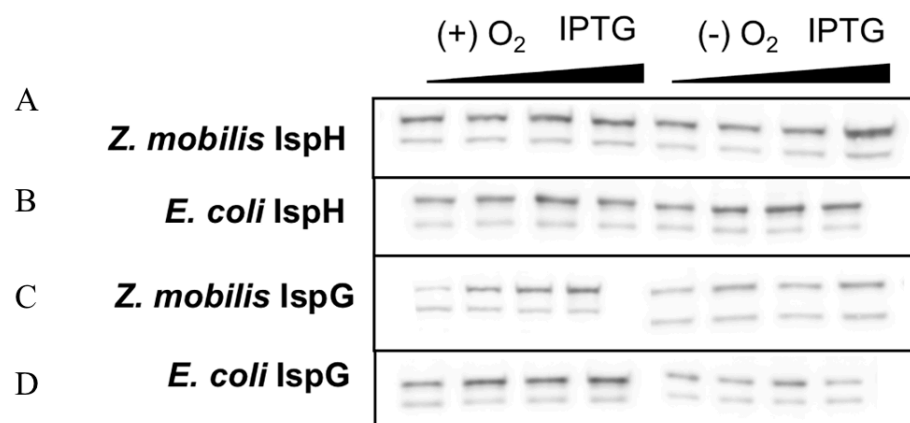


Figure A1-4. Mean values of IspH and IspG protein levels quantified by antibody against strep-tag II under anaerobic conditions

IspH and IspG strep-tag II in MG1655 (MVA⁺) $\Delta ispH$, $\Delta ispG$, $\Delta ispG \Delta ispH$ under anaerobic conditions. Data represent averages of protein levels from at least three replicates. Error bar show standard errors of the mean.

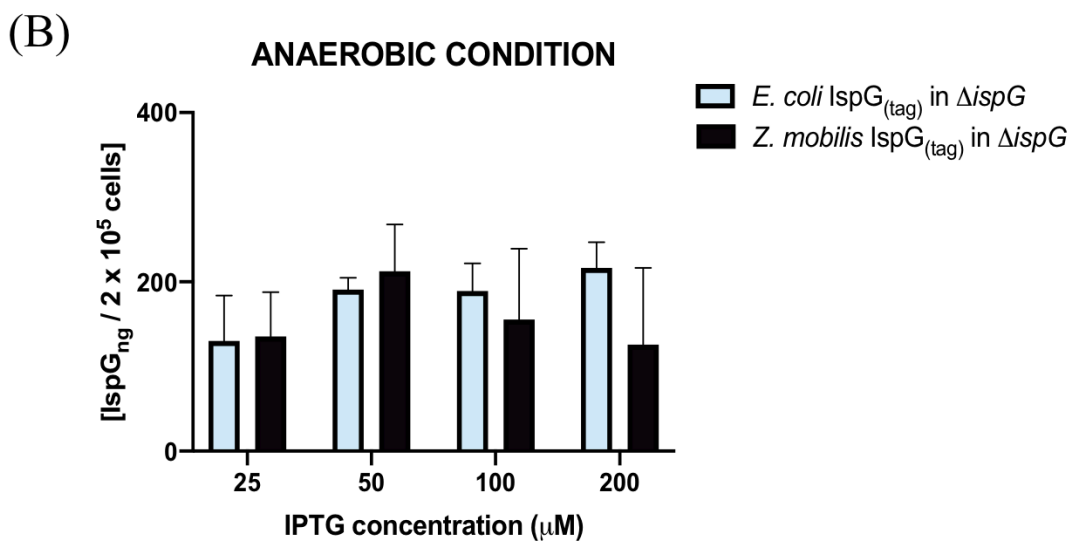
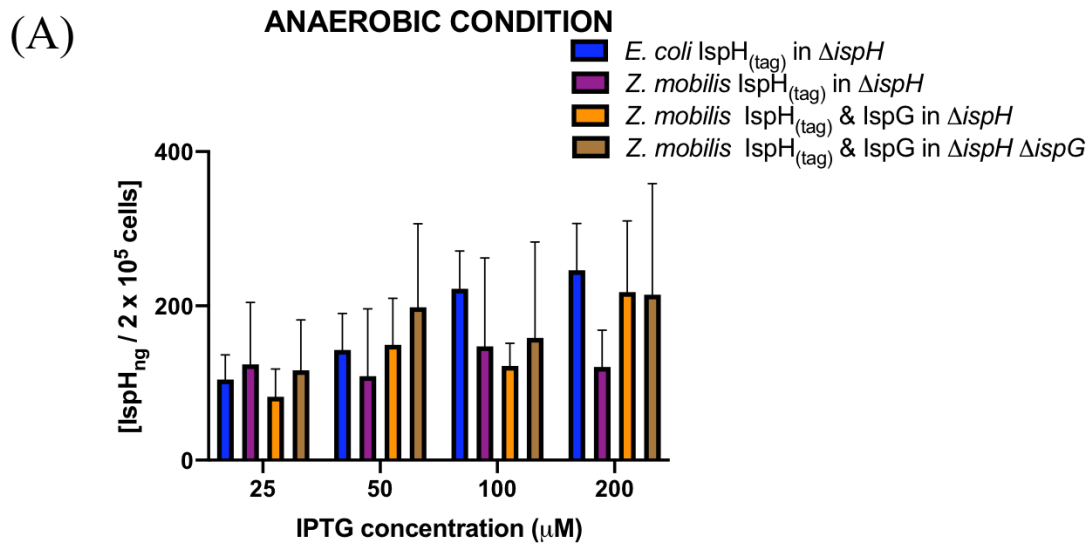


Figure A1-5. Mean values of IspH and IspG protein levels quantified by antibody against strep-tag II under aerobic conditions

IspH and IspG strep-tag II in MG1655 (MVA⁺) $\Delta ispH$, $\Delta ispG$, $\Delta ispG \Delta ispH$ under aerobic conditions. Data represent averages of protein levels from at least three replicates. Error bar show standard errors of the mean.

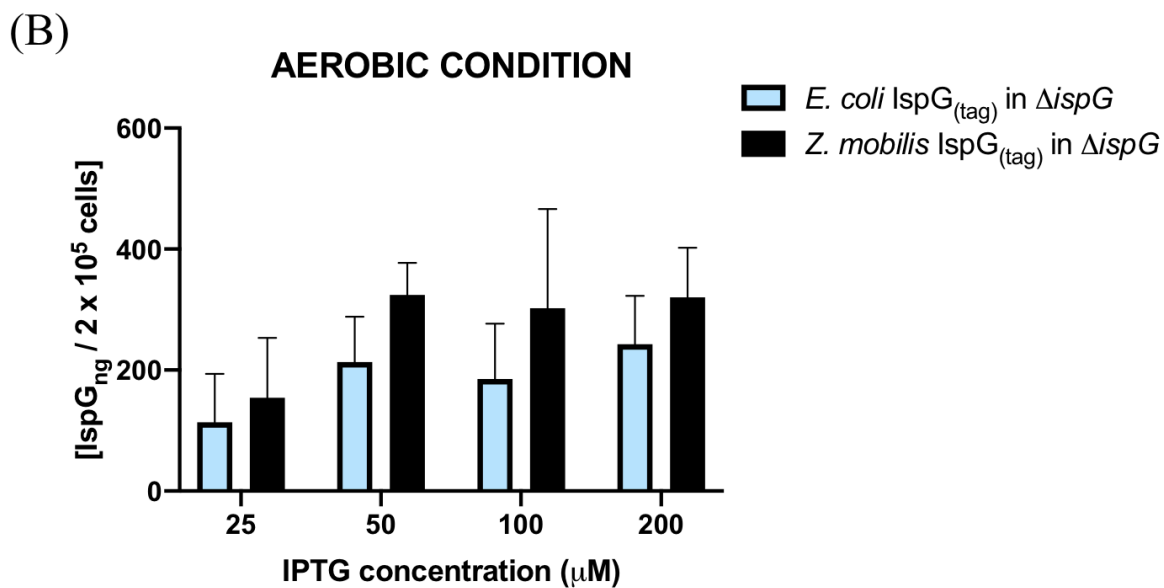
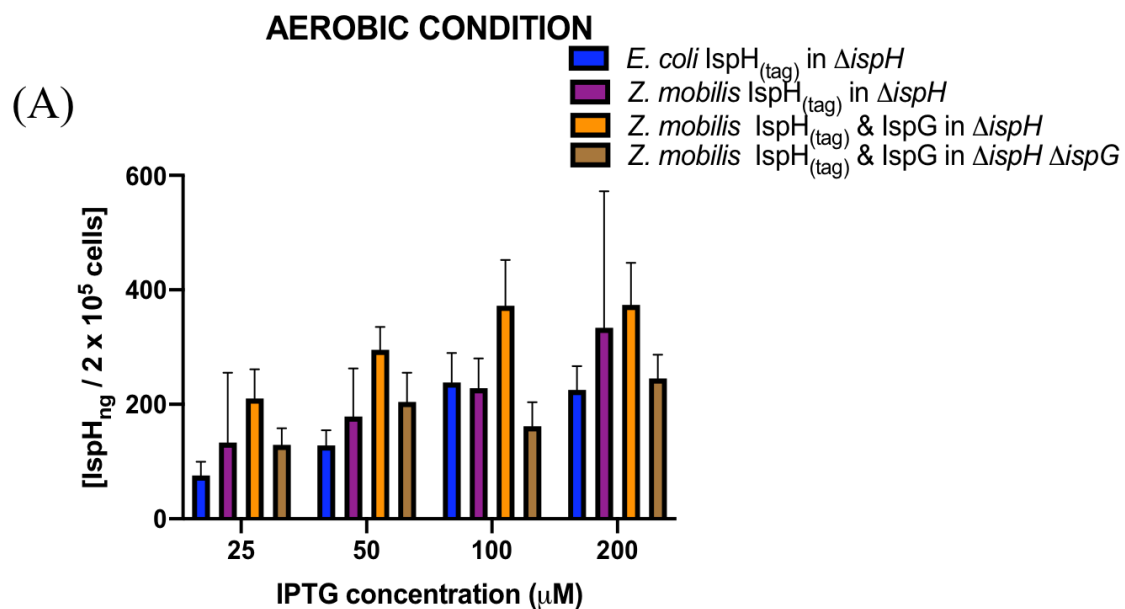


Figure A1-6. Viability of cells assayed at 100 & 200 μ M IPTG under aerobic and anaerobic conditions

MG1655 (MVA⁺) with plasmid variants containing *ispH* from *Z. mobilis* (*ispH_{ZM}*) or with point mutations E127A or C13A were grown in LB with mevalonate, arabinose and spectinomycin.

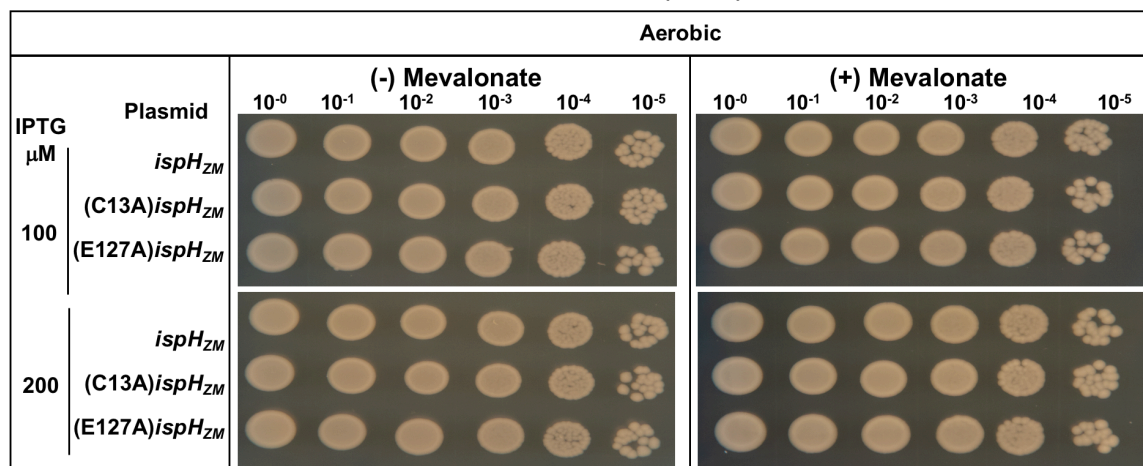
MG1655 (MVA⁺)

Figure A1-7. Comparison of Suf D levels under aerobic conditions.

MG1655 (MVA⁺) Δ *ispH* and MG1655 (MVA⁺) Δ *ispH* *P*_{fur}, *suf*_{EC} were grown under aerobic conditions. Equivalent amount of cell lysates was separated on SDS-PAGE, transferred to nitrocellulose membrane and probed with antibody against Suf D. The blot was imaged using an Azure imager.

MG1655 (MVA⁺)
 Δ ispH, P_{fm} *sufl*_{EC}
MG1655 (MVA⁺)
 Δ ispH

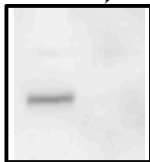


Figure A1-8. Multiple sequence alignment of *E. coli* and *Z. mobilis* IspG.

The residues (Cys, Glu) that ligand the [4Fe-4S] cluster is in red box and the catalytic Glu is in blue box. The percent identity between the two sequences is 48.4%.

Figure A1-9. Multiple sequence alignment of *E. coli* and *Z. mobilis* IspH.

The residues (Cys) that ligand the [4Fe-4S] cluster is in red box and the catalytic Glu is in blue box. The percent identity between the two sequences is 52.5%.

REFERENCES

1. Beauchene NA, Mettert EL, Moore LJ, Keles S, Willey ER, Kiley PJ. O₂ availability impacts iron homeostasis in *Escherichia coli*. *Proc Natl Acad Sci U S A*. 2017;114(46):12261-12266.
2. Ghosh IN, Martien J, Hebert AS, et al. OptSSeq explores enzyme expression and function landscapes to maximize isobutanol production rate. *Metab Eng*. 2019;52:324-340.

Appendix 2

Additional assays of *Z. mobilis* IspH and IspG

This appendix contains preliminary results that may inform future approaches on this project. The first part describes results using defined transcriptional reporters to determine if overexpression of *Z. mobilis* IspH was causing oxidative stress in *E. coli*. The second part describes results using ferrene to confirm that the cluster was completely degraded versus just losing one iron of cluster. The third part describes results with tagged IspH and IspG in pull down experiments to assay for a physical interaction. None of the results obtained thus far were conclusive.

1. Does IspH overexpression induce oxidative stress in *E. coli*?

Bacteria use relatively conserved mechanisms to counteract the damaging effects of O₂ and its derived reactive oxygen species (ROS). One such mechanism is the action of the enzyme superoxide dismutase, which catalyzes the dismutation of superoxide to hydrogen peroxide and oxygen. In *E. coli*, *sodA* encodes the Mn²⁺ containing superoxide dismutase and its regulation under aerobic conditions occurs by various transcription factors. IscR, the regulator of the Isc and Suf Fe-S cluster biogenesis pathways, also regulates *sodA* expression by acting as an activator under aerobic conditions^{4,5}. Fur (ferric uptake regulator) represses *sodA* transcription when Fe²⁺ is readily available¹⁻³. SoxS also acts as an activator of *sodA* in response to redox cycling agents that increase superoxide. In addition to SoxS, IscR also plays a role in the upregulation of *sodA* in response superoxide generating redox cycling agents.

Under aerobic conditions, expression of *PsodA-lacZ* increases ~2-fold when expression of *Z. mobilis* IspH is induced, compared to the vector only control (A2-1A). Under anaerobic conditions, expression of *PsodA-lacZ* is low, as expected, and expression of *ispH* has no effect.

One interpretation of this result is that O₂ destabilizes the [4Fe-4S] of the cluster of IspH, increasing free Fe, which could increase ROS, increasing expression of *PsodA*. Anaerobic conditions where the [4Fe-4S] cluster of IspH is presumed stable does not induce this promoter. Expression of *E. coli* IspH does not induce *sodA* expression under aerobic conditions, suggesting its [4Fe-4S] cluster is more stable to O₂ compared to its *Z. mobilis* counterpart or that more substrate is bound in the active site, which should be protective against degradation. Co-expression of IspG & IspH decreased the expression of *sodA* promoter under aerobic conditions, which perhaps indicates an increase in substrate (HMBDP) bound to *Z. mobilis* IspH in the presence of IspG. However, this effect was small. Lastly, expression of P *fepB*, which is regulated by Fur, does not change significantly in the presence of *Z. mobilis* IspH, making it difficult to argue there is an increase in free iron from the cluster (A2-1B).

Figure A2-1 β - galactosidase assay of *PsodA* upon expression of IspH and IspG under aerobic and anaerobic conditions

(A) MG1655 *psodA-lacZ* with the plasmid variants overexpressing *E. coli* IspH, *Z. mobilis* IspH and *Z. mobilis* IspG and IspH were grown in MOPS minimal media until OD 0.4 and beta-galactosidase assay was performed after cells lysis. Vector backbone was used as a control. Error bars represent standard error of three replicate datasets.

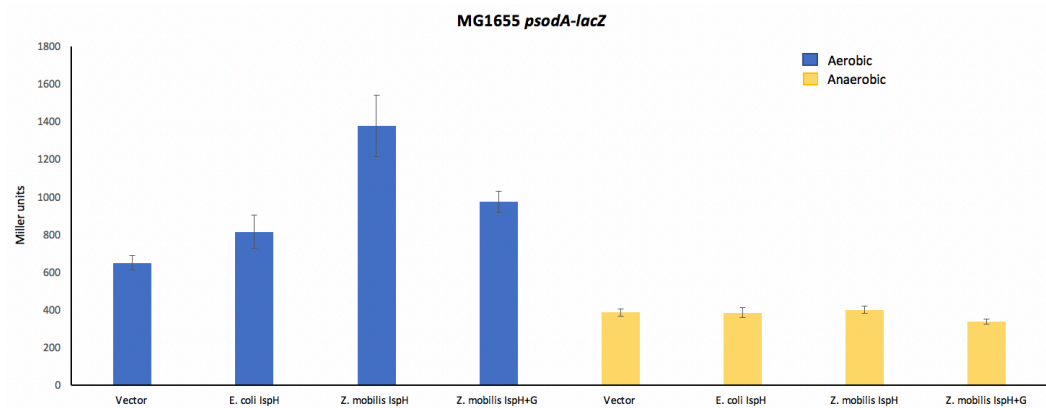
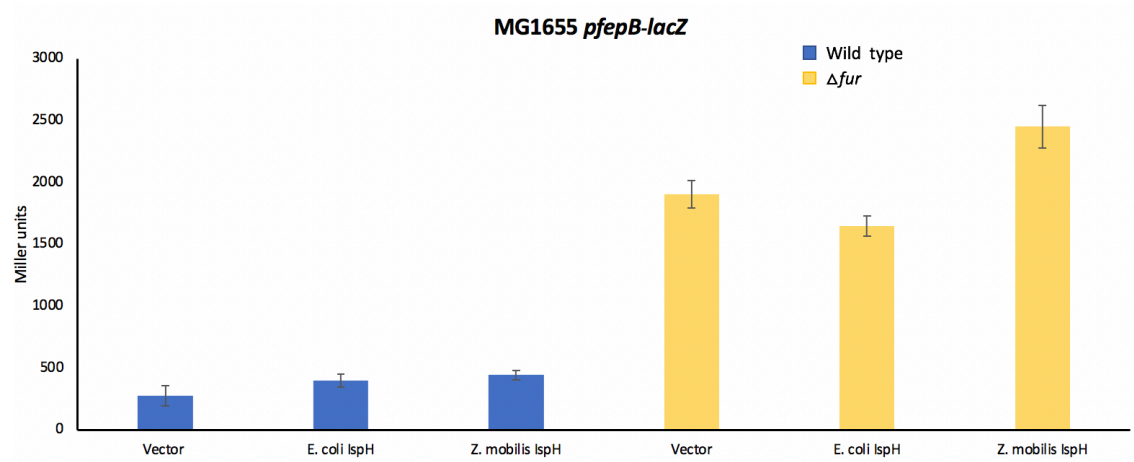


Figure A2-1 β - galactosidase assay of Fur regulated promoter under aerobic conditions

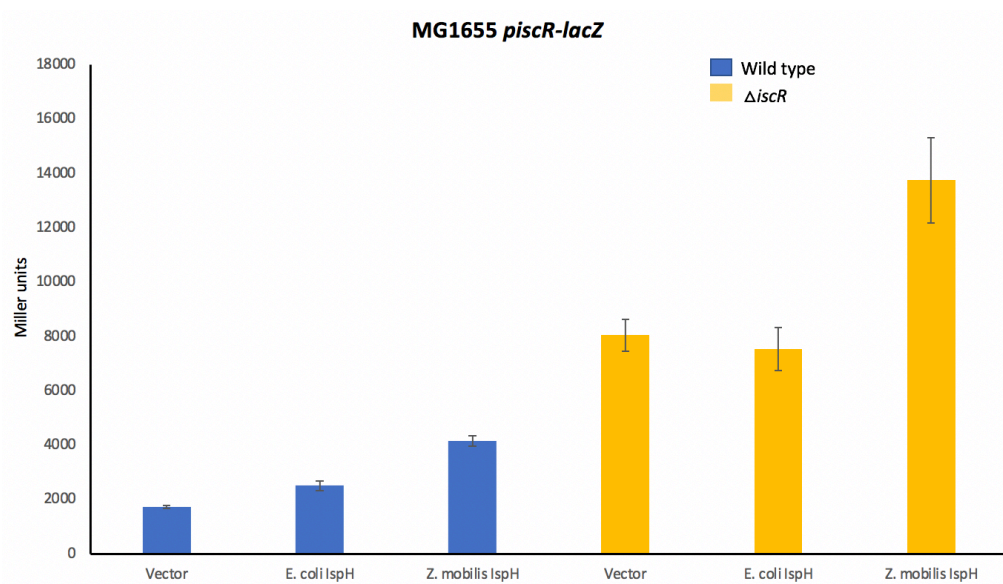
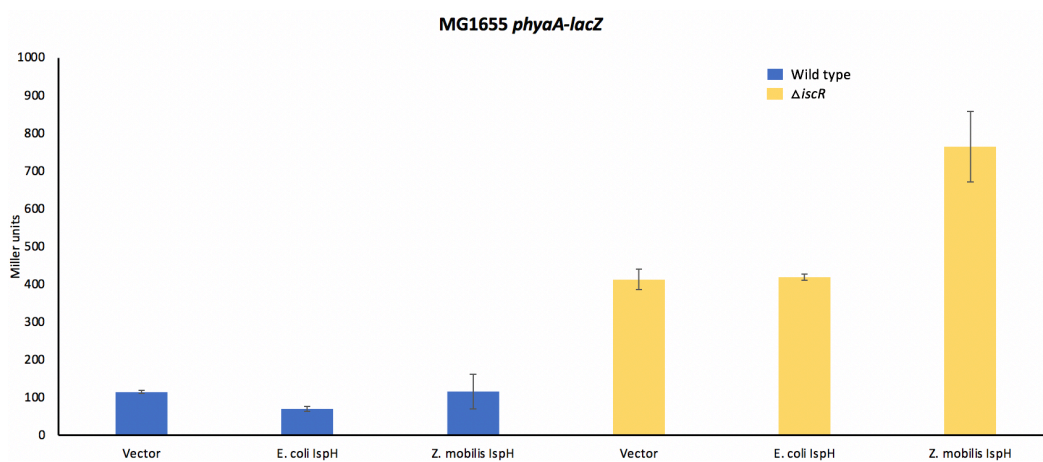
(B) MG1655 *pfepB-lacZ* with the plasmid variants overexpressing *E. coli* IspH, *Z. mobilis* IspH were grown in MOPS minimal media until OD 0.4 and beta-galactosidase assay was performed after cells lysis. Vector backbone was used as a control. Error bars represent standard error of three replicate datasets.



IscR regulates expression of the Isc and Suf Fe-S cluster biogenesis pathway. IscR represses the transcription of the *isc* operon under anaerobic conditions. Under oxidative stress IscR upregulates the expression of the *isc* and the *suf* pathway. We found that expression of *iscR* and *hyaA* promoter increased during overexpression of *Z. mobilis* IspH under aerobic growth conditions (A2-1C, D). Although the trends observed suggest that IscR activation would be required to synthesize Fe-S clusters and replace the damaged clusters of IspH, the overall effects were quite small.

Figure A2-1 β - galactosidase assay of *PiscR* and *PhyaA* upon expression of IspH under aerobic conditions

(C, D) MG1655 *piscR-lacZ*, *phyaA-lacZ* with the plasmid variants overexpressing *E. coli* IspH, *Z. mobilis* IspH were grown in MOPS minimal media until OD 0.4 and beta-galactosidase assay was performed after cells lysis. Vector backbone was used as a control. Error bars represent standard error of three replicate datasets.

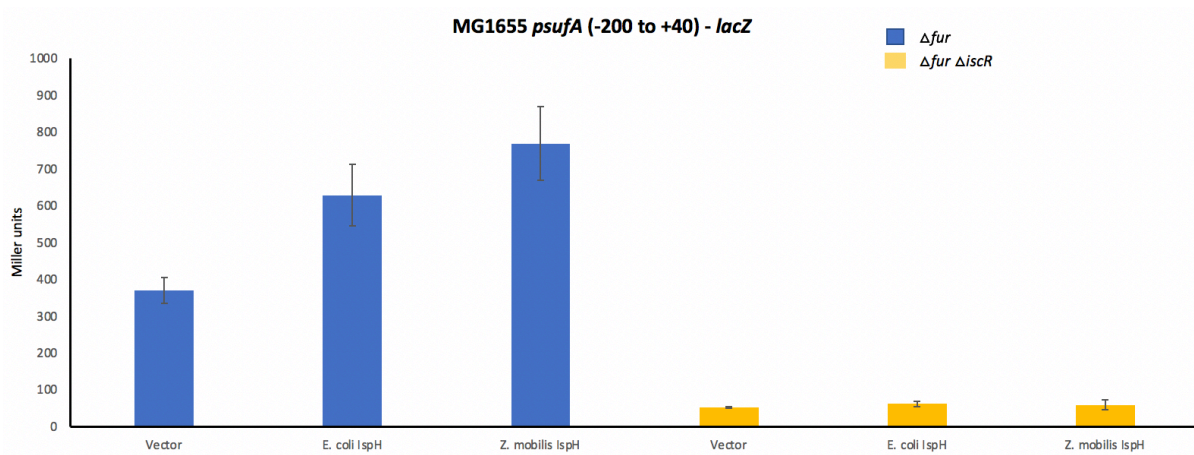
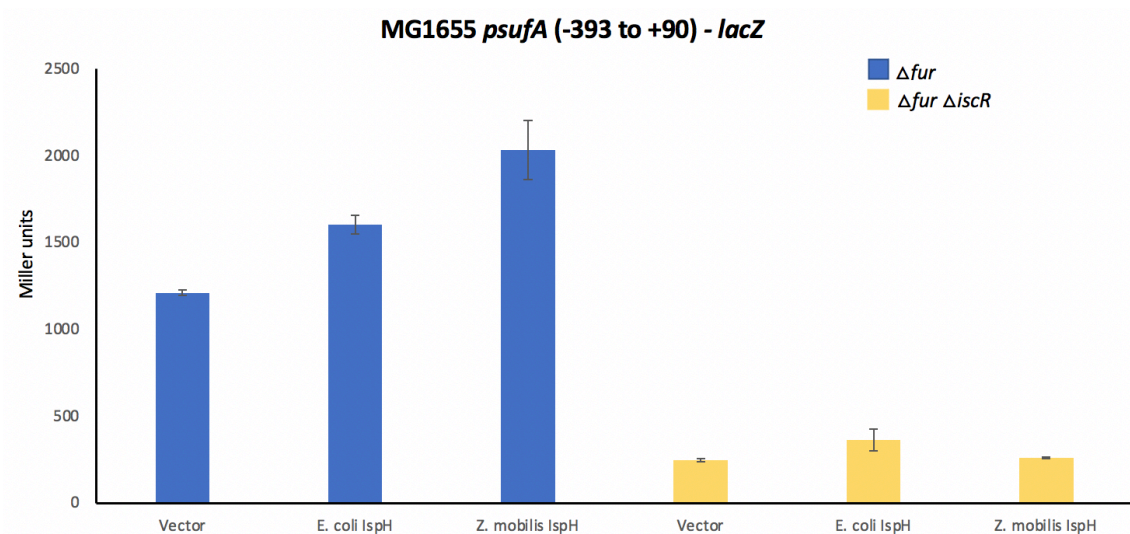


The *suf* operon is also upregulated under oxidative stress conditions. OxyR, the peroxide stress regulator activates the expression of the *suf* operon⁵ and many antioxidant genes including those that metabolize peroxide. Fur also represses expression of *suf* by primarily antagonizing IscR binding site to P_{*sufA*}⁶. We found that the *sufA* promoter does not show a significant difference in expression in presence of *Z. mobilis* IspH (Figure A2-1E, F).

Taken together we observed only small effects on these reporter constructs making it difficult to draw any firm conclusions.

Figure A2-1 β -galactosidase assay of *PsufA* upon expression of IspH under aerobic conditions

(E, F) MG1655 *psufA-lacZ* (-393 to +90), (-200 to +40) with the plasmid variants overexpressing *E. coli* IspH, *Z. mobilis* IspH were grown in MOPS minimal media until OD 0.4 and beta-galactosidase assay was performed after cells lysis. Vector backbone was used as a control. Error bars represent standard error of three replicate datasets.

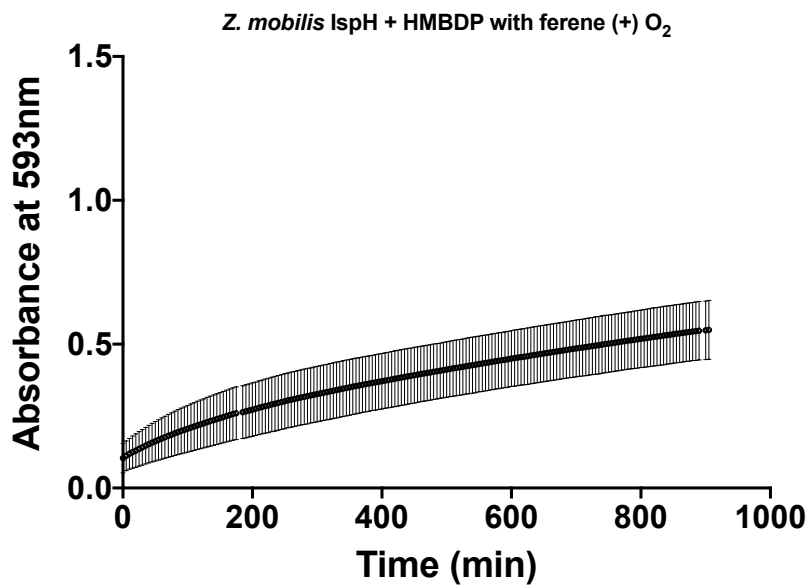
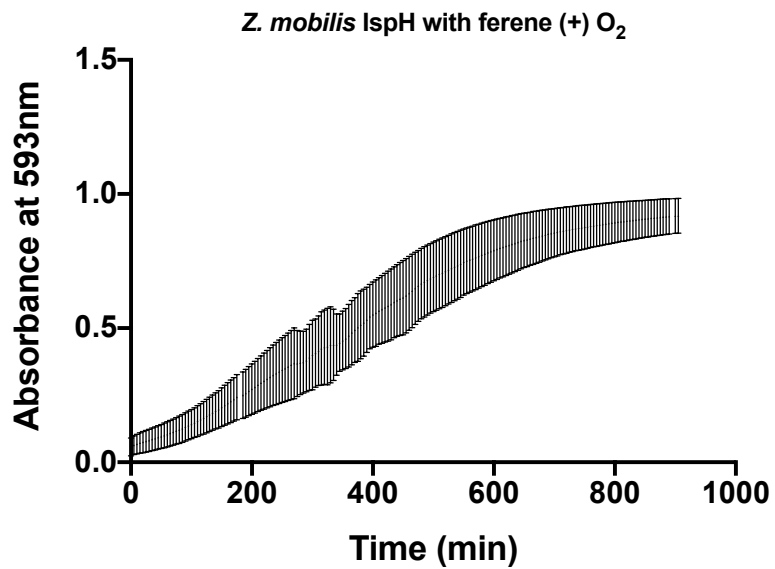


2. Using ferene to measure iron release from IspH and IspG [4Fe-4S] clusters under aerobic conditions

The absorbance at 593nm with ferene is indicative of Fe^{2+} release from the Fe-S cluster⁷ of *Z. mobilis* IspH. Our results from this assay suggest that in the presence of ferene, *Z. mobilis* IspH loses ~ 63% Fe^{2+} from the oxidized [4Fe-4S] cluster under aerobic conditions as 12.6 μM Fe released is divided by total Fe (20 μM) present in the sample. This is calculated as the final $A_{593\text{nm}}$ value 0.5 which divided by extinction coefficient of ferene is 39.6 $\text{mM}^{-1}\text{cm}^{-1}$ equals 12.6 μM Fe is released. The concentration of Fe in IspH used is 20 μM . The increase in $A_{593\text{nm}}$ was around ~ 2-fold more compared to presence of HMBDP in the reaction mixture. These results suggests that *Z. mobilis* IspH cluster is labile under aerobic conditions as the destabilized cluster loses its Fe. However, as the substrate acts as the fourth ligand of the cluster, the cluster is more stable with oxygen presumably because of protection of the "labile" Fe atom of the [4Fe-4S] cluster.

Figure A2-2. Measurement of Fe²⁺ release from the [4Fe-4S] cluster of *Z. mobilis* IspH

Purified *Z. mobilis* IspH was incubated with ferene only and also with ferene and HMBDP under aerobic condition. Absorbance was monitored at 593 nm using UV-Vis spectrophotometer. Error bars represent standard error of three replicate datasets.

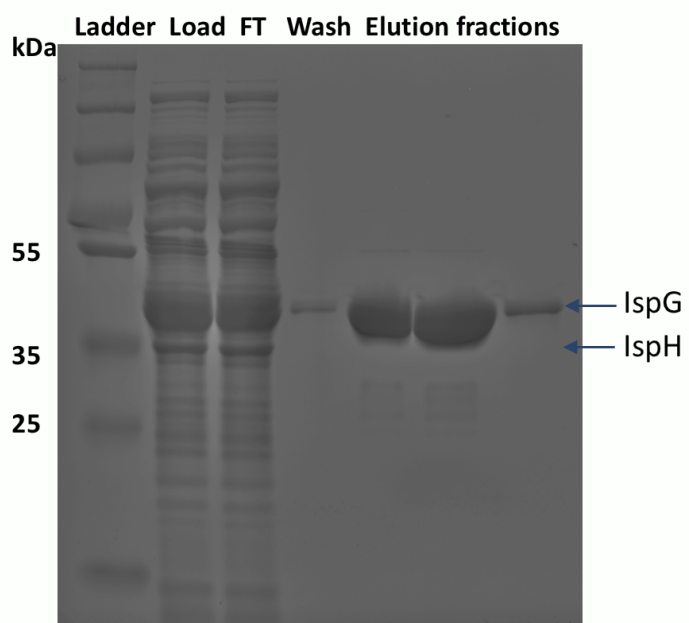


3. Pull-down assays to test *Z. mobilis* IspG and IspH interaction under anaerobic conditions

To test IspG and IspH interactions, pull down assays were performed under anaerobic conditions to protect the [4Fe-4S] cluster of IspG and IspH from oxidative damage. We found the strep-tag II IspG pulldown fractions did not co-elute with IspH when electrophoresed on 12% SDS PAGE gel.

Figure A2-3. *Z. mobilis* IspH does not co-elute with *Z. mobilis* IspG C- terminus strep-tag II.

Pull-down fractions of co-expressed *Z. mobilis* IspG strep-tag II and *Z. mobilis* IspH non-tagged separated on 12% SDS-PAGE gel.



MATERIALS AND METHOD

Strain construction

Plasmids encoding *E. coli* IspH, *Z. mobilis* IspH, *Z. mobilis* IspG & IspH and vector backbone which lacks gene encoding GFP were transformed in strains PK 7564, PK 12028, PK 12029, PK 7573, PK 6886, PK 11099, PK 11100, PK 10864, PK 10865 for β -galactosidase experiments. Plasmids pPK 13650 containing *Z. mobilis* IspH strep-tag II was transformed in PK13681 that contains the repaired *suf* operon which is controlled by arabinose induced *P_{BAD}* promoter⁸, resulting in PK 13654 strain which was used for isolation.

Expression and purification of IspH

Cells were grown aerobically at 37°C in 1L of terrific broth (Research Products International) containing final concentration of ferric ammonium citrate 10mg/L, 2 mM cysteine, 10 mM arabinose, and ampicillin (100 μ g/L). At an OD₆₀₀ of 0.3, synthesis of IspH or IspG was induced by adding IPTG to a final concentration of 0.4 mM for 2 hours. The induced culture was sparged overnight (20 hours) with argon at 4°C. The culture was centrifuged at 8000 rpm in a Beckman JLA 10.500 rotor for 15 min at 4°C, resuspended in 50 mM Tris-HCl, 150 mM NaCl, 1mM DTT, 100 μ M PMSF, pH 8 under anaerobic conditions and lysed in a French Press at 20,000 psi (1 psi~6.9kPa). The lysate was centrifuged at 45,000 rpm in a Beckman 70.1 Ti rotor for 1h at 4°C. The supernatant was fractionated using a FPLC instrument (AKTA pure chromatography system, cytiva) equipped with a StrepTrapTM HP column (5ml, GE Healthcare), equilibrated with 50 mM Tris-HCl, 150 mM NaCl, 1 mM DTT, pH 8. IspH proteins were eluted with 50 mM Tris-HCl, 150 mM NaCl, 2.5 mM desthiobiotin, 1 mM DTT, pH 8. DTT and desthiobiotin in the pooled protein fraction was separated using PD-10 desalting column containing 8.3 ml of SephadexTM G-25 resin

(cytiva) with 50 mM Tris-HCl, 150 mM NaCl pH 7.5., The concentration of the protein was measured using Bradford assay⁹. The isolation of protein was carried out anaerobically inside a Coy anaerobic chamber with an atmosphere of 80% N₂, 10%CO₂ and 10%H₂.

Measurement of Fe²⁺ release

IspH with ferene reaction mixture was made in anaerobic chamber in sealed screw cap cuvette containing 5 μM IspH and 1 mM ferene (Fe²⁺ specific iron chelator) (Sigma) in the presence of 50 mM Tris-HCl, 150 mM NaCl pH 7.5. Release of Fe²⁺ from the [4Fe-4S]²⁺ cluster of *Z. mobilis* IspH was measured in triplicate by monitoring A_{593nm}, characteristic of ferene-Fe²⁺ complex during the reaction of 5 μM 4Fe-IspH under aerobic conditions in the presence of 1 mM ferene. Fe²⁺ release was also monitored in the presence of 50 μM HMBDP and 5 μM 4Fe-IspH and 1 mM ferene. A_{593nm} was monitored using UV-Vis spectrophotometer (Perkin Elmer).

β-galactosidase assay

Strains were grown to an OD₆₀₀ of 0.4 in MOPS minimal medium and IspH and IspG genes were induced from plasmid with 100 μM IPTG. Cells were grown by shaking at 37°C, 250 r.p.m. or by incubating cultures anaerobically in filled screw-capped tubes at 37°C. The cultures were then subsequently assayed for β-galactosidase activity¹⁰.

REFERENCES

1. Tardat B, Touati D. Iron and oxygen regulation of Escherichia coli MnSOD expression: competition between the global regulators Fur and ArcA for binding to DNA. *Mol Microbiol.* 1993;9(1):53-63.
2. Beauchene NA, Myers KS, Chung D, et al. Impact of Anaerobiosis on Expression of the Iron-Responsive Fur and RyhB Regulons. *mBio.* 2015;6(6):e01947-01915.
3. Beauchene NA, Mettert EL, Moore LJ, Keles S, Willey ER, Kiley PJ. O₂ availability impacts iron homeostasis in Escherichia coli. *Proc Natl Acad Sci U S A.* 2017;114(46):12261-12266.
4. Giel JL, Rodionov D, Liu M, Blattner FR, Kiley PJ. IscR-dependent gene expression links iron-sulphur cluster assembly to the control of O₂-regulated genes in Escherichia coli. *Mol Microbiol.* 2006;60(4):1058-1075.
5. Mettert EL, Kiley PJ. Coordinate regulation of the Suf and Isc Fe-S cluster biogenesis pathways by IscR is essential for viability of Escherichia coli. *J Bacteriol.* 2014;196(24):4315-4323.
6. Lee KC, Yeo WS, Roe JH. Oxidant-responsive induction of the suf operon, encoding a Fe-S assembly system, through Fur and IscR in Escherichia coli. *J Bacteriol.* 2008;190(24):8244-8247.
7. Sutton VR, Stubna A, Patschkowski T, Munck E, Beinert H, Kiley PJ. Superoxide destroys the [2Fe-2S]²⁺ cluster of FNR from Escherichia coli. *Biochemistry.* 2004;43(3):791-798.

8. Sourice M, Askenasy I, Garcia PS, et al. A Diverged Transcriptional Network for Usage of Two Fe-S Cluster Biogenesis Machineries in the Delta-Proteobacterium *Myxococcus xanthus*. *mBio*. 2023;14(1):e0300122.
9. Kielkopf CL, Bauer W, Urbatsch IL. Bradford Assay for Determining Protein Concentration. *Cold Spring Harb Protoc*. 2020;2020(4):102269.
10. Griffith KL, Wolf RE, Jr. Measuring beta-galactosidase activity in bacteria: cell growth, permeabilization, and enzyme assays in 96-well arrays. *Biochem Biophys Res Commun*. 2002;290(1):397-402.
11. Nesbit AD, Fleischhacker AS, Teter SJ, Kiley PJ. ArcA and AppY antagonize IscR repression of hydrogenase-1 expression under anaerobic conditions, revealing a novel mode of O₂ regulation of gene expression in *Escherichia coli*. *J Bacteriol*. 2012;194(24):6892-6899.

Appendix 3

Metabolomics profiling to study flux through the MEP pathway in *E. coli*

In collaboration with Julia Martien, Daniel-Amador Noguez lab

Under aerobic conditions, complementation assays in *E. coli* (MVA+) Δ *ispH* showed a severe oxygen sensitive growth phenotype when *Z. mobilis* IspH was expressed at all tested IPTG concentrations. However, co-expression of *Z. mobilis* IspG and IspH partially improved the phenotype at higher IPTG concentrations. One possible explanation is that the presence of IspG is delivering sufficient substrate to IspH, which is improving the flux through the MEP pathway. To test this hypothesis, we did metabolomic profiling studies in the *E. coli* (MVA+) Δ *ispH*. MEP pathway intermediates were measured in strains containing plasmids with *E. coli* IspH, *Z. mobilis* IspH, *Z. mobilis* IspG & IspH, or the vector backbone plasmid after growth with 100 μ M IPTG and normalized to *E. coli* IspH. MEcDP and HMBDP levels accumulated in the *E. coli* (MVA+) Δ *ispH* that overexpressed only vector backbone plasmid as expected. Small increase in MEcDP levels was also observed as the strains were transferred from anaerobic to aerobic growth conditions as reported earlier in *Z. mobilis*¹. IDP and DMADP levels were unaffected when comparing the different plasmid bearing strains, which was not surprising since these intermediates would also be produced by the mevalonic acid pathway and mevalonate was included in the growth media in order to maintain viability of the strains. IDP levels produced from the MVA pathway maybe causing feedback inhibition of DXS enzyme to regulate the flux of the MEP pathway, precluding any conclusions from this experiment. It has been reported earlier that in plants, DXS is a major metabolic control point in the MEP pathway^{2,3} and that DXS is subject to feedback inhibition from IDP and DMADP⁴. Also, it is reported that recombinant IspF from *E. coli* can be feedforward activated by methylerythritol 4-phosphate (MEP) and that IspF is subject only to feedback inhibition from the downstream isoprenoid farnesyl diphosphate when IspF is complexed with MEP^{5,6}.

Figure A3-1. Fold change of various metabolites of the MEP pathway. [(A) DXP (B) MEcDP (C) HMBDP (D) IDP-DMADP] of the MEP pathway upon transfer from anaerobic to aerobic growth conditions in MG1655 (MVA+) $\Delta ispH$ with plasmid variants containing *ispG* or *ispH* from either *Z. mobilis* or *E. coli* at 100 μ M IPTG.

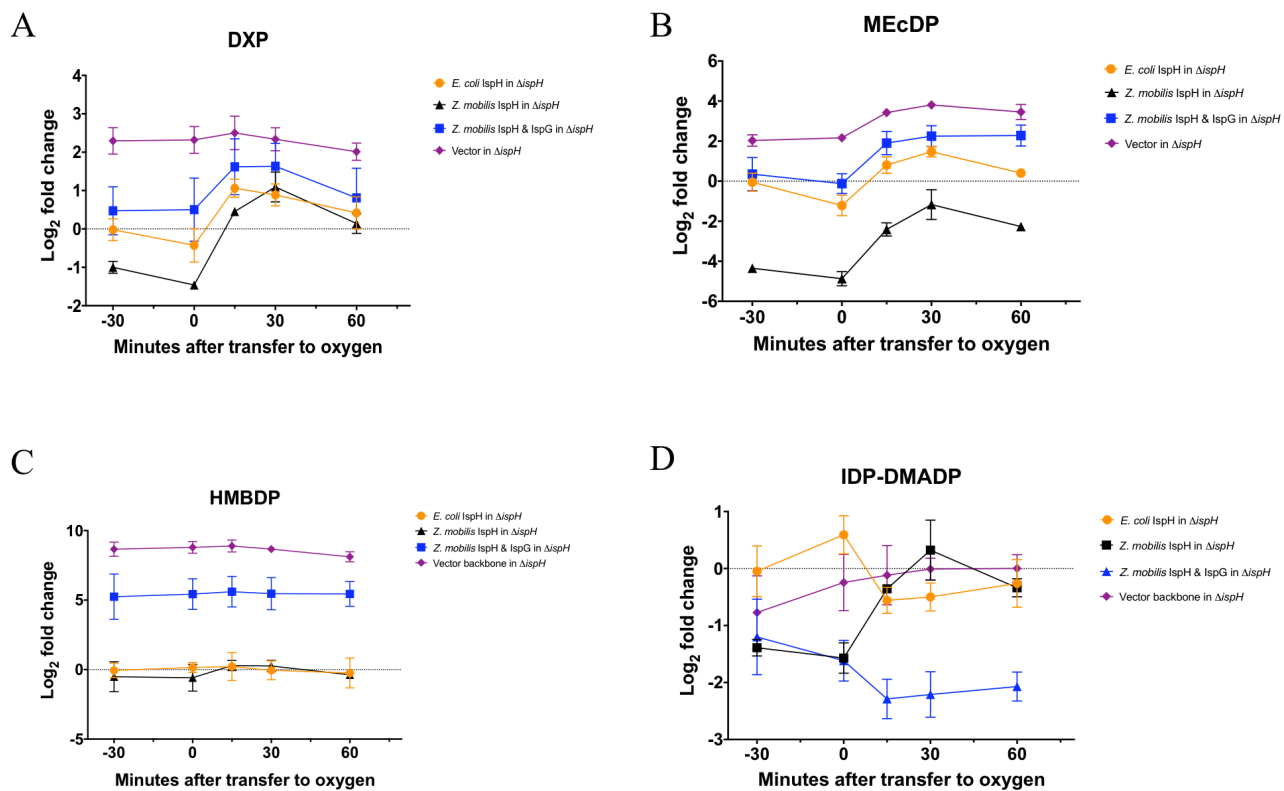
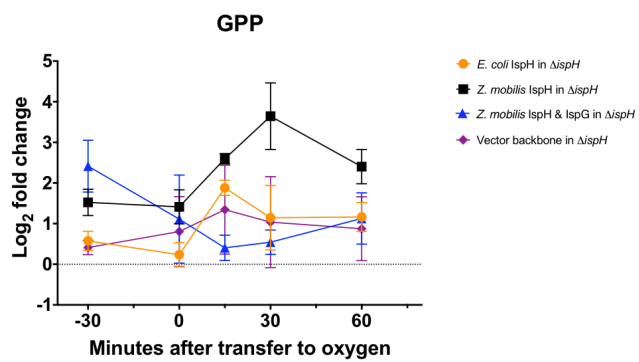
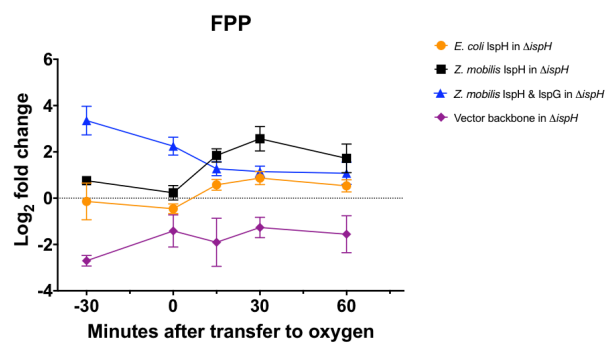


Figure A3-2. Fold change of downstream metabolites [(A) GPP (B) FPP] of the MEP pathway upon transfer from anaerobic to aerobic growth conditions in MG1655 (MVA+) $\Delta ispH$ with plasmid variants containing *ispG* or *ispH* from either *Z. mobilis* or *E. coli*

A



B



MATERIALS AND METHOD

Cell culturing and experimental design. Strains PK 13591, PK13592, PK13593 and PK13976 were inoculated from a frozen glycerol stock into LB rich media containing 10 mM arabinose, 0.9 mM mevalonate, 100 μ M IPTG and 100 μ g/mL spectinomycin. The culture tubes were shaken under atmospheric conditions at 37°C for 16 hours. These cultures were then used to inoculate a reduced nutrients media consisting of M9 media (6g/L Na_2HPO_4 anhydrous, 3g/L KH_2PO_4 anhydrous, 0.5 g/L NaCl, 1g/L NH_4Cl , 0.4% Glucose, 1mM MgSO_4 , 0.1 mM CaCl_2 , 0.0072 mM FeSO_4) with 2 g/L yeast extract, 10 mM arabinose, 0.9 mM mevalonate, 100 M IPTG and 100 μ g/mL spectinomycin. Cultures were grown anaerobically in reduced nutrient media for two passages before being used to inoculate experimental flasks with a starting OD between 0.07 and 0.01 under anaerobic conditions. Three biological replicates of each strain were then grown up in 70 mL of reduced nutrient media (with 50 μ g/mL spec instead of 100) in a 250 mL baffled flask at 37°C anaerobically without shaking. Cultures were grown for 3 to 5 hours, until OD reached approximately 0.4 at which point an anaerobic baseline ($t = -30$) metabolite extraction was performed. 30 minutes later, another ($t = 0$) metabolite extraction was performed and immediately after the extraction, cultures were transferred out of the anaerobic chamber and started shaking under atmospheric aerobic conditions. Subsequent metabolite extractions were performed 15, 30, and 60 minutes following the transfer to aerobic conditions.

Metabolite extraction. At the time of extraction, 10 mL of liquid culture was extracted using a serological pipet. The culture was then rapidly filtered through a 0.45 μ m nylon filter (Millipore catalog no. HNWP04700) using a vacuum flask fitted with a sintered glass funnel, separating cells from the growth media. Immediately after the media passed through the filter, the cells captured

on the filter were plunged into cold extraction solvent, simultaneously quenching metabolism, lysing cells, and dissolving intracellular metabolites. This was done by placing the filter face-down in a small (5.5 cm diameter) plastic Petri dish containing 1.5 mL extraction solvent (40:40:20 methanol:acetonitrile:water; all HPLC-grade). The dish containing extraction solvent was kept on dry ice or an aluminum block that had been stored at -80 °C. The entire process of extraction was done in 30 seconds or less. The filter was then rinsed in the extraction solvent within the dish using a pipet to dislodge remaining cell debris and metabolites. The 1.5 mL of extract was then transferred to a microcentrifuge tube and centrifuged at $16,000 \times g$ for 3 minutes to remove debris. The supernatant was stored at -80°C until analysis by LC-MS. For analysis, 300 to 200 uL of extract was dried down under N₂ gas. Samples were concentrated 3x by re-suspending in one third the dry-down volume of Solvent A (see Metabolomics LC-MS), vortexed for 10 seconds, and centrifuged at $16,000 \times g$ for 3 minutes to remove any remaining cell debris. 50uL of the supernatant was then transferred to an HPLC vial for LC-MS analysis.

Metabolomics LC-MS analysis. Metabolomics analysis by LC-MS was performed using a Vanquish™ UHPLC system (Thermo Scientific) coupled to a hybrid quadrupole orbitrap mass spectrometer (Q exactive, Thermo Scientific). The chromatography was done using a reverse-phase C18 column (1.7 μm particle size, 2.1 x 100mm column, Acquity UPLC® BEH). Solvent A was 97% H₂O and 3% methanol with 10mM tributylamine (TBA) and ~10mM acetic acid for a pH of 8.2. Solvent B was 100% methanol. Total run time was 25 minutes. Flow rate was held constant at 0.2 mL/min. The chromatography gradient was as follows: 5% solvent B for 2.5 min, linear increase to 95% B over 14.5 min, maintain 95% B for 2.5 min, linear decrease back to 5% B over 0.5 min, maintain 5% B for 5 min. Eluent from the column was analyzed by mass

spectrometry from the start of the run until 19 min, at which time flow was directed to waste for the remainder of the run. Compounds separated by HPLC were ionized by electrospray ionization (negative polarity) and analyzed by full MS-selected ion monitoring (MS-SIM) with a scanning range of 70 to 1000 m/z, an automatic gain control (AGC) target value of 1×10^6 , maximum injection time (IT) of 40 ms, and resolution of 70,000.

Metabolomics computational analysis. LC-MS raw files were converted to mzXML format and visualized using MAVEN. Peaks were chosen by comparison with retention times obtained using analytical standards. For each metabolite, signal intensity was divided by OD_{600nm} to account for variation in culture density between samples. These values were then divided by the average of the three replicates in the 13592 t = -30 sample to generate fold-change values. The Log_2 of the fold-change values was then averaged to obtain the data displayed in this study.

REFERENCES

1. Martien JI, Hebert AS, Stevenson DM, et al. Systems-Level Analysis of Oxygen Exposure in *Zymomonas mobilis*: Implications for Isoprenoid Production. *mSystems*. 2019;4(1).
2. Wright LP, Rohwer JM, Ghirardo A, et al. Deoxyxylulose 5-Phosphate Synthase Controls Flux through the Methylerythritol 4-Phosphate Pathway in Arabidopsis. *Plant Physiol*. 2014;165(4):1488-1504.
3. Ghirardo A, Wright LP, Bi Z, et al. Metabolic flux analysis of plastidic isoprenoid biosynthesis in poplar leaves emitting and nonemitting isoprene. *Plant Physiol*. 2014;165(1):37-51.
4. Banerjee A, Wu Y, Banerjee R, Li Y, Yan H, Sharkey TD. Feedback inhibition of deoxy-D-xylulose-5-phosphate synthase regulates the methylerythritol 4-phosphate pathway. *J Biol Chem*. 2013;288(23):16926-16936.
5. Bitok JK, Meyers CF. 2C-Methyl-d-erythritol 4-phosphate enhances and sustains cyclodiphosphate synthase IspF activity. *ACS Chem Biol*. 2012;7(10):1702-1710.
6. Khana DB, Tatli M, Rivera Vazquez J, et al. Systematic Analysis of Metabolic Bottlenecks in the Methylerythritol 4-Phosphate (MEP) Pathway of *Zymomonas mobilis*. *mSystems*. 2023;8(2):e0009223.